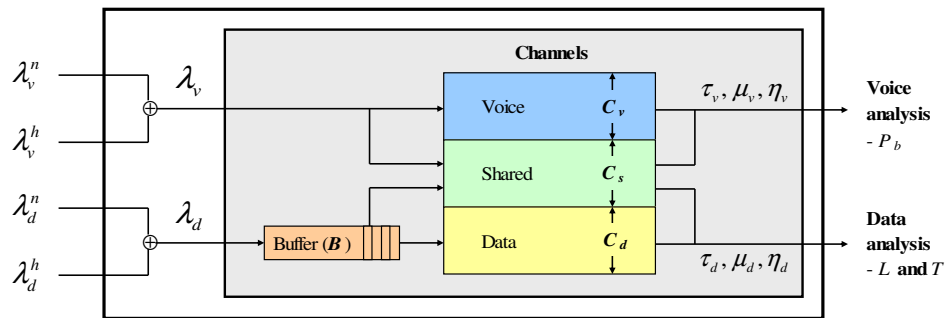




INSTITUTO
SUPERIOR
TÉCNICO

UNIVERSIDADE TÉCNICA DE LISBOA INSTITUTO SUPERIOR TÉCNICO



An analytical traffic model for the UMTS radio interface

Cristina Büchel Marques dos Reis
(Licenciada)

Dissertation submitted for obtaining the degree of
Master in Electrical and Computer Engineering

Supervisor: Doctor Luís Manuel de Jesus Sousa Correia

Jury:

President: Doctor Luís Manuel de Jesus Sousa Correia

Members: Doctor Américo Manuel Carapeto Correia

Doctor José Manuel Rego Lourenço Brázio

December 2003

To my Family

Acknowledgements

First of all, I wish to thank most sincerely Professor Luís Correia, for providing me with all information and support on the elaboration of this thesis. The excellent guidelines that were provided, sometimes even more than once a week, were determinant on the completion of this work.

I am thankful for having been able to use the working space and facilities from *Instituto de Telecomunicações*. I am also extremely grateful to have shared, for some months, the room with a very friendly team, who, in addition, provided me with important documentation and good tips for this work.

Special thanks are due to my Family, for their unconditional support and great incentive given during this hard time.

Abstract

This work is centred on the analysis of the performance of UMTS, based on the implementation of a traffic model that integrates voice and data users, mixing circuit- and packet-switch with a finite-buffering capacity. The model is adapted in such a way that the main 3rd generation system characteristics are reflected in it. The generation of voice and data events are modelled by a Poisson distribution, the service time being exponentially distributed. Two ways of allocating channels to users are analysed: either equitably between voice and data, or as a proportion of the number of users for each service. As expected, the system behaves worse when the number of users or the traffic per user increases, as it imposes a rise in the interference and a reduction on the number of channels made available by the system. Mobility being a key issue in UMTS, its integration in the model is also accounted for. Users' speed is studied and the corresponding impact evaluated. Some limited heterogeneous routing towards neighbouring cells is considered as well on the analysis of the traffic model. The buffer size is also studied, and, as expected, it comes out that this network element is determinant on the system performance. The analysis of a predominant voice users' scenario, done for a cell with 250 m radius, showed that a blocking probability of 2 % is not exceeded for average speeds lower than 90 or 100 km/h. Considering a larger data users' scenario, and assuming a buffer with 15 or 20 MB, losses of 1 % become rather scarce for any average users' speed. In general, a reduction on the cell dimensions leads to a remarkable improvement on the overall system performance.

Keywords

UMTS. Traffic models. Analytical model. Multi-service. System performance. Network planning.

Resumo

Este trabalho centra-se na análise do desempenho de um sistema UMTS, com base na implementação de um modelo de tráfego que integra utilizadores de voz e dados e considera uma capacidade limitada para armazenamento de chamadas de dados. O modelo foi adaptado por forma a contemplar as principais características de sistemas 3G. A geração de eventos de voz e dados é modelada pela distribuição de Poisson, sendo a sua duração caracterizada pela distribuição Exponencial. São analisadas duas formas de distribuir os canais pelos utilizadores: equitativamente entre voz e dados ou proporcionalmente ao número de utilizadores por serviço. Tal como esperado, o sistema comporta-se pior quando o número de utilizadores ou o tráfego por utilizador cresce, dado que a interferência aumenta e o número de canais disponibilizado pelo sistema é inferior. Sendo a mobilidade um ponto chave em sistemas UMTS, impunha-se a sua integração no modelo. É estudada a velocidade dos utilizadores e o correspondente impacto. Considera-se igualmente um movimento heterogéneo limitado para células vizinhas na análise do modelo de tráfego. A capacidade de armazenamento de pacotes é igualmente estudada, e, tal como esperado, condiciona de forma determinante o desempenho do sistema. A análise de um cenário com um número predominante de utilizadores de voz, para uma célula de 250 m de raio, mostra que não é excedida uma probabilidade de bloqueio de 2 % para a voz para velocidades médias inferiores a 90 ou 100 km/h. Considerando um cenário com maior número de utilizadores de dados, e, assumindo uma capacidade de armazenamento de 15 ou 20 MB, obtêm-se, para qualquer velocidade, perdas inferiores ou na ordem de 1 %. Em geral, a redução das dimensões das células leva a uma notável melhoria nos parâmetros que medem o desempenho do sistema.

Palavras Chave

UMTS. Modelos de tráfego. Modelo analítico. Multi-serviços. Desempenho do sistema. Planeamento de rede.

Table of Contents

- Acknowledgements.....iii**
- Abstract v**
- Keywords..... v**
- Resumovi**
- Palavras Chavevi**
- Table of Contents.....vii**
- List of Figuresix**
- List of Tables.....xiv**
- List of Acronymsxv**
- List of Symbols.....xix**
- 1 Introduction 1**
- 2 UMTS fundamentals 9**
 - 2.1 Network architecture 9
 - 2.2 Air interface..... 11
 - 2.3 Radio resource management 15
 - 2.4 Services and applications 17
 - 2.5 Network dimensioning 18
- 3 Traffic analysis 25**
 - 3.1 Coverage estimation 25
 - 3.2 Capacity estimation 32

Table of Contents

3.3	Code planning.....	37
3.4	General traffic aspects	41
4	Traffic model.....	49
4.1	Model formulation.....	49
4.2	Adaptation of the model to UMTS.....	53
4.3	The algorithm	65
5	Analysis of results.....	75
5.1	Description of scenarios under study	75
5.2	Analysis of the number of channels	79
5.3	Comparison of traffic model results with known models	81
5.4	Results for a single cell	87
5.5	Results for multi-cells	98
6	Conclusions	103
Annex A	COST231–Walfisch-Ikegami Model.....	109
Annex B	Statistical distributions	113
Annex C	Scenario A, Program results.....	115
Annex D	Scenario B, Program results.....	133
References	151

List of Figures

Figure 1.1 – International allocations for IMT-2000 (extracted from [CEPT00]).	1
Figure 1.2 – Third generation environment (adapted from [CEPT00]).	3
Figure 2.1 – General UMTS network architecture (adapted from [3GPP01a]).	9
Figure 2.2 – UMTS Spectrum allocations in Europe (based on [CEPT02]).	12
Figure 2.3 – Example of services and applications in UMTS (adapted from [UMTS01]).	18
Figure 3.1 – Cell radius.	31
Figure 3.2 – Coverage vs. capacity on UL and DL.	36
Figure 3.3 – Code-tree for generation of OVSF codes (extracted from [3GPP01b]).	37
Figure 3.4 – Maximum number of DL users per service (based on [FCSC02]).	40
Figure 3.5 – Maximum number of users for more than one service.	40
Figure 3.6 – General call access mechanism for CS (extracted from [Corr03]).	44
Figure 3.7 – General call access mechanism for PS (adapted from [Leon94]).	46
Figure 4.1 – Traffic model for the base station (adapted from [HaLH00]).	49
Figure 4.2 – DL Code check.	54
Figure 4.3 – E_b/N_0 values (adapted from [RFHL03]).	55
Figure 4.4 – Orthogonal factor as a function of users' speed.	56
Figure 4.5 – Link budget parameters adapted to a varying users' speed.	57
Figure 4.6 – Call arrival rate vs. cell radius.	60
Figure 4.7 – p_{ij} matrix.	61
Figure 4.8 – Steady-states $[(\tau_v, \tau_d), (\lambda_v, \lambda_d)]$.	62
Figure 4.9 – Steady-states $[(2\tau_v, 2\tau_d), (\lambda_v, \lambda_d)]$ or $[(\tau_v, \tau_d), (2\lambda_v, 2\lambda_d)]$.	62
Figure 4.10 – Users' motion along a ring of six cells.	65

List of Figures

Figure 4.11 – Channel distribution.....	68
Figure 4.12 – Traffic model algorithm, main flowchart.....	70
Figure 4.13 – System load verification, flowchart A.	71
Figure 4.14 – Code verification, flowchart B.....	72
Figure 4.15 – BS power verification, flowchart C.	73
Figure 4.16 – Traffic model computation, flowchart D.	74
Figure 5.1 – Possible cell radii.	78
Figure 5.2 – Number of codes for Scenario A.	79
Figure 5.3 – Number of codes for Scenario B.....	80
Figure 5.4 – Blocking probability for Erlang-B model.	82
Figure 5.5 – Available voice channels versus users’ speed.....	83
Figure 5.6 – Traffic model blocking probability for Scenario B.....	84
Figure 5.7 – Erlang-B model blocking probability, Scenario A.....	85
Figure 5.8 – Erlang-B model blocking probability, Scenario B.....	86
Figure 5.9 – Equitable distribution of channels.	88
Figure 5.10 – Proportional distribution of channels, predominant voice users.....	89
Figure 5.11 – Proportional distribution of channels, predominant data users.....	90
Figure 5.12 – Blocking probability as a function of users’ speed.....	92
Figure 5.13 – Data loss probability as a function of users’ speed.....	93
Figure 5.14 – Mean data delay as a function of users’ speed.....	94
Figure 5.15 – P_b and L as a function of the users’ speed, for $R = 100$ m.	95
Figure 5.16 – P_b and L as a function of the users’ speed, for $R = 200$ m.	96
Figure 5.17 – Mean data delay vs. speed for a heterogeneous scenario.....	100
Figure 5.18 – Mean data delay per cell for a heterogeneous scenario.	101

Figure A.1 – Parameters used in the COST231-Walfisch-Ikegami model (extracted from [Corr99]).	109
Figure B.1 – Discrete distribution of events (extracted from [Keis89]).	113
Figure C.1 – Number of codes for Scenario A with a 150 and 250 m cell radius.	115
Figure C.2 – System performance versus users’ speed (150 m cell radius; 20 MB buffer size).	116
Figure C.3 – System performance versus users’ speed (250 m cell radius; 20 MB buffer size).	117
Figure C.4 – System performance versus users’ speed (150 m cell radius; 10 MB buffer size).	118
Figure C.5 – System performance versus users’ speed (250 m cell radius; 10 MB buffer size).	119
Figure C.6 – System performance versus buffer size (150 m cell radius; 15 km/h average speed).	120
Figure C.7 – System performance versus buffer size (250 m cell radius; 15 km/h average speed).	121
Figure C.8 – System performance versus buffer size (150 m cell radius; 60 km/h average speed).	122
Figure C.9 – System performance versus buffer size (250 m cell radius; 60 km/h average speed).	123
Figure C.10 – Steady-states $[(\tau_v, \tau_d), (\lambda_v, \lambda_d)]$, equitable distribution of resources and 150 m cell radius.	124
Figure C.11 – Steady-states $[(2\tau_v, 2\tau_d), (\lambda_v, \lambda_d)]$ or $[(\tau_v, \tau_d), (2\lambda_v, 2\lambda_d)]$, equitable distribution of resources and 150 m cell radius.	125
Figure C.12 – Steady-states $[(\tau_v, \tau_d), (\lambda_v, \lambda_d)]$, proportional distribution of resources and 150 m cell radius.	126
Figure C.13 – Steady-states $[(2\tau_v, 2\tau_d), (\lambda_v, \lambda_d)]$ or $[(\tau_v, \tau_d), (2\lambda_v, 2\lambda_d)]$, proportional distribution of resources and 150 m cell radius.	127

List of Figures

Figure C.14 – Steady-states $[(\tau_v, \tau_d), (\lambda_v, \lambda_d)]$, equitable distribution of resources and 250 m cell radius..... 128

Figure C.15 – Steady-states $[(2\tau_v, 2\tau_d), (\lambda_v, \lambda_d)]$ or $[(\tau_v, \tau_d), (2\lambda_v, 2\lambda_d)]$, equitable distribution of resources and 250 m cell radius..... 129

Figure C.16 – Steady-states $[(\tau_v, \tau_d), (\lambda_v, \lambda_d)]$, proportional distribution of resources and 250 m cell radius..... 130

Figure C.17 – Steady-states $[(2\tau_v, 2\tau_d), (\lambda_v, \lambda_d)]$ or $[(\tau_v, \tau_d), (2\lambda_v, 2\lambda_d)]$, proportional distribution of resources and 250 m cell radius. 131

Figure D.1 – Number of channels for Scenario B..... 133

Figure D.2 – System performance versus users’ speed (150 m cell radius; 20 MB buffer size)..... 134

Figure D.3 – System performance versus users’ speed (250 m cell radius; 20 MB buffer size)..... 135

Figure D.4 – System performance versus users’ speed (150 m cell radius; 10 MB buffer size)..... 136

Figure D.5 – System performance versus users’ speed (250 m cell radius; 10 MB buffer size)..... 137

Figure D.6 – System performance versus buffer size (150 m cell radius; 15 km/h average speed)..... 138

Figure D.7 – System performance versus buffer size (250 m cell radius; 15 km/h average speed)..... 139

Figure D.8 – System performance versus buffer size (150 m cell radius; 60 km/h average speed)..... 140

Figure D.9 – System performance versus buffer size (250 m cell radius; 60 km/h average speed)..... 141

Figure D.10 – Steady-states $[(\tau_v, \tau_d), (\lambda_v, \lambda_d)]$, equitable distribution of resources and 150 m cell radius..... 142

Figure D.11 – Steady-states $[(2\tau_v, 2\tau_d), (\lambda_v, \lambda_d)]$ or $[(\tau_v, \tau_d), (2\lambda_v, 2\lambda_d)]$, equitable distribution of resources and 150 m cell radius. 143

Figure D.12 – Steady-states $[(\tau_v, \tau_d), (\lambda_v, \lambda_d)]$, proportional distribution of resources and 150 m cell radius..... 144

Figure D.13 – Steady-states $[(2\tau_v, 2\tau_d), (\lambda_v, \lambda_d)]$ or $[(\tau_v, \tau_d), (2\lambda_v, 2\lambda_d)]$, proportional distribution of resources and 150 m cell radius. 145

Figure D.14 – Steady-states $[(\tau_v, \tau_d), (\lambda_v, \lambda_d)]$, equitable distribution of resources and 250 m cell radius..... 146

Figure D.15 – Steady-states $[(2\tau_v, 2\tau_d), (\lambda_v, \lambda_d)]$ or $[(\tau_v, \tau_d), (2\lambda_v, 2\lambda_d)]$, equitable distribution of resources and 250 m cell radius. 147

Figure D.16 – Steady-states $[(\tau_v, \tau_d), (\lambda_v, \lambda_d)]$, proportional distribution of resources and 250 m cell radius..... 148

Figure D.17 – Steady-states $[(2\tau_v, 2\tau_d), (\lambda_v, \lambda_d)]$ or $[(\tau_v, \tau_d), (2\lambda_v, 2\lambda_d)]$, proportional distribution of resources and 250 m cell radius. 149

List of Tables

Table 2.1 – Main characteristics of channelisation and scrambling codes (based on [HoTo01]).	14
Table 2.2 – UMTS traffic classes (extracted from [3GPP02a]).	19
Table 2.3 – Radio bearer attributes per UMTS QoS class (as defined in [3GPP02a]).	20
Table 3.1 – MTs and BSs assumptions (based on [HoTo01]).	27
Table 3.2 – E_b/N_0 used for link budget calculations (extracted from [FCSC02]).	28
Table 3.3 – Services vs. UL/DL spreading factors and UL/DL codes (adapted from [FCSC02]).	39
Table 4.1 – L_{in-car} , G_{SHO} and $M_{fast-fading}$ vs. number of channels.	58
Table 5.1 – Number of users forming Scenarios A and B.	75
Table 5.2 – Services characteristics (adapted from [FCXV03]).	76
Table 5.3 – Input parameters common to Scenarios A and B.	77
Table 5.4 – No. of codes for $R = 200$ m at 30 km/h, Scenarios A and B.	77
Table 5.5 – System tendency due to the traffic model.	98

List of Acronyms

2.5G	Interim step towards 3 rd Generation of mobile system
2G	2 nd Generation of mobile systems
3G	3 rd Generation of mobile systems
3GPP	3 rd Generation Partnership Project
AICH	Acquisition Indication Channel
BCCH	Broadcast Control Channel
BCH	Broadcast Channel
BHCA	Busy Hour Call Attempt
BS	Base Station
BSC	Base Station Controller
BSS	Base Station Subsystem
CCCH	Common Control Channel
CCPCH	Common Control Physical Channel
CDMA	Code Division Multiple Access
CN	Core Network
CPCH	Common Packet Channel
CPICH	Common Pilot Channel
CS	Circuit Switched
CTCH	Common Traffic Channel
DCCH	Dedicated Control Channel
DCH	Dedicated Channel

List of Acronyms

DL	Downlink
DPCCH	Dedicated Physical Control Channel
DPCH	Dedicated Physical Channel
DPDCH	Dedicated Physical Data Channel
DS-CDMA	Direct Sequence Code Division Multiple Access
DSCH	Downlink Shared Channel
DTCH	Dedicated Traffic Channel
EDGE	Enhanced Data for Global Evolution
EIRP	Equivalent Isotropic Radiated Power
E-Mail	Electronic Mail
ETSI	European Telecommunications Standards Institute
FACH	Forward Access Channel
FCFS	First-Come-First-Served
FDD	Frequency Division Duplex
FDMA	Frequency Division Multiple Access
FDwnld	File Download
FTP	File Transfer Protocol
GPRS	General Packet Radio Service
GSM	Global System for Mobile communications
HLR	Home Location Register
HO	Handover
HSCSD	High Speed Circuit Switched Data
iid	Independent and identically distributed
IP	Internet Protocol

ITU-T	International Telecommunications Union, Telecommunications Sector
LocBas	Location Based
MAC	Medium Access Control
MMS	Multimedia Messaging Service
MSS	Mobile Satellite Service
MT	Mobile Terminal
NSS	Network Subsystem
OSI	Open Systems Interconnection
OVSF	Orthogonal Variable Spreading Factor
PCCH	Paging Control Channel
P-CCPCH	Primary Common Control Physical Channel
PCH	Paging Channel
PCPCH	Physical Common Packet Channel
PDSCH	Physical Downlink Shared Channel
PHY	Physical Layer
PICH	Page Indication Channel
PN	Pseudo Noise
PRACH	Physical Random Access Channel
PS	Packet Switched
QoS	Quality of Service
RAB	Radio Access Bearer
RACH	Random Access Channel
RLC	Radio Link Control
RNC	Radio Network Controller

List of Acronyms

RNS	Radio Network Subsystems
RRM	Radio Resource Management
S-CCPCH	Secondary Common Control Physical Channel
SCH	Synchronisation Channel
SF	Spreading Factor
SIR	Signal to Interference Ratio
SMS	Short Message Service
SNR	Signal-to-Noise Ratio
Speech	Speech-Telephony
StrMMHQ	Streaming Multimedia High Quality
StrMMLQ	Streaming Multimedia Low Quality
TDD	Time Division Duplex
TDMA	Time Division Multiple Access
UE	User Equipment
UL	Uplink
UMTS	Universal Mobile Telecommunications System
USCH	Uplink Shared Channel
USIM	UMTS Subscriber Identity Module
UTRAN	UMTS Terrestrial Radio Access Network
VideoT	Video-Telephony
WCDMA	Wideband Code Division Multiple Access
WWW	Web Browsing

List of Symbols

α	Angle between horizon (at h_b-H_B) and h_b , seen by building diffraction point
$\bar{\alpha}$	Average orthogonality factor in the cell
ϕ	Road orientation with respect to the direct radio path
η	Cell load
η_d	Cell cross-over rate for data users
η_{DL}	DL load factor
η_h	Cell cross-over rate
η_{UL}	UL load factor
η_v	Cell cross-over rate for voice users
λ	Arrival rate
λ_d	Data call rate
λ_{d100}	Data call rate for a 100 m cell radius
λ_d^h	HO data call rate
λ_d^n	New data call rate
λ_h	HO call arrival rate
λ_n	New call arrival rate
λ_v	Voice call rate
λ_{v100}	Voice call rate for a 100 m cell radius
λ_v^h	HO voice call rate
λ_v^n	New voice call rate

List of Symbols

μ_{cd}	Data channel occupancy rate
μ_{cv}	Voice channel occupancy rate
μ_d	Data call service rate
μ_v	Voice call service rate
ρ	Utilisation of a system
σ_τ	Standard deviation of τ
τ	Average call duration
τ_c	Channel occupancy time in the cell
τ_d	Data call duration
τ_h	Average dwell time in a cell
τ_v	Voice call duration
v_j	Activity factor of user j at physical level
ξ_h	HO rate
A	Amount of traffic
B	Buffer size
c	Number of servers (channels)
C	Number of channels
C_τ^2	Coefficient of variation of the service time
C_d	Number of data channels
C_g	Number of channels for new generated calls
C_h	Number of channels for HO calls
C_s	Number of shared channels
C_v	Number of voice channels
d	Distance

E_b	Energy per user bit
f	Frequency
F_N	Noise figure
G_{div}	Diversity gain
G_r	Antenna gain at the reception
G_{SHO}	Soft handover gain
G_t	Antenna gain at the transmission
h_b	BS height
H_B	Heights of buildings
h_m	MT height
H_{roof}	Roof height
i	Other cell to own interference ratio seen by the BS
k_a	BS height correction factor
k_d	Distance correction factor
k_f	Frequency correction factor
L	Data loss probability
L_0	Free space loss
L_{bsh}	Loss due to BS height
$L_{building}$	Building penetration loss
L_c	Cable losses at the BS
L_{in-car}	In-car loss
L_{msd}	Multi-screen loss
L_{ori}	Loss due to orientation
L_p	Allowed propagation loss

List of Symbols

L_{rts}	Roof-top-to-street diffraction and scatter loss
$M_{body-loss}$	Body loss margin
$M_{fast-fading}$	Fast fading margin
M_{int}	Interference margin
$M_{log-normal}$	Log-normal fading margin
N	Number of users per cell
N_0	Noise power
$N_{pole_{DL_n}}$	DL pole capacity for the n^{th} RAB
$N_{pole_{UL_n}}$	UL pole capacity for the n^{th} RAB
N_{rf}	Noise spectral density of the MT receiver front-end
p_0	Probability at state 0
P_b	Probability of blocking calls
p_c	Probability at state c
P_d	Drop call probability
$p_d(j)$	Probability of having j data packet transmissions
P_h	Probability of performing HO
P_{hf}	Probability of HO failure
P_{i_i}	Probability generating function
p_{ij}	Steady-state probability of i voice calls and j data packets
P_r	Power at the reception
$P_{r\ min}$	Receiver sensitivity
P_t	Power at the transmission
P_{Tx}^{BS}	BS transmitted power

$p_v(i)$	Probability of having i voice calls
P_w	Probability that a call waits in a queue
q_{ij}	Tail probability of j data packets when there are i voice calls
R	Cell radius
R_b	Service bit rate
R_{bj}	Service bit rate of user j
R_c	WCDMA chip rate
r_{ij}	Routing probability from cell i to cell j
R_{ij}	Routing matrix
R_n	Service bit rate of the n^{th} RAB
T	Mean data delay
v	Mean velocity
w_B	Building separation
W_B	Widths of roads considering building walls
w_s	Widths of roads
z	Complex number

1 Introduction

A long way has been left behind since it was first heard about the 3rd generation of mobile systems (3G), namely IMT-2000 or even UMTS. Many thoughts were discussed within the standardisation bodies, leading to the presentation of a variety of multiple radio access techniques and several standards. Originally, and in a wide sense, 3G aimed at:

- converging to a common world standard;
- allowing both voice and high speed data;
- using in a more efficient way the available spectrum;
- simplifying international roaming;
- attaining economies of scale in equipment production.

It was then shown that it was not possible to achieve a common standard, as consensus of worldwide views was completely impossible to attain at the standardisation *fora*; on the other hand, spectrum allocations are not completely overlapped around the world, Figure 1.1, leading to the need of having multimode terminals to allow international roaming.

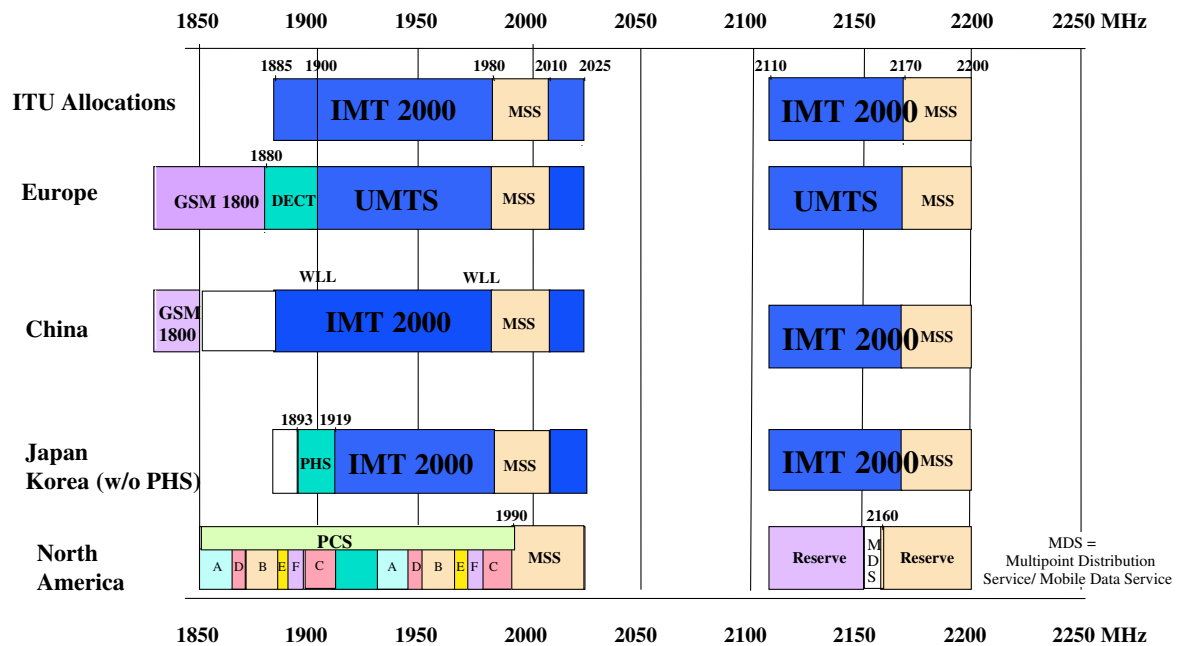


Figure 1.1 - International allocations for IMT-2000 (extracted from [CEPT00]).

1. Introduction

3G will extensively introduce the Wideband Code Division Multiple Access (WCDMA) approach. Despite of the huge investment already done in 2nd generation (2G) Time Division Multiple Access (TDMA) systems in Europe and in other parts of the world, e.g., Global System for Mobile communications (GSM), this new access method was the one approved for UMTS. Operators that work with TDMA systems need to change a considerable amount of network elements in order to get on track with CDMA.

An intermediate step between 2G and 3G, namely the 2.5G (interim step towards 3rd Generation, based on upgrading the GSM network to provide data services faster than 2G GSM), was envisaged to fit in the timeframe within which 3G was still under development, and where 2G could no longer satisfy the users requirements and needs. *High Speed Circuit Switched Data* (HSCSD), with up to 57.6 kbps by using several traffic channels, *General Packet Radio Service* (GPRS), with up to 115 kbps by using additional network elements that allow the Mobile Terminal (MT) to form a packet switched connection through the GSM network to an external packet data network, or even the *Enhanced Data for Global Evolution* (EDGE), with up to 384 kbps by implementing a new air interface modulation (8-PSK) and sophisticated channel coding techniques, were the strongest proposed predecessors for 3G systems.

UMTS data rates, as promised, would make it possible to offer all kinds of new services to 3G users. The most common examples of service are [FCSC02]:

- Speech- and Video-telephony;
- Streaming multimedia;
- Web browsing;
- Location based;
- Short message service (SMS) and Multimedia messaging service (MMS);
- E-Mail;
- File download.

The majority of users will certainly keep, for a rather long time, voice as one of the most requested services. Short messages, as used in 2G, especially by youth, which corresponds to the first data service possible through an MT, will probably tend to disappear in the meantime, as the awakening of multimedia messages seem to attract a lot of people. Internet

access, from everywhere, at any time and at a reasonable price, is one of the most interesting promises that are being announced by many 3G operators; interactivity on the mobile phones is, as well, a wish for many persons. These tempting examples and users' expectations do not summarise the wish list of the majority of people; there are many other services and applications, some even still being studied, which will certainly be disclosed as soon as the commercial use of 3G networks is launched.

UMTS was, from the start, conceived to be a global system, comprising national terrestrial and satellite components, while 2G systems are expected to be used to extend coverage for less demanding services. Roaming from a private cordless or fixed network into a pico- or micro-cellular public network, and then into a wide area macro-cellular network, and, if necessary, into a satellite mobile one, and, in each case, with a minimal break in communication, seems to be the greatest challenge for the current 3G drivers. Contemporary mobile users live in a multi-dimensional world, moving between indoor, outdoor urban and outdoor rural environments, with a degree of mobility ranging from essentially stationary through pedestrian, up to very high vehicular speeds, as shown in Figure 1.2.

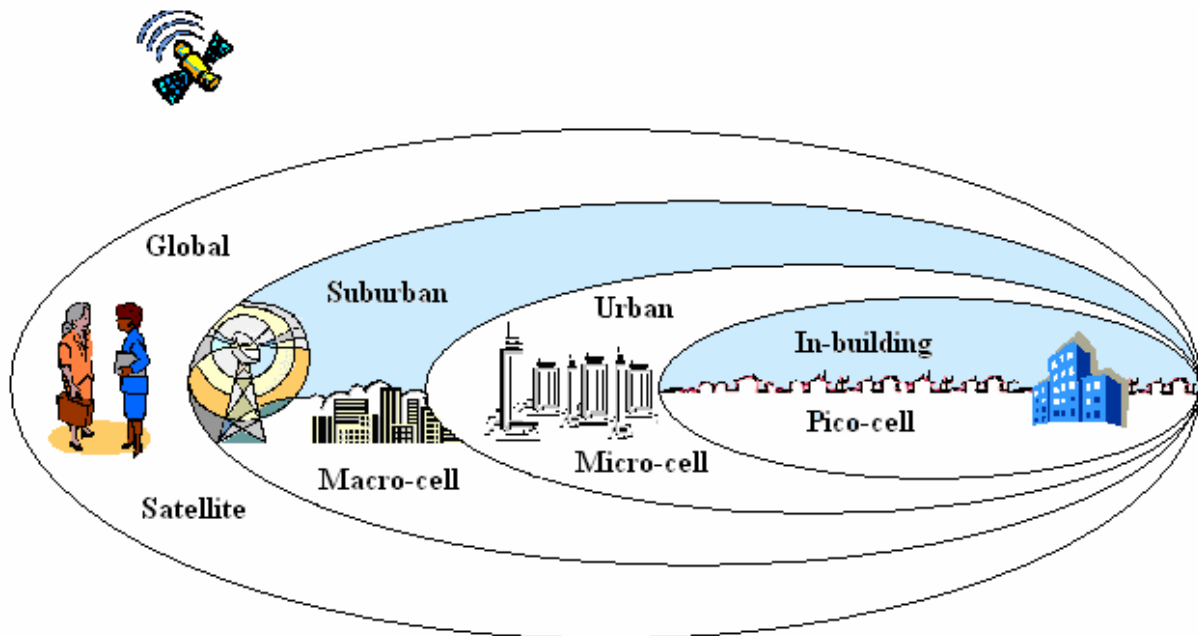


Figure 1.2 – Third generation environment (adapted from [CEPT00]).

This seems to be achievable if boundaries between networks, operators and countries are blurred. Great cooperation is thus required in the future, to enable not only international

1. Introduction

roaming to the demanding 3G users, but also seamless roaming on a national basis, to allow access to diverse environments and/or miscellaneous networks, ruled by distinct technologies, and which will not disappear in the coming years or decades, due to the fact that they complement each other.

After knowing which services may be used by future UMTS subscribers, it becomes important to understand their spatial and temporal incidence; along the day, as well as during a week period, some typical usage behaviours are important to be depicted, as they will absolutely determine the overall system capacity. To characterise the diversity of service usage patterns that UMTS can sustain, it is worthwhile to distinguish between three customer segments [FCSC02]:

- *Business*, with intensive and almost entirely professional use, primarily during working hours;
- *Small Office Home Office (SOHO)*, with both professional and private use, during the day and in the evening;
- *Mass-market*, with low use, staying within flat traffic levels.

Users of distinct customer segments are spread differently over the operational environment, according to their specific characteristics; the amount of calls generated per service may, thus, assume different values per customer segment.

It is known that there is currently very little information, besides marketing estimates, on the amount of traffic that UMTS networks are expected to cope with. It is also difficult to find any information on models that show adequately the behaviour of UMTS users and consequences in terms of system performance, allowing multi-service traffic to be estimated.

Due to the scarce information and experience with 3G systems, it is of great interest to predict the amount of traffic generated by all kinds of users, so that the performance of UMTS networks is studied and a better dimensioning of the systems is carried out. Although voice in 3G may have some similarities with 2G, and the well-known traffic models could still be appropriate if adapted (e.g., the Erlang-B model), the same does not apply for data services over the CDMA technology that is behind the new mobile network's generation, where so many parameters influence the overall system performance and an extensive analysis of the subject is required, before the first accurate results are available.

The idea of studying traffic matters for UMTS is a popular one these days, in view of finding and investigating a model that could deal with both voice and data services; UMTS reality implies that many new aspects, not considered as 2G systems' key issues, are as well accounted for during the planning of activities for 3G, e.g., asymmetric bandwidth requirements and code planning needs.

Several research projects and groups already tackled this very challenging subject, providing some valuable contributions in this area. The IST-MOMENTUM European project [MOME01], for example, developed a considerable amount of work and documentation on the analysis of UMTS system-behaviour and the optimisation of radio network design, through the deployment of new planning methods, with support of system manufacturers, network operators, service providers and university research teams. Additionally, [CaVa02] provided traffic modelling for UMTS, basing many assumptions on criteria resulting from *Population and Housing Census in Portugal*, performed in 2001, and topographic information. Moreover, [Serr02] resulted in a valuable contribution on optimisation of cell radius in UMTS-FDD networks, presenting a new tool that was developed to perform many system calculations, converting its output in the optimum cell radius for a given scenario. More recently, [Dias03] further improved the work presented in [Serr02], by complementing it with specific traffic source models for each service, combining, for various scenarios, different services with distinct call rates and penetration factors, and analysing, as a consequence, the overall system performance. Last, but not least, [HaLH00] proposed an analytical model to investigate the performance of an integrated voice/data mobile network with finite data buffer, which served as a starting point for the current work.

This thesis deals with an analytical traffic model that integrates voice and data services, mixing circuit- and packet-switch, and considering a finite data-buffering capacity. The model is adapted to reflect 3G system characteristics, a detailed study from the system performance perspective being presented. Parameters like users' speed, cell radii, call characteristics (rates and average duration) and capacity to store data, are analysed. To accomplish this ambitious task, some approximations are made, in order to avoid an extreme complexity of the model, allowing it to be practical and functional.

1. Introduction

It is worthwhile saying that the present work will exclusively be focused on the UMTS Frequency Division Duplex (FDD) mode of operation; the standardisation of the Time Division Duplex (TDD) mode is still not completely finished by the corresponding entities. Nevertheless, it is of great importance to consider, as soon as there is any supporting documentation, this mode of operation, as it may improve considerably the efficient use of resources in UMTS, especially for asymmetric services.

The current analytical model introduces an innovative approach when performing the integration of distinct services, voice and data, commonly supported by networks with separate structures, circuit- and packet-switched, allowing, through a single model, the estimation of the traffic amount generated by a UMTS network and its corresponding system performance. The scenarios in terms of number of users per service may be varied; the main system parameters (e.g., call rates, system load, Base Station (BS) power, types of services and corresponding duration) may as well be modified, allowing the model to suit the purposes of the environment particularities and specific UMTS users' characteristics.

The present work is composed of six chapters, including the current one; in addition, four Annexes are appended to this document. In Chapter 2, a brief overview of essential UMTS fundamentals is presented. Chapter 3 provides a general description covering the main particular UMTS aspects that need to be reflected in the traffic model analysis; more specifically, the major coverage, capacity and code planning guidelines are depicted, as well as the most important traffic aspects that are required for the subsequent work. Chapter 4 is devoted to the analytical traffic model; first of all, its formulation is presented in detail; afterwards, all aspects where a model adaptation is required are described; at the end of the chapter, the algorithm as implemented is explained, with the aid of the corresponding detailed flowcharts. In Chapter 5, the output of the analytical traffic model is extensively analysed: the scenarios under study are described, an explanation on the variable channel number is provided, and a comparison of the output of the model with that of other traffic models is performed; finally, the results of the traffic model applied to a single cell are analysed; a multi-cell scenario, where users' movement is not homogeneous, is summarised as well and the motion repercussions depicted. Chapter 6 presents the final conclusions and further suggestions of work to be done in the future. Finally, Annex A contains the formulation of the COST231-Walfisch-Ikegami propagation model, required for the estimation of the cell radius;

Annex B comprises the statistical distributions referred along the thesis; Annexes C and D contain the complete set of results for the two scenarios under study.

2 UMTS fundamentals

2.1 Network architecture

UMTS is divided into Core Network (CN), UMTS Terrestrial Radio Access Network (UTRAN) and User Equipment (UE), [3GPP01a], Figure 2.1.

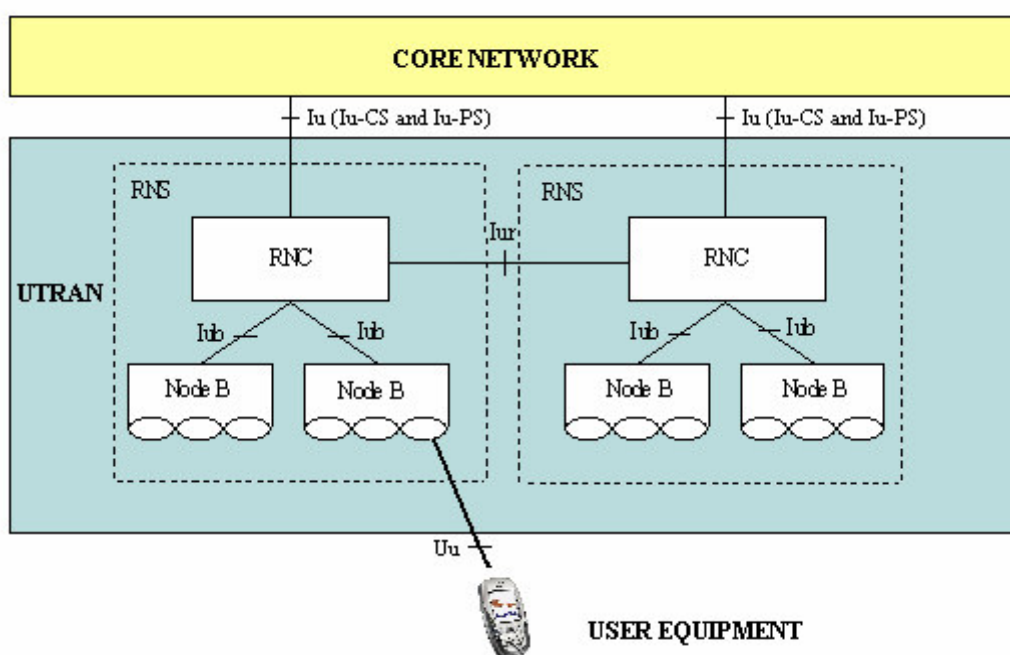


Figure 2.1 – General UMTS network architecture (adapted from [3GPP01a]).

The UMTS architecture was designed in such a way that the CN can be connected to a variety of UTRAN subsystems, which is a step forward when compared to 2G; it is known that GSM operators that had on their network Base Station Subsystems (BSSs) and Network Subsystems (NSSs) from different vendors experienced considerable problems of interoperability. The Iu interface in UMTS was conceived to be an open one, meaning that, in theory at least, different vendors' equipment could be put together, if they fulfilled the standards. This allows the coexistence of different standards, not only 3G, but also the enhanced 2G technologies, and a cost efficient deployment, maximising the use of the GSM/GPRS infrastructure, as well as the implementation of Internet Protocol (IP) technologies.

2. UMTS fundamentals

The UMTS CN consists of two specific domains, the circuit (CS) and the packet (PS) switched ones, the latter being the major novelty introduced by UMTS when compared with 2G systems, which were clearly CS oriented at the beginning. The separation between the CS and PS domains inside the CN allows a simpler evolution from GSM/GPRS, with lower risks, an earlier availability and service continuity. On the other hand, operators need to build and manage two different networks, perform separate engineering and dimensioning, and invest on two distinct infrastructures. CN functions may be summarised as follows:

- Switching;
- Service availability;
- Transmission of user traffic between UTRAN(s) and/or fixed network(s);
- Mobility management;
- Operations, Administration and Maintenance.

The UTRAN consists of one or several Radio Network Subsystems (RNSs) connected to the CN through the Iu interface. Each RNS contains one Radio Network Controller (RNC) and one or several Node Bs. The RNC owns and controls the radio resources in its domain, and acts as the service access point for all services that UTRAN provides to the CN; the Node B corresponds to the radio BS and converts the data flow between the Iub and the Uu interfaces. The major difference in the radio access network between GSM and UMTS corresponds to the fact that in UMTS, the RNC (the counterpart of the Base Station Controller (BSC) in GSM) is partly in charge of the mobility management, whereas the BSC is not responsible for this function. UTRAN functions may be summarised as follows:

- Provision of radio coverage;
- System access control;
- Security and privacy;
- Handover;
- Radio resource management and control.

The UE consists of two parts: the MT, which corresponds to the radio terminal used for radio communication over the Uu air interface, and the UMTS Subscriber Identity Module (USIM), the GSM equivalent smart card, that holds the subscriber identity, performs authentication algorithms, stores authentication and encryption keys, etc. There are no major differences between the 2G and 3G MTs, except for the fact that 3G terminals are expected to have a

completely new layout, with a tempting and attractive monitor to encourage data calls. UE functions may be summarised as follows:

- Display of the user interface;
- Holding of the authentication algorithms and keys;
- User and termination of the air interface;
- Application platform.

There are four major interfaces defined in UMTS, as presented in Figure 2.1:

- **Iu**
The Iu interface connects the CN to the UTRAN and is split into two parts: Iu-CS, the interface between the RNC and the CS part of the CN, and Iu-PS, the interface between the RNC and the PS part of the CN.
- **Iur**
The Iur interface connects different RNCs, allowing soft Handover (HO) between RNCs.
- **Iub**
The Iub interface connects the Node B and the RNC. Contrarily to GSM, this interface is envisaged to be fully open in UMTS, thus, more competition is expected.
- **Uu**
The Uu interface is the WCDMA radio interface within UMTS, being the interface through which the UE accesses the fixed part of the network.

2.2 Air interface

The UMTS air interface supports two transmission modes of operation [HoTo01]: FDD and TDD.

The FDD mode uses a pair of 5 MHz band carrier frequencies, one for the uplink (UL) and another for the downlink (DL), and uses wideband Direct Sequence Code Division Multiple Access (DS-SS-CDMA), also known as WCDMA. This operation mode is suited for applications in macro- and micro-cell environments, with typical data rates up to 384 kbps and high mobility (but not both at the same time).

2. UMTS fundamentals

The TDD mode uses a single 5 MHz band carrier frequency, shared between the up- and the downlink connections, being the result of the combination of TDMA and CDMA, and exploiting spreading as part of its CDMA component. This mode of operation is advantageous for public micro- and pico-cell environments, since it facilitates the efficient use of the unpaired spectrum and supports data rates up to 2 Mbps. Therefore, the TDD mode is suited for environments with high traffic densities and indoor coverage, where applications require high data rates and tend to create asymmetric traffic.

The combined deployment of the FDD and TDD modes will enable a more efficient use of the available spectrum, by considering the advantages and avoiding the disadvantages of each of these modes. Nevertheless, there are still some ongoing standardisation activities for definition of the UMTS TDD mode. It is expected that the first TDD networks will appear some two years after the FDD mode is put into operation.

As shown in Figure 2.2, the amount of spectrum allocated in Europe to the FDD and TDD modes, as well as to its satellite component, corresponds to:

- 2×60 MHz of paired spectrum for use in FDD mode;
- 35 MHz of unpaired spectrum for use in TDD mode;
- 2×30 MHz for use in the satellite component.

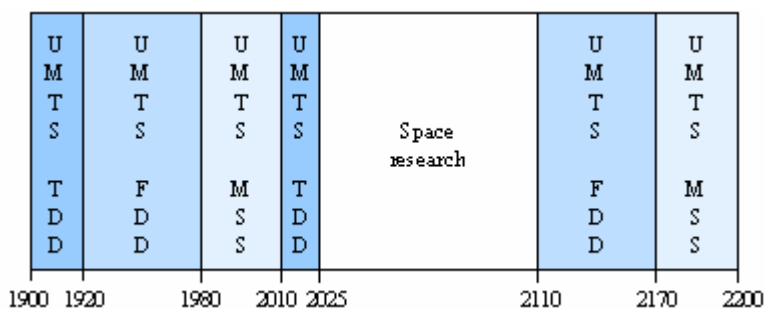


Figure 2.2 – UMTS spectrum allocations in Europe (based on [CEPT02]).

In Portugal, the terrestrial component of the available spectrum for UMTS is split among three operators that were awarded a 3G license. Each of the operators owns, for the 15-year period of duration of its license, 2×20 MHz of paired spectrum (FDD) and one additional carrier frequency, 5 MHz, of unpaired spectrum (TDD).

There are three different channel types for data transmission and signalling in the UTRAN FDD mode [HoTo01]:

- **Logical channels**, interface between Layers 3 and 2 of the Open Systems Interconnection (OSI) protocol stack, i.e., between Radio Link Control (RLC) and Medium Access Control (MAC) layers. Logical channels specify “which” data is to be transferred. These channels are generally classified into two groups: Traffic channels (e.g., DTCH and CTCH) for the transfer of user plane information, and Control channels (e.g., BCCH, PCCH, DCCH, CCCH) for the transfer of control plane information.
- **Transport channels**, interface between Layers 2 and 1 of the OSI protocol stack, i.e., between MAC and Physical (PHY) layers. Transport channels specify “how” data is transferred over the radio interface. Dedicated channels are one type of Transport channel (e.g., UL / DL DCH); they are UE specific, assigned on a per call basis, and are kept only as long as the call remains. Common channels (e.g., FACH, RACH, CPCH) and Shared channels (e.g., DSCH and USCH) are the other types of Transport channels, and they are cell specific.
- **Physical Channels**, Layer 1 of the OSI protocol stack, i.e., between the Physical layers at the Node B and UE. Physical channels specify “where” data is transferred. On the UL, there are Dedicated physical channels (e.g., DPCCH, DPDCH) and Common physical channels (e.g., PRACH, PCPCH); on the DL, the division is also done between Dedicated (e.g., DL DPCH) and Common physical channels (e.g., CPICH, P-CCPCH, S-CCPCH, SCH, PDSCH, AICH, PICH).

Physical channels are defined by a specific carrier frequency, scrambling and channelisation codes, time start and stop (giving a duration) and, on UL, relative phase (0 or $\pi/2$). Time durations are defined by start and stop instants, measured in integer multiples of chips. Physical channels will be time multiplexed by using:

- (i) **radio frames**, which consist of 15 slots, with a duration of 10 ms; the length of a radio frame corresponds to 38 400 chips;
- (ii) **slot**, a duration that consists of fields containing bits; the length of a slot corresponds to 2 560 chips.

A detailed description of the logical, transport and physical channels, their individual frame structures, as well as the mapping of logical onto transport channels, and these onto physical

2. UMTS fundamentals

channels, may be found in [3GPP02b] or in [HoTo01]. Reference [3GPP02c] presents this same information, but for the TDD mode of operation.

It is mentioned above that physical channels are defined, among others, by specific channelisation and scrambling codes. In fact, these are the two types of codes used in WCDMA networks. Channelisation codes are used to separate channels from a single cell or terminal; they allow multiple users in each cell to transmit on the same channel. Scrambling codes are used to separate cells and terminals from each other; they allow multiple BSs on the same channel and each user in a cell uses the same scrambling code.

Table 2.1 lists the main characteristics of both channelisation and scrambling codes. Further detailed information may be found in 3GPP recommendations [3GPP99a], [3GPP01b] and [3GPP00a].

Table 2.1 – Main characteristics of channelisation and scrambling codes (based on [HoTo01]).

	Channelisation codes	Scrambling codes
Uplink	Separates channels (physical and control data) from same terminal	Separates terminals in one cell
Downlink	Separates connections to different users in a same cell	Separates cells
Type of codes	Orthogonal Variable Spreading Factor (OVSF) codes	Gold codes
Length	4–256 chips in UL 4–512 chips in DL	38 400 chips
Duration	1.04 – 133.34 μ s in UL 1.04 – 66.67 μ s in DL	10 ms
Number of codes available	Equal to the spreading factor: 4 ... 256 in the UL 4 ... 512 in the DL	Several million in the UL (no. of users) and 512 in the DL (no. of cells)
Spreading factor (SF)	Yes, increases bandwidth	No, does not change bandwidth
Orthogonality of codes	Yes	No (not synchronised to each other at the receiver)

While in GSM there was the need to plan the frequencies to be used in each cell, in order to allow efficient re-use of spectrum and simultaneously avoid interference to grow, in UMTS that is not required – each 5 MHz carrier will be used in each cell, thus, following a 1/1 pattern. Nevertheless, scrambling codes need to be planned to conveniently separate the BSs.

2.3 Radio resource management

The use of the air interface resources is a Radio Resource Management (RRM) task of extreme importance, which has strong impact on the fulfilment of the Quality of Service (QoS) requirements. There are three basic aspects that need to be considered: power control, admission control, and handover.

The power control mechanism in UMTS is not focused on selecting *a priori* a power level to be used by the transmitter. Instead, it is based on a quality level (the Signal to Interference Ratio (SIR)) that has to be achieved by transmitting with an appropriate power level; if the SIR is too low, the received signal cannot be de-spread and reconstructed any more. Since all users are transmitting simultaneously, the noise level depends, among others, on the number of users. A good power control algorithm will optimise the usage of the radio resources, thus, increase system capacity.

There are 2 types of power control:

- **Open Loop Power control:** it consists in setting the transmit power by measuring the path loss of the direct link via the received signal and adding the interference level of the Node B.
- **Closed Loop Power control:** it is intended to reduce interference in the system by maintaining the quality of air interface communication as close as possible to the minimum quality required for the type of service requested by the user.

The closed loop power control consists of two parts, an inner loop and an outer one:

- The inner part of the closed loop power control is also called fast power control (at 1500 Hz), since it is intended to respond to fast variations in propagation characteristics of the radio link (e.g., fast-fading at slow or medium speeds) as well as rapidly changing interference conditions. The power control loop is closed because the receiver of the radio

2. UMTS fundamentals

signal provides commands back to the sender to adjust its transmitted power. Fast power control is considered to be a function of the UTRA physical layer, and it is performed in both the Node B and the UE.

- The outer loop power control algorithm determines the parameter level used by Layer 1 to perform the inner loop power control decisions. The outer loop control function manages the inner loop process by setting the SIR target parameter and the power up/down step sizes. The frequency of the outer loop power control is typically in the range of 10 – 100 Hz.

Admission control (restrict access to more voice / data calls) and congestion control (either by lowering bit rates of services, or by carrying out intra-frequency handovers, or even disconnecting calls) need to be performed in order to avoid the increase of interference. Users located on the edge of a cell are those who require from the corresponding BS more power, and, consequently, those who should be pushed out of the cell effective coverage area. By powering off the major interferers, an immediate interference decrease is achieved, the transmitted power from the BS may consequently be reduced and the system becomes more stable – more users will be further allowed to enter the cell. This is known as the cell breathing phenomena, i.e., a reduction / increase on the size of the cell to control interference.

Handovers are mainly required when MTs are moving around. Users may be served in other cells in a more efficient way (like lower transmission power, or less interference), nevertheless, handovers might also be performed for other reasons, such as system load control. There are three categories of handovers:

- **Hard handover** means that all the old radio links in the UE are removed before the new radio links are established, and they can be seamless, meaning that the handover is not perceptible to the user. In practice a handover that requires a change of the carrier frequency (inter-frequency handover) is always performed as hard handover.
- **Soft handover** means that the radio links are added and removed in a way that the UE always keeps at least one radio link to the UTRAN, and it is performed by means of macro diversity, which refers to the condition that several radio links are active at the same time.
- **Softer handover** is a special case of soft handover, where the radio links that are added and removed belong to the same Node B (i.e., the site of co-located BSs from which several sector-cells are served). In softer handover, macro diversity with maximum ratio

combining can be performed in the Node B, whereas generally in soft handover on the DL, macro diversity with selection combining is applied.

2.4 Services and applications

While estimating both coverage and capacity of a UMTS network, operators aim at dimensioning the equipment to provide services and applications that meet users' needs. The notion of "service" is used within the UMTS world with a variety of meanings: at a first glance, one would associate the word "service" to the user application, like web-browsing or e-mail. Being more rigorous, and depicting the definitions presented in [3GPP03], it may be said that a service is a component of the portfolio of choices offered by service providers to a user, whereas an application is a service enabler deployed by service providers, manufacturers or users. SMS is an example of a mobile service, while the ability to make flight bookings via a specific provider corresponds to an example of a mobile application.

Figure 2.3 represents an example of choices of such services and applications, as defined by the UMTS Forum [UMTS01].

Services and applications may be grouped into different classes or categories, according to their own characteristics. The classifications presented by well known standardisation bodies, namely ITU-T, 3GPP, ETSI and UMTS Forum, are summarised in [FMSC01]. Taking into consideration the fact that the leading UMTS vendors are basing their equipment deployment in 3GPP standards, the classification of services considered in this thesis is the one as proposed by 3GPP.

The UMTS drivers will be responsible for providing to the users the most adequate set of services and applications, by making the difference not only from the technical / quality point of view, but also by considering the inherent economical aspects. UMTS is expected to offer the user the provision of a contracted end-to-end QoS (throughput, transfer delay, data error); it will be possible to negotiate and renegotiate the characteristics of a bearer service at session or connection establishment, and during ongoing sessions or connections.

2. UMTS fundamentals

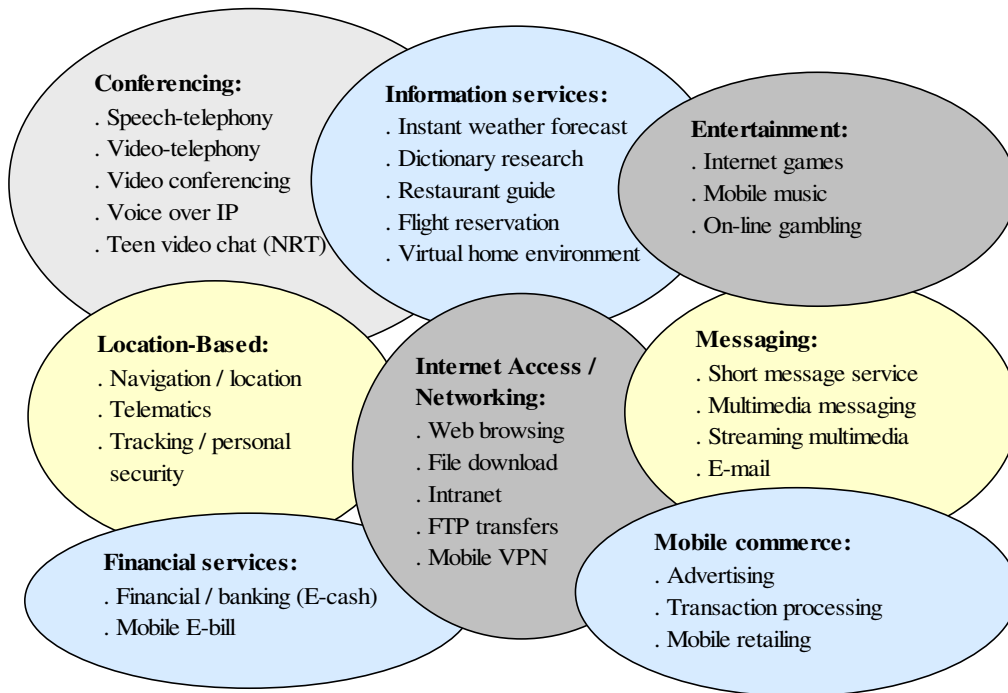


Figure 2.3 – Example of services and applications in UMTS (adapted from [UMTS01]).

From an end-user and application points of view, four major traffic classes with different QoS requirements can be identified. The main characteristics of these traffic classes are listed in Table 2.2.

Each application is always associated to a certain Radio Access Bearer (RAB). When the terminal is being activated, the QoS profile of the application is sent and a comparison of the attributes values with the user profile as registered in the Home Location Register (HLR) is done, before a radio bearer is either established or not. The radio bearer attributes per traffic class are presented in Table 2.3.

2.5 Network dimensioning

Network dimensioning is a process through which an initial estimation of the amount of network equipment and possible configurations is determined. Key parameters of this dimensioning phase will be coverage and capacity planning.

Table 2.2 – UMTS traffic classes (extracted from [3GPP02a]).

Traffic class	Conversational	Streaming	Interactive	Background
Type of traffic	Real Time	Real Time	Best Effort	Best Effort
Fundamental characteristics	- Preserve time relation (variation) between information entities of the stream - Conversational pattern (stringent and low delay)	- Preserve time relation (variation) between information entities of the stream	- Request response pattern - Preserve payload content	- Destination is not expecting the data within a certain time - Preserve payload content
Transfer delay requirements	$\ll 1$ s	< 1 s	< 10 s	> 10 s
Examples of the application	Voice, video telephony, video games	Multimedia, video on demand, webcast	Web browsing, network gaming, Telnet	Email delivery, SMS, Downloading of databases

With respect to **coverage planning**, there are four basic aspects that require analysis: *coverage regions*, *area type information*, *propagation conditions*, and *link budget*. The *coverage region* is either a licence obligation or an operator's strategic decision. The *area type information* results from both geographic and demographic information. The *propagation conditions* need to be completely identified, in order to avoid unexpected propagation behaviours and results. By knowing those, the related parameters may be adjusted in the planning tools and the channel model used within its validation limits. *Link budgets* are used to calculate maximum propagation losses (detailed examples of link budget calculations may be found in [HoTo01]). The main inputs required are:

- Interference margin (inter- and intra-cell);
- Fast-fading margin;
- Soft handover gain;
- MT characteristics (maximum transmit power, antenna gain, body loss);
- BS characteristics (noise figure, antenna gain, required Signal-to-Noise Ratio (SNR), cable losses);
- Assumptions on cell loading and applications (services) offered.

2. UMTS fundamentals

Table 2.3 – Radio bearer attributes per UMTS QoS class (as defined in [3GPP02a]).

Traffic class	Conversational	Streaming	Interactive	Background
Maximum bit rate	X	X	X	X
Delivery order	X	X	X	X
Maximum Service Data Unit (SDU) size	X	X	X	X
SDU format information	X	X		
SDU error ratio	X	X	X	X
Residual bit error ratio	X	X	X	X
Delivery of erroneous SDUs	X	X	X	X
Transfer delay	X	X		
Guaranteed bit rate	X	X		
Traffic handling priority			X	
Allocation/Retention priority	X	X	X	X

The obtained path losses are converted into cell radiuses for different environments, from which the typical coverage areas may be derived, as well as a rough estimation of number of sites per environment area.

After predicting the coverage area, the complex activity of site acquisition – field activity and site negotiation – needs to be performed. Sometimes, the search area needs to be enlarged due to the non-possibility to position the BS in the most suitable site location. After having the definitive positions of the BSs, new predictions of the coverage areas may be obtained from the planning tools, and, if any further parameter adjustment is required, network optimisation will follow.

In terms of **capacity planning**, three main aspects need to be analysed: *spectrum availability*, *subscriber growth forecast*, *traffic density information*. The *spectrum available* in Portugal corresponds to 4 paired carriers (FDD) and 1 unpaired carrier (TDD) per UMTS operator, as mentioned in Section 2.2. Operators may start by using exclusively one FDD carrier all over

the network, as long as the generated traffic does not increase, or already introduce more spectrum right from the beginning. FDD carriers may be used on a hierarchical cell structure, covering umbrella, macro-, micro- or pico-cells, while TDD spectrum is mainly planned to cover hot spot areas, where low mobility is necessary, but capacity for asymmetric traffic with high bit rates is required. *Subscriber growth forecasts* result from marketing projections. *Traffic density information* for UMTS networks is still non-existing, the currently required figures being estimated as long as real values are not available.

Capacity dimensioning in UMTS is a very complex task. It depends not only on the three aspects mentioned above, but also on other parameters like:

- Interference and noise (depend on cell loading, frequency reuse and sectorisation efficiency);
- UL pole capacity (depends on the mixed service rates considered – target SNR and processing gain);
- DL capacity and transmitted Equivalent Isotropic Radiated Power (EIRP) (depend on the link balance and on the power per traffic channel).

It will basically correspond to the number of active links that achieve, in a given coverage area and at a specific time instant, the QoS requirements in an antenna sector.

Capacity dimensioning in GSM is a completely different task. The area to be covered is overlaid with a regular cell pattern, the available spectrum (40 frequencies in the 900 MHz and another 40 in the 1800 MHz band, per operator, in Portugal) is distributed among a group of cells (cluster) and then repeated all over the network, bearing in mind that a good compromise between minimisation of adjacent channel interference and maximisation of traffic capacity has to be attained. When more capacity is required, a couple of additional actions can be undertaken, if no more spectrum is available: change of cell pattern, cell splitting, frequency borrowing from neighbouring cells, use of overlaid / underlaid cells, or cell sectorisation. System capacity depends mainly on the available spectrum and on the interference caused by adjacent channels, and can easily be estimated.

There is almost no experience with data over CDMA networks, and the user's behaviour is also still unknown. Before 3G operators are able to collect real values that allow more

2. UMTS fundamentals

consolidated conclusions, two main aspects may be considered for the estimation of traffic figures required for network dimensioning:

- *Prediction of the total number of users per service type and per geographical area*

It will not be enough to know the traffic per cell, as it was the case in GSM: in UMTS, it is even required to know the traffic distribution inside the cell, since it affects intra-cell interference. Rough traffic distributions may be obtained by using district information (where, among others, population, income and business are known) and clutters (used to distribute traffic within districts).

- *Prediction of the usage for each service type*

Up to now, the user profile and his/her needs in terms of service types required were obtained through marketing studies. It is expected that, if an attractive set of applications is offered to the user at a reasonable price, an increase on the use of 3G may occur. The creation of new services and user needs will be a major point in the success of the introduction of 3G, although some uncertainty on the real behaviour of the 3G users is still present.

Among others, the MT speed, multipath channel profile, power control, handover, bit rate and type of services, play a more important role in WCDMA systems than in 2G TDMA/FDMA systems. A growth on the number of users, or simply on the transmission data rates within a certain coverage area, is power demanding and may cause an increase in the overall interference, meaning that other users (especially those more distant from the BS) may see their requirements affected / restricted.

As in WCDMA all users share the same interference resources in the air interface, they cannot be analysed independently: each user influences the others and causes others' transmission powers to change. Therefore, the whole prediction process required to complete the UMTS radio network planning has to be done iteratively, until transmission powers stabilise.

The traffic models that shall be considered need to be able to reflect the various characteristic features of the upcoming UMTS services, namely real-time and non-real-time. Further analysis on the identification of adequate traffic models for UMTS, considering voice and data services over CS and PS domains, as well as a description of the interdependent

parameters, like system capacity, coverage and interference, are done in detail in the following chapter.

3 Traffic analysis

3.1 Coverage estimation

In UMTS, coverage, capacity and QoS planning are items that depend on each other and support the overall network planning process. The cell radius in UMTS is a factor that depends, among others, on the traffic allowed inside the cell, meaning that a complex cell range analysis is required in order to achieve an accurate dimensioning (equipment and configuration) of the network.

The first key element required for this complex radio network planning process is the link budget estimation – it is used to derive the maximum path loss allowed between the UE and the Node B, leading to a first indicative maximum cell radius that meets the quality objectives defined in advance, and allows a rough estimation of the required network elements (CN elements, RNCs, Node Bs, and others). Operators' requirements, like areas to be covered, subscriber and traffic forecasts, throughput, blocking probability (for CS) or maximum allowed delay or loss per type of service (for PS), are inputs that need to be clearly specified prior to the final dimensioning of the network.

Three distinct situations are evaluated hereafter for service rates at 12.2, 64, 128 and 384 kbps:

- **Vehicular:** MTs moving at 120 km/h on suburban environments, where users are located inside cars (in-car loss and exclusive data terminals considered); no fast-fading margin will be taken into account due to the impossibility to compensate, at that speed, for the fast power control;
- **Pedestrian:** MTs moving at 3 km/h on metropolitan centres / large cities, where users walk around on streets;
- **Indoor:** MTs moving as well at 3 km/h on metropolitan centres / large cities, but located inside buildings – an additional building penetration margin is considered for this particular situation, as it is assumed that coverage is provided by outdoor BSs.

3. Traffic analysis

Both UL and DL link budgets are calculated, aiming at concluding if there is any of these connections that systematically impose a restriction on the coverage area (radius of the cell).

The allowed propagation loss for the cell range is given by [HoTo01]:

$$L_p[\text{dB}] = P_t[\text{dBm}] + G_t[\text{dBi}] - L_c[\text{dB}] - P_{r\text{ min}}[\text{dBm}] + G_r[\text{dBi}] + G_{div}[\text{dB}] + G_{SHO}[\text{dB}] - M_{body-loss}[\text{dB}] - M_{log-normal}[\text{dB}] - M_{fast-fading}[\text{dB}] - L_{in-car}[\text{dB}] - L_{building}[\text{dB}] \quad (3.1)$$

where:

- P_t Transmission power
- G_t Antenna gain at the transmission
- L_c Cable losses in the BS
- $P_{r\text{ min}}$ Receiver sensitivity
- G_r Antenna gain at the reception
- G_{div} Diversity gain
- G_{SHO} Soft-handover gain
- $M_{body-loss}$ Body loss margin
- $M_{log-normal}$ Log-normal fading margin
- $M_{fast-fading}$ Fast-fading margin
- L_{in-car} In-car loss
- $L_{building}$ Building penetration loss

The resulting propagation losses obtained on both UL and DL connections are the input values required for the cell radius calculations. An appropriate propagation model is selected and, consequently, the maximum cell radius is derived.

As with GSM, the user interfaces to the RNCs are not completely specified within the 3GPP standards, meaning that distinct vendors may use slightly different parameter settings. The particular UMTS link budget parameter values used on the link budget calculations are summarised hereafter.

Both UMTS MT and BS characteristics differ from those used in GSM. The assumptions presented in Table 3.1 are recommended by the most well-known vendors, which are used in the next section for the link budget calculations:

Table 3.1 – MTs and BSs assumptions (based on [HoTo01]).

Mobile Terminals	Speech terminals	Data terminals
Maximum transmission power (P_t [dBm])	21	24
Antenna gain (G_t [dBi] or G_r [dBi])	0	2
Body loss margin ($M_{body-loss}$ [dB])	3	0
Noise figure (F_N [dB])	7	7
Base Stations		
Maximum transmission power (P_t [dBm])		43
Antenna gain (G_r [dBi] or G_t [dBi]) (3-sector BS)		18
Cable losses (L_c [dB])		2
Noise figure (F_N [dB])		5

There are four power classes that define the nominal UE maximum output power, P_t , as specified in [3GPP01c]: class 1 with 33 dBm, class 2 with 27 dBm, class 3 with 24 dBm, and class 4 with 21 dBm. Classes 3 (for data services) and 4 (for voice) will be the ones to be considered, as they correspond to the most stringent values and are expected to correspond to the majority of the terminals that will enter the market.

The MT antenna gain, G_t or G_r , considered in [HoTo01] is 0 dBi for terminals with data and voice capabilities, and 2 dBi for MT exclusively oriented towards data services (where different antennas, with slightly higher gains, may be built in).

A 3 dB body loss margin, $M_{body-loss}$, is assumed when the MT is used for voice services, as its position will mainly be close to the user's head and the signal absorption is higher. When this same terminal is used for data services, it is assumed that the user is holding it on his/her hand, body absorption being negligible.

A 5 dB noise figure, F_N , is considered for the BS (parameter that corresponds to the reception level above the noise level), whereas 7 dB is assumed for the MT noise figure.

The ratio E_b/N_0 , energy per bit over noise spectral density, corresponds to another parameter that needs to be considered, which is commonly obtained through complex simulations; the values used for the link budget calculations are extracted from [FCSC02], Table 3.2.

3. Traffic analysis

Table 3.2 – E_b/N_0 used for link budget calculations (extracted from [FCSC02]).

E_b/N_0 [dB]	3 km/h		120 km/h	
	UL	DL	UL	DL
12.2 kbps	6.8	10.4	5.0	6.2
64 kbps	3.8	6.2	2.8	4.4
128 kbps	3.4	5.0	2.4	4.2
384 kbps	3.8	4.6	2.8	4.2

Nevertheless, these values should be dynamically obtained, as they depend on numerous factors, like type of service, bit rate, multipath profile, mobile speed, receiver algorithms and BS antenna structure.

The receiver sensitivity, $P_{r \min}$, which corresponds to the minimum signal required in the reception, is given by [HoTo01]:

$$P_{r \min [\text{dBm}]} = N_{rf [\text{dBm/Hz}]} + 10 \log(R_{c [\text{chip/s}]}) - 10 \log\left(\frac{R_{c [\text{chip/s}]} }{R_b [\text{bps}]}\right) + \frac{E_b}{N_0 [\text{dB}]} + M_{int [\text{dB}]} \quad (3.2)$$

where:

- N_{rf} Noise spectral density of the MT receiver front-end

$$N_{rf [\text{dBm}]} = -174.0_{[\text{dBm}]} + F_N [\text{dB}] \quad (3.3)$$

- R_c WCDMA chip rate ($R_c = 3.84$ Mchip/s)
- R_b Service bit rate
- M_{int} Interference margin

An interference margin, M_{int} , is considered to account for the increase in the interference levels within the cell due to other users. It introduces a way to take into consideration the loading of the cell in the link budget:

$$M_{int[\text{dB}]} = -10 \log(1 - \eta) \quad (3.4)$$

where:

- η Cell load

When the cell loading increases, a larger margin is needed in the UL and, consequently, a smaller cell radius is obtained. Typical values for the interference margin are of the order of 3 dB, corresponding to 50 % loading.

A diversity gain, G_{div} , is included as well in the estimation of the propagation loss for the cell range, in case diversity is used on the reception of the signal. This is a feature that may be implemented on the BS.

The soft handover gain, G_{SHO} , takes into account the diversity gain achieved during soft handover conditions: the receiver is allowed to compensate for both slow- and fast-fadings, since it receives information arriving from different BSs with almost uncorrelated paths. The typical values found in the literature for this parameter range between 2 and 4 dB. A 3 dB value will be considered for fast moving MTs, while 1 dB less is assumed for lower speeds.

The values of the log-normal fading margin, $M_{log-normal}$, considered in the link budget calculations are the ones used in [HoTo01]: 7.3 dB when 95 % coverage probability is assumed, and 4.2 dB when an 80 % coverage probability is considered. The coverage probability corresponds to the percentage of area within the cell radius where the received signal level exceeds a certain threshold. This parameter is related to the quality of radio planning and radio network capacity, and depends on the variation of non-controlled propagation elements: shadowing, penetration characteristics, fast-fading, different environment, etc. The probability of coverage at the cell edge is one of the parameters that define the QoS. For link budget purposes, the following thresholds are assumed:

- 95 % of coverage probability for outdoor scenarios;
- 80 % of coverage probability for indoor scenarios served by outdoor BSs.

The fast-fading margin, $M_{fast-fading}$, is included to account for the additional headroom needed in the MT transmission power to maintain the adequate power level. This is a consequence of the fast power control used in UMTS, and applies specifically to slow moving pedestrian

3. Traffic analysis

mobiles. Typical values for this parameter range between 2 and 5 dB; a 4 dB margin is assumed for the scenarios where a slow moving MT is considered.

Penetration losses account for the type of environment in which MTs operate. The most typical scenarios and corresponding loss values are:

- In-car (L_{in-car}), 8 dB
- Indoor ($L_{building}$), 15 dB

Measurements for the local conditions are usually recommended, in order to use a good estimate of the penetration losses in each environment type.

All these parameters are directly or indirectly used in link budget calculations that need to be performed. Afterwards, an appropriate propagation model needs to be selected, in order to describe signal propagation in particular conditions (namely for specific environments, frequency bands, range of radius, and BS and MT heights). The maximum allowed propagation loss calculated through (3.1) is converted by the propagation model formulation into the maximum cell range, i.e., the area that may be served by a BS. The well-known propagation models COST231-Okumura-Hata or COST231-Walfisch-Ikegami might be applied.

The COST231-Okumura-Hata [DaCo99] propagation model, an empirical prediction method for signal strength calculation, results from extensive series of measurements in and around Tokyo at frequencies up to 1 920 MHz. Its applicability is nevertheless restricted to frequencies up to 1 500 MHz. COST231 has extended this model to the frequency band [1 500, 2 000] MHz by analysing Okumura's propagation curves in the upper frequency band. This model is usually used in macro-cells.

The COST231-Walfisch-Ikegami [DaCo99] model turns out to be a more complex model than COST231-Okumura-Hata's, as it allows improved path loss estimation by considering more data describing the urban environments: building heights and separation, road widths and orientation with respect to the direct radio path. This model is based on a deterministic approach, and it may distinguish between line-of-sight and non-line-of-sight situations, being usually applied to micro-cells.

Both propagation models should be calibrated for the environments where they are to be used; after analysing the measurement results, a clutter correction factor may be required. Taking into consideration the characteristics and applicability conditions of each of the above mentioned propagation models, it was considered adequate to use the COST231-Walfisch-Ikegami model for all scenarios (its complete formulation, as well as the ranges over which these models are applicable, can be found in Annex A), since it is the one that has a lower error in urban centre scenarios, where the larger variety of services use is expected.

The result of the application of the COST231-Walfisch-Ikegami model, in conjunction with the allowed propagation losses obtained through (3.1), leads to the maximum cell radius on both UL and DL connections as presented in Figure 3.1.

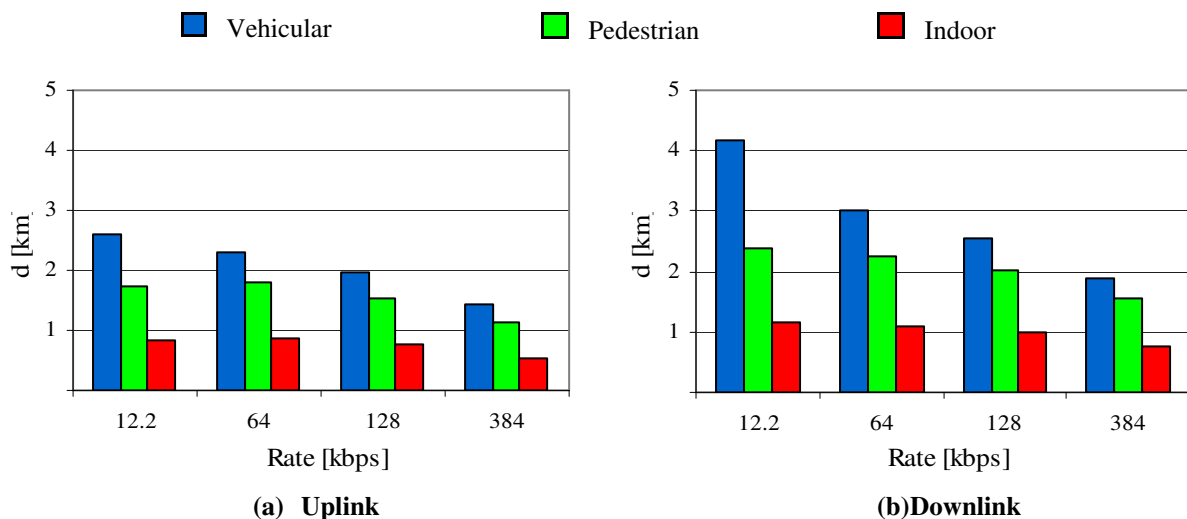


Figure 3.1 – Cell radius.

One of the major conclusions that may be drawn after analysing the results presented above is that macro-cell coverage is UL limited. This is basically due to the fact that the MT's power level is restricted to 21 dBm for voice, or 24 dBm for data terminals, instead of the 43 dBm maximum BS transmitted power on the DL. Consequently, the coverage planning study does not require the DL coverage information, but should consider exclusively its UL connection characteristics, and, especially, its constraints.

Another fact that may be pointed out is the direct relationship between data rate and cell radius: considering a fixed load / interference on the cell, as the service rates increase, the

3. Traffic analysis

radius of the cell shrinks. One clear exception exists for the 12.2 kbps data rate for pedestrian and indoor users: on the UL, a maximum transmitted power of 21 dBm is considered, and a MT antenna gain of 0 dBi is taken, together with an additional loss due to the body absorption, leading to a slightly smaller cell radius than the obtained for the remaining service rates considered; on the DL, the E_b/N_0 value for the pedestrian and indoor scenarios is considerably higher than the one used for the larger bit rates, leading as well to a cell radius smaller than the ones obtained for the bit rate immediately higher. In a real network, the dependence of the cell radius on the data rates is one of the aspects that should be closely monitored, as new service demands may need to be kept on hold in order to avoid the “cell breathing” phenomena to occur.

The indoor scenarios served by outdoor BSs are the most demanding ones in terms of coverage. In order to avoid an excessive number of outdoor BSs, which reverts into an extremely high investment, it is common to perform the coverage planning analysis solely for outdoor environments, considering then additional indoor BSs for some indoor areas, namely airports, exhibitions / fairs halls, business areas, shopping centres, etc..

The section that follows is dedicated to a capacity analysis, whose results need to be weighed against the ones obtained under the current section, and further conclusions are drawn.

3.2 Capacity estimation

Another fundamental element required for the network planning process is the estimation of the maximum number of simultaneous users that a cell can support, i.e., the system capacity. The frequency reuse in WCDMA systems is 1, and only one 5 MHz carrier is considered here. The system is proven to be typically interference-limited by the air interface; thus, the amount of interference / capacity per cell must be obtained.

A capacity study on both UL and DL is presented hereafter, aiming at identifying if any of the connections is more restrictive than the other, and extracting the limiting factors for further calculations and comparison with the coverage analysis performed earlier. The capacity per cell is therefore dependent on the UL and DL load factors.

The UL load factor as defined in [HoTo01] is given by:

$$\eta_{UL} = (1+i) \cdot \sum_{j=1}^N \frac{1}{1 + \frac{R_c / R_{b_j}}{(E_b / N_0)_j} \cdot \frac{1}{v_j}} \quad (3.5)$$

where:

- i Other cell to own interference ratio, seen by the BS (typically 65 %)
- N Number of users per cell
- R_{b_j} Service bit rate of user j (depends on the service)
- v_j Activity factor of user j at physical level (0.67 for speech and 1 for data)

The system pole capacity in the UL corresponds to the theoretical limit for the number of MTs that a cell can cope with. At this limit, the interference level in the system is infinite and consequently the coverage is reduced to zero. By grouping together the users into the offered RABs, the pole capacity for the n^{th} RAB is thus obtained when assuming an UL load factor close to 100 %:

$$N_{pole_{UL_n}} = \frac{1 + \frac{R_c / R_n}{(E_b / N_0)_n} \cdot \frac{1}{v_n}}{(1+i)} \quad (3.6)$$

where:

- R_n Service bit rate of the n^{th} RAB (12.2, 64, 128 or 384 kbps).

The transmitted power in the UL leads to an increase on the interference to adjacent cells, whereas the power received by MTs is considered as interference for all other users in the same cell.

The more loaded the system is, the higher is the generated interference (as shown through (3.4)). This implies that the receiver noise floor is greater in a highly loaded system than in an unloaded one, as results from (3.2).

Another aspect that needs to be considered is the BSs power delivered to each user on DL; it will basically correspond to the minimum amount of power required to establish each

3. Traffic analysis

connection, as it will revert in interference to other cells' users. The BS power may be expressed by [HoTo01]:

$$P_{Tx}^{BS} = \frac{N_{rf} \cdot R_c \cdot \sum_{j=1}^N v_j \cdot \frac{(E_b / N_0)_j}{R_c / R_j} \cdot L_{p j}}{1 - \eta_{DL}} \quad (3.7)$$

where:

- $L_{p j}$ Attenuation between BS and MT
- η_{DL} DL load factor

By knowing the users' locations, it is possible to check the amount of power that a given scenario is requesting to each BS, and if there is enough power to deliver to all users (based on the value set up by the operators, e.g., the one presented in Table 3.1). When a considerable number of users is no longer closely located to the BS, they will require more power to the BS, and this will revert in interference to other users either in that cell or neighbouring ones. The system may, thus, turn to be limited due to the "lack" of BS power.

The DL load factor, also defined in [HoTo01], is obtained through:

$$\eta_{DL} = \sum_{j=1}^N v_j \cdot \frac{(E_b / N_0)_j}{R_c / R_j} \cdot [(1 - \bar{\alpha}) + i] \quad (3.8)$$

where:

- $\bar{\alpha}$ Average orthogonal factor in the cell (depends on the multipath propagation, ranging from 1, fully orthogonal, up to 0; the values considered hereafter correspond to 60 % for vehicular and 90 % for pedestrian)

The pole capacity per cell in the DL is also obtained when assuming a DL load factor of 100 %:

$$N_{pole_{DLn}} = \frac{R_c / R_n}{(E_b / N_0)_n} \cdot \frac{1}{\left[(1 - \bar{\alpha}) + i \right]} \cdot \frac{1}{v_n} \quad (3.9)$$

The air interface capacity in the DL is directly determined by the required transmission power. As the BS transmission power increases, more interference is generated in the system and less capacity will be available for MTs. In order to overcome this limitation, it is necessary to reduce to the maximum possible extent the BS transmitted power per link, leading to an interference reduction and an increase in system capacity.

Figure 3.2 shows the maximum path loss vs. the throughput on both UL and DL, for each of the RAB under study (12.2, 64, 128 and 384 kbps), considering two different scenarios – vehicular and pedestrian; the indoor scenario is left out of this analysis, as its coverage requirements are too stringent if outdoor BSs are to be used, and its inclusion would lead to an over dimensioning of the network.

Each plot is based on the assumption that there is a unique RAB; the throughput is obtained by increasing the number of users until the system is 100 % loaded; the system load is used as an input to obtain the maximum path loss, from which the cell radius may be derived. The throughput values correspond to the product of the RAB and the number of users. This is clearly a study case, in order to further understand the relationship between capacity and coverage, as well as the parameters that influence those two aspects.

With respect to both UL and DL curves, the starting maximum path loss (lowest system load) for the vehicular and the pedestrian scenarios differ slightly due to the variation on the link budget parameters considered: E_b/N_0 , $M_{fast-fading}$, L_{in-car} and G_{SHO} . By analysing the UL curves, it is visible that while the load increases, the pole capacity on the cell is approached (as said earlier, this is a theoretical value as it would lead to an infinite system interference level and a null coverage). It is also possible to observe that an increase on the RAB on the UL leads to a higher load value supported by the system. There is one exception to this, the 12.2 kbps case, which receives the weigh of an activity factor lower than 1, namely 0.67, influencing positively the overall system load.

3. Traffic analysis

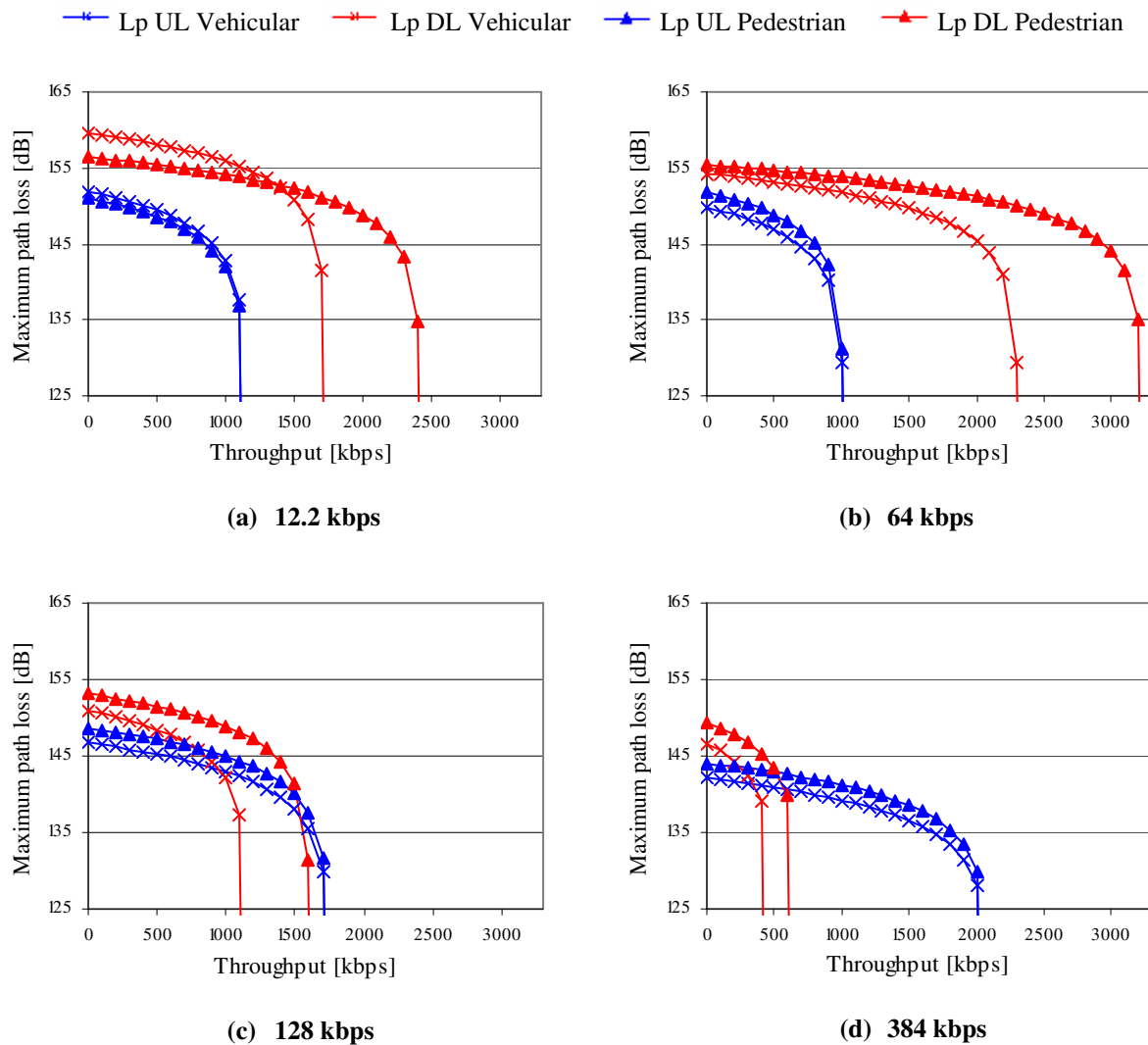


Figure 3.2 – Coverage vs. capacity on UL and DL.

Considering now the DL curves, several conclusions may be drawn. The DL power (from the BS) is to be divided among all users on the cell, the coverage on the DL being more dependent on the load than on the UL (where each user contributes with its power amplifiers). The more demanding RABs will allow fewer users per cell. The non-orthogonal factor on the DL leads to a decrease on the overall system load: the 60 % for vehicular users makes its corresponding pole capacity to be even smaller than the one for pedestrian users, where a 90 % average orthogonal factor in the cell is used.

While analysing together the UL and the DL, it is possible to observe that for lower RABs, namely 12.2 and 64 kbps, the UL coverage is always the limiting factor; the MT power is

very low and it does not allow the user to be too distant from the BS. The system itself does not show any restriction in terms of capacity for lower RABs. On the other hand, for higher RABs, 128 and 384 kbps, an intersection on the UL and DL curves is visible on Figure 3.2. This means that, for higher data rates but low system load, the UL coverage is still the most severe factor to be considered on the dimensioning, whereas the DL capacity is the aspect that will restrict the system when an increasing number of users are to be served. This is due to the fact that the BS transmission power, despite of being considerably higher than the MT's one (critical factor on low load), has to be divided among all users.

Real scenarios involve all service types at the same time, both on UL and DL, with potentially asymmetric traffic on the two links. Each service is mapped onto the most adequate RAB, as defined by the operators.

3.3 Code planning

It is mentioned in Section 2.2 that there are two types of operations that affect the physical channels in UMTS: channelisation and scrambling.

The channelisation operation allows the transformation of each bit into a SF number of chips, by increasing the bandwidth of the signal. It uses the Orthogonal Variable Spreading Factor (OVSF) codes, aiming at preserving the orthogonality of the user's different physical channels. The OVSF codes can be defined using the code tree presented in Figure 3.3.

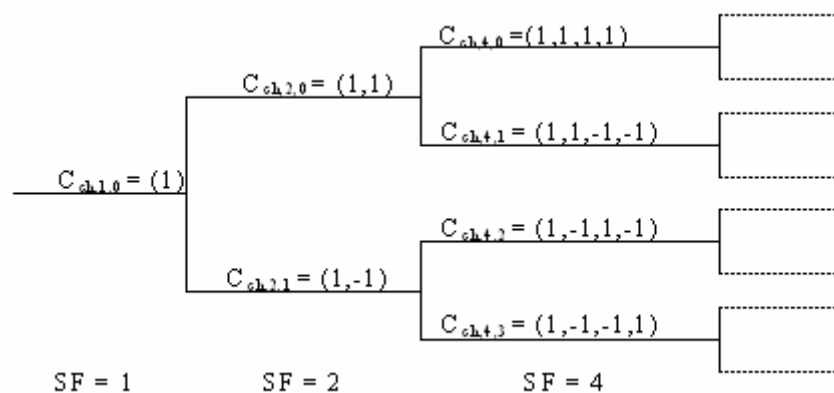


Figure 3.3 – Code-tree for generation of OVSF codes (extracted from [3GPP01b]).

3. Traffic analysis

In the UL, the channelisation codes separate physical and control channels from one same terminal; in the DL, they make the distinction between the DL connections to different users in the same cell. The number of channelisation codes depends directly on the SFs, which are related to the channel bit rates: they may vary between a SF of 4 (960 kbps) and 256 (15 kbps) in the UL, and a SF of 4 (1920 kbps) and 512 (15 kbps) in the DL. The utilisation of a specific code causes the unavailability of the sub-tree of higher SFs descending from that code, meaning that a limit on the number of channelisation codes is imposed mainly by high bit rate services with low spreading factors. As there are some restrictions on the use of a 512 SF in case soft handover needs to be performed, it is common to use only SFs up to 256 in the DL; this upper limit will as well be used in this thesis.

The scrambling operation corresponds to the application of “scrambling” codes (Gold sequence of 38 400 chips) to the spread signal, and is used to distinguish among terminals in one cell in the UL, or cells from each other in the DL. There are 2^{24} scrambling codes available in the UL, meaning that there is a very remote chance that all these codes are used. The maximum number of scrambling codes in the DL is a little bit smaller, i.e., $2^{18}-1$. Nevertheless, not all of these DL codes may be employed – the scrambling codes that are used are divided into 512 sets of primary codes, each one encompassing 15 secondary scrambling codes. This makes a total of 512×15 codes, i.e., 7 680. Each cell receives only one primary code in the DL, meaning that in total only 512 cells may be distinguished – 512 correspond to the scrambling code reuse factor. The P-CCPCH uses always a primary scrambling code, while the other DL physical channels use either the primary or the secondary scrambling codes associated with the primary scrambling code that identifies the cell.

Especially in the DL, it has to be confirmed if the number of available channelisation codes is limiting the system capacity or not. Considering the set of services presented in [FCSC02], which is further used in the next chapters, the corresponding SFs and numbers of codes, Table 3.3, determine the number of users in the system, Figure 3.4; the channel bit rate is obtained through:

$$ChannelBitRate_{[kbps]} = \frac{7680}{DL SF} \quad (3.10)$$

The maximum number of users per service, presented in Figure 3.4, reflects the particular situation when, for the DL, all MTs are making use of a unique service at a time; no mixture of services is considered here. Services requiring fewer codes, e.g., Speech-Telephony or Location Based, will leave more resources to other users, thus, letting more MTs to access the system; in contrary, code consuming services, e.g., Streaming Multimedia, utilise the total amount of resources with few users in the system.

Considering now a mix of two services at a time, the resulting number of users allowed to enter the system depends on the codes required per service. In Figure 3.5 (a), the number of Speech users is varied between 0 and 128, and analysed against the other services' users (only one of the remaining services can be considered); an increase on the number of Speech users leads consequently to a reduction of the number of the other services' users that attempt to access the system simultaneously. Similarly, in Figure 3.5 (b) StrMMLQ is weighed against the other services.

Table 3.3 – Services vs. UL/DL spreading factors and UL/DL codes (adapted from [FCSC02]).

Service	SF UL	SF DL	UL codes	DL codes
Speech-Telephony (Speech)	64	128	4	2
Video-Telephony (VideoT)	16	32	16	8
Streaming Multimedia Low Quality (StrMMLQ)	128	16	2	16
Streaming Multimedia High Quality (StrMMHQ)	128	8	2	32
Web Browsing (WWW)	128	32	2	8
Location Based (LocBas)	128	128	2	2
Multimedia Messaging Service (MMS)	16	32	16	8
Electronic Mail (E-Mail)	32	64	8	4
File Download (FDwnld)	128	32	2	8

3. Traffic analysis

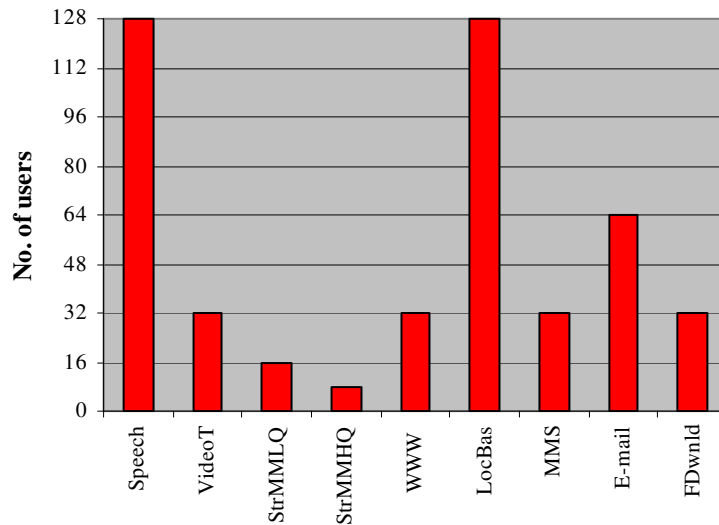


Figure 3.4 – Maximum number of DL users per service (based on [FCSC02]).

More demanding services in terms of codes will disable the possibility of a higher number of other services' users to access the system. This is visible in Figure 3.5, (b), when compared to (a), where, e.g., 8 StrMMLQ users (16 codes per user) will leave the chance to 64 Speech users, or 32 E-mail users, or even 4 StrMMHQ users to access the system at the same time. On the other hand, it is shown in Figure 3.5, (a), that 8 Speech users (2 codes per user) allow either 15 StrMMLQ users, or 60 E-mail users, or even 7 StrMMHQ.

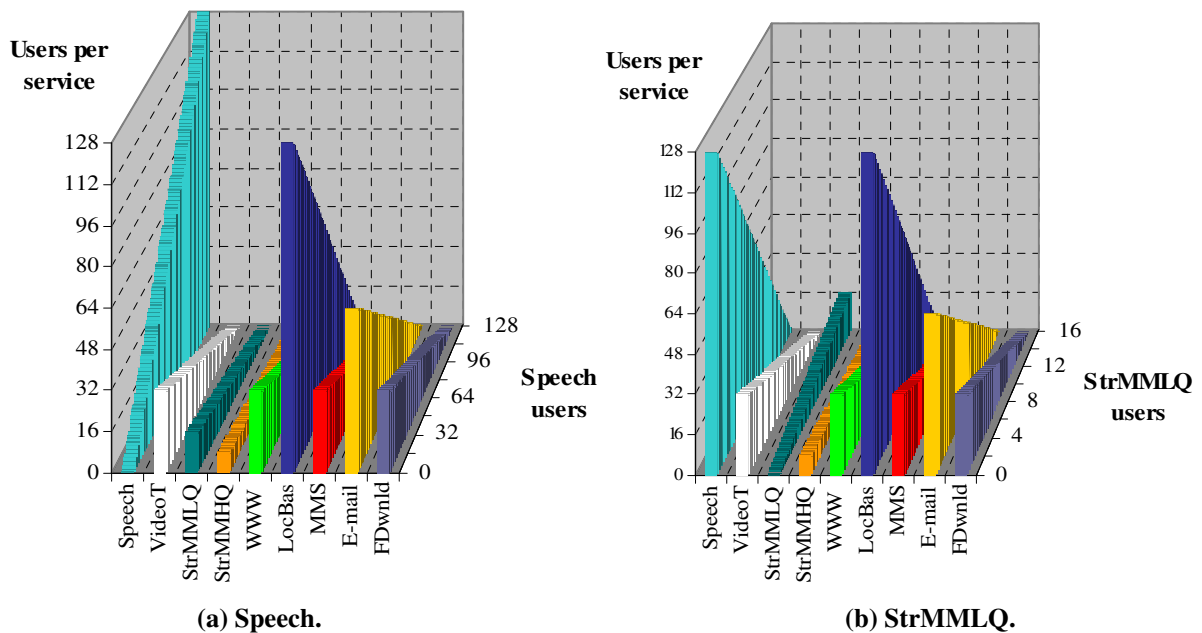


Figure 3.5 – Maximum number of users for more than one service.

The possible combinations of each type of service (considering the required codes) to complete the amount of DL available codes is high, but the effective number of users is relatively limited. One possible way to overcome the lack of these codes, in order to increase the number of users in the system, is to use more than one code tree, combined with distinct scrambling codes. It is thus possible to assign up to 15 code trees (secondary scrambling codes) per cell, reducing significantly the possibilities to run out of codes.

3.4 General traffic aspects

In UMTS, real-time and non-real-time services need to be handled in a different way: real-time (conversational and streaming) use the CS part of the network, to guarantee that there are no unacceptable delays on the provision of the services, whereas non-real-time (interactive and background) may be satisfied through the PS part, as they can wait until there are resources available on the network and support delivery delays.

CS traffic is characterised through four main parameters: *call arrival patterns* (usually random, modelled by a Poisson process), *blocked calls* (calls that cannot be completed at the time of request, due to congestion, and that are lost or held in a queue), *number of channels* (the resource that has to be shared among users) and *holding times* (average call duration). In order to optimise the available resources, the CS traffic should be limited to symmetrical services, i.e., the same amount of traffic on UL and DL. The traffic models with widest adoption in 2G are Erlang-B, Erlang-C and Engset (see, e.g., [Rapp96] and [Yaco93]).

PS traffic needs a different characterisation with respect to the CS one, as it is usually of an asymmetric nature and arrives in bursts. A packet service session may be further characterised through the following parameters, in order to reflect its typical behaviour [ETSI98]: *session arrival process* (how data packets arrive to the system, usually modelled as a Poisson process), *number of packet transmissions per session* (typically a Geometrically distributed random variable), *reading time between packet transmissions* (a Geometrically distributed random variable as well), *number of packets within a session* (different statistical distributions can be used to generate the number of packets that better describe each traffic case; it is common to use the Geometrical distribution to determine this parameter), its *inter-arrival*

3. Traffic analysis

time (usually a Geometrically distributed random variable) and *size* (typically a Pareto distribution).

In order to simulate the behaviour of a UMTS network, typical source models for traffic generation need to be considered [TWPL02]: Voice model (Speech-Telephony), Video traffic (Video-Telephony), ETSI WWW (Streaming Multimedia, Web Browsing, Location Based), ON-OFF (SMS and MMS) and Specific WWW (E-mail, File Download). There are many other aspects that need, in addition, to be addressed, and for which HO and mobility assume extremely high importance, aiming at fulfilling the expectations of 3G users.

It is expected, as it was mentioned in Section 2.3, that MTs may need to perform HOs between cells, or cell sectors, i.e., users may be crossing the cell / sector coverage limits while a call is still ongoing. Mobility is a very important aspect that needs to be accounted for in UMTS, especially in areas where high bit rate services are to be offered (where, as seen in Section 3.1, the smallest cell radii are observed). As one is talking about users that may move around, it is important to distinguish between calls that are originated and terminated in one single cell and calls that cross the border(s) towards adjacent cells, generating HO traffic. Some considerations in terms of mobility for homogeneous systems are drawn in [Corr03] and [Jabb96], where important parameters in terms of mobility are addressed: channel occupancy time, i.e., the time spent by an user in a cell prior to HO attempt or call completion, and probability of cell boundary crossing, which may be modelled through fluid flow assumptions. In particular, it is considered that MTs are uniformly distributed over a uniform cell structure with a given cell radius, R , that users move at a specific mean velocity, v , and that their direction of movement is uniformly distributed over $[0, 2\pi]$; the cell cross-over rate, η_h , is then given by:

$$\eta_h = \frac{4}{\sqrt{3} \cdot \pi} \cdot \frac{v}{R} \quad (3.11)$$

The call duration, τ , is commonly obtained through a random variable exponentially distributed (Annex B). The HO rate, ξ_h , is influenced by the cell cross-over rate and the average call duration:

$$\xi_h = \eta_h \cdot \tau \quad (3.12)$$

The completed calls, μ , known as well by service time, may be obtained by knowing the average call duration:

$$\mu = \frac{1}{\tau} \quad (3.13)$$

The average dwell time, τ_h , also known as residence time in a cell, is given by the inverse of the cell cross-over rate:

$$\tau_h = \frac{1}{\eta_h} \quad (3.14)$$

Another important and useful relation is the mean channel occupancy time in a cell, τ_c , which is given by:

$$\tau_c = \frac{1}{\mu + \eta_h} \quad (3.15)$$

The mean arrival rate, λ , corresponds to the sum of both new calls, λ_n , and HO calls, λ_h , the system entries being:

$$\lambda = \lambda_n + \lambda_h \quad (3.16)$$

The amount of traffic per user, represented henceforth by A , for c servers, is given by:

$$A = \frac{\lambda}{c \cdot \mu} \quad (3.17)$$

In any communication system, channels need to be shared among many users. Users' demands are placed randomly, and the call duration has usually an unpredictable duration. As some requests may arrive while all resources are in use, it is required to define a general access mechanism to the available channels: Figure 3.6 shows how the general call access

3. Traffic analysis

mechanism for voice through CS is accomplished. Afterwards, a similar access mechanism of a queuing system fitting PS purposes is presented.

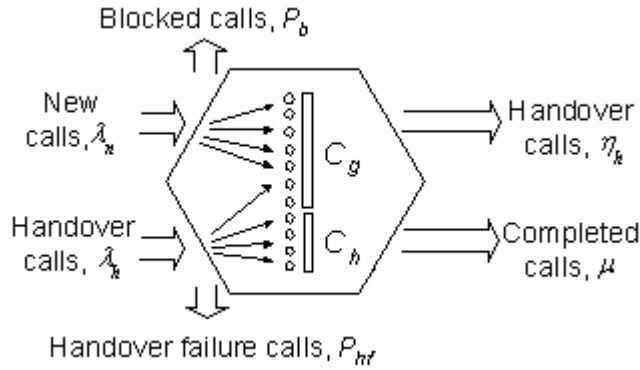


Figure 3.6 – General call access mechanism for CS (extracted from [Corr03]).

Part of the total system resources, C channels, is used for both new generated and HO calls, C_g , while the remaining ones, C_h , are allocated exclusively to handover calls.

$$C = C_g + C_h \quad (3.18)$$

If, at any instant, a CS user arrives to the system and there is no available resources, the call cannot be completed and will be either held (kept in a queue, if there is one), or lost (blocked, in case of a new user, P_b , or failed, for a HO user, P_{hf}). The probabilities of blocking calls and handover failure are given by [Jabb96]:

$$P_b = \frac{A^{C_g} \sum_{k=C_g}^C \frac{A_h^{k-C_g}}{k!}}{\sum_{k=0}^{C_g-1} \frac{A^k}{k!} + A^{C_g} \sum_{k=C_g}^C \frac{A_h^{k-C_g}}{k!}} \quad (3.19)$$

$$P_{hf} = \frac{A^{C_g} \frac{A_h^{C_h}}{C!}}{\sum_{k=0}^{C_g-1} \frac{A^k}{k!} + A^{C_g} \sum_{k=C_g}^C \frac{A_h^{k-C_g}}{k!}} \quad (3.20)$$

where A_h is the traffic load due exclusively to HO. New and HO calls will be dealt with in the same way, leading to $P_{hf} = P_b$.

Another arising probability that affects the call behaviour is the drop call probability, P_d , which occurs when there are calls lost in HO; this probability is given by [Jabb96]:

$$P_d = \frac{P_h P_{hf}}{1 - P_h (1 - P_{hf})} \quad (3.21)$$

P_h is the probability of performing HO and can be obtained through:

$$P_h = \text{Prob}(\tau > \tau_h) = \frac{\tau_c}{\tau_h} = \frac{\eta_h}{\mu + \eta_h} \quad (3.22)$$

The HO call rate, λ_h , is given by:

$$\lambda_h = \frac{P_h (1 - P_b)}{1 - P_h (1 - P_{hf})} \lambda_n \quad (3.23)$$

In case P_b and P_{hf} assume small values, which is usually the case, the HO call rate may be further simplified into:

$$\lambda_h \cong \frac{P_h}{1 - P_h} \lambda_n = \xi_h \lambda_n = \frac{\eta_h}{\mu} \lambda_n \quad (3.24)$$

When the system reaches a steady-state, the HO rate at the entry is equal to the outgoing HO rate; in steady-state, P_b may be obtained through the Erlang-B model [Leon94]:

$$P_b = \frac{\frac{A^c}{C!}}{\sum_{i=0}^c \frac{A^i}{i!}} \quad (3.25)$$

In traditional 2G CS networks, like GSM, which were planned from the begin to provide a unique service (voice), traffic dimensioning is based on the Erlang-B model, an M/M/c/c

3. Traffic analysis

queuing system according to Kendall's classification of queuing systems (1953). The Erlang-B model is based on the assumption that there is an infinite number of users per cell, and it does not account for users' mobility, thus, it does not consider handover; in addition, calls that cannot be established due to lack of resources are simply lost. For GSM networks, typical values for the blocking probability range between 1 and 2 %.

Similarly to what was seen for CS, a general call access mechanism for data through PS may be established, Figure 3.7. There are now different system parameters that may be measured: the data loss probability, L , and the mean waiting time, τ_w , which is a direct result of including a buffer to store data until there are resources to serve the users. Adequate models are, thus, required to obtain those parameter values.

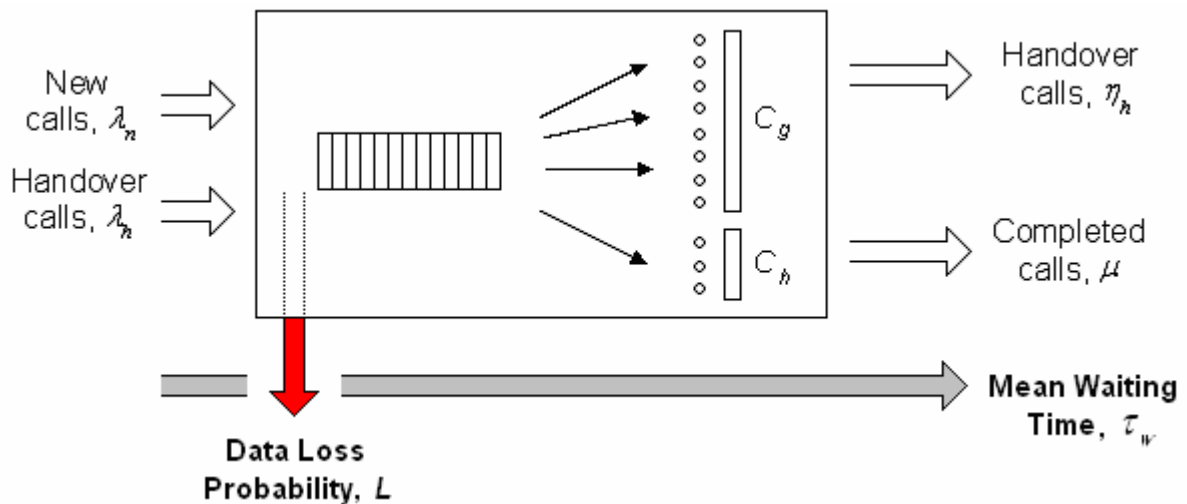


Figure 3.7 – General call access mechanism for PS (adapted from [Leon94]).

A model that is commonly used to account for data is the M/G/1 queuing system, which is a single-server system. Arrivals follow again a Poisson process, but the service times are no longer exponentially distributed.

The mean waiting time in an M/G/1 system is given by [Leon94]:

$$\tau_w = \frac{A(1+C_\tau^2)}{2(1-A)} \cdot \frac{1}{\mu} \quad (3.26)$$

C_τ^2 being the coefficient of variation of the service time, obtained through:

$$C_\tau^2 = \frac{\sigma_\tau^2}{(1/\mu)^2} \quad (3.27)$$

(3.26) is frequently referred to be the Pollaczek-Khinchin mean value formula.

There is another model, the Erlang-C, which corresponds to an M/M/c queuing system; contrarily to the Erlang-B model, this one accounts for the possibility to hold in a queue all calls that could not be served until there are available resources. The probability that a call will wait in a queue is given by [Leon94]:

$$P_w = \frac{P_c}{1-A} \quad (3.28)$$

where p_c is the probability for state c , given by:

$$p_c = \frac{(\lambda/\mu)^c}{c!} \cdot \left\{ \sum_{j=0}^{c-1} \frac{(\lambda/\mu)^j}{j!} + \frac{(\lambda/\mu)^c}{c!} \frac{1}{1-A} \right\}^{-1} \quad (3.29)$$

The mean waiting time, period of time elapsed since the customer arrives until he starts to be served, is found from Little's formula [Leon94]:

$$\tau_w = \frac{1/\mu}{c \cdot (1-A)} \cdot P_w \quad (3.30)$$

It is worth to say that the system is stable and has a steady-state if $A < 1$, or, equivalently:

$$\lambda < c\mu \quad (3.31)$$

In cellular systems like GSM, a fixed amount of frequencies allocated to the service are reused in a regular pattern of areas – usually hexagonal cells – each covered by one BS. In order to avoid harmful interference, the same channels cannot be used in adjacent cells, and a

3. Traffic analysis

safety distance needs to be preserved, meaning that a careful frequency planning is required to maximise the system capacity and the quality of the service provided to the user.

In UMTS, the frequency reuse factor is 1, and the resource that needs to be shared by users is no longer a preset number of frequencies, but the available system capacity, which is limited and varies according to instantaneous conditions – among the most critical, the number of active users and their exact location in the cell, the type of services that are being required, and the interference (intra- or inter-cells); this leads basically to a constantly changing number of “UMTS channels”.

Thus, traffic estimation in UMTS requires the consideration of a model more complex than the ones used in 2G, as it has to reflect the possibility of having multi-service traffic, with different bandwidth and QoS requirements, for scenarios that are constantly varying, and, last but not least, that account for mobility. While mixing up voice and data traffic, its complexity becomes very high and an accurate planning turns out to be an extremely difficult task to achieve. It would be worthwhile to consider a model that would differentiate each traffic type, in order to better reflect all services and its characteristics, and perform a valid study of the network behaviour. In the absence of such an optimal theoretical model for mobile communications, the adaptation of existing ones that already account for both voice and data traffic is a possible way to proceed with.

A traffic model that integrates voice and data calls in a mobile communications system, considers a finite-buffer for data, accounts for mobility, and is able to adjust the boundaries of the available resources per service type, is adapted to the particularities of UMTS, and, therefore, studied for various scenarios and input parameters. Its detailed description is presented in the next chapter, a further analysis in terms of system performance being the main objective of Chapter 5.

4 Traffic model

4.1 Model formulation

The traffic model that is studied in detail intends to integrate voice and data services, considers a finite-buffer to store data packets, accounts for mobility and adapts the boundaries of the available resources to the users' requirements, Figure 4.1. The aim of this section is to present the general model formulation [HaLH00]; in the next section, the adaptation of the model to UMTS is detailed, the last section containing a description of the algorithm as implemented.

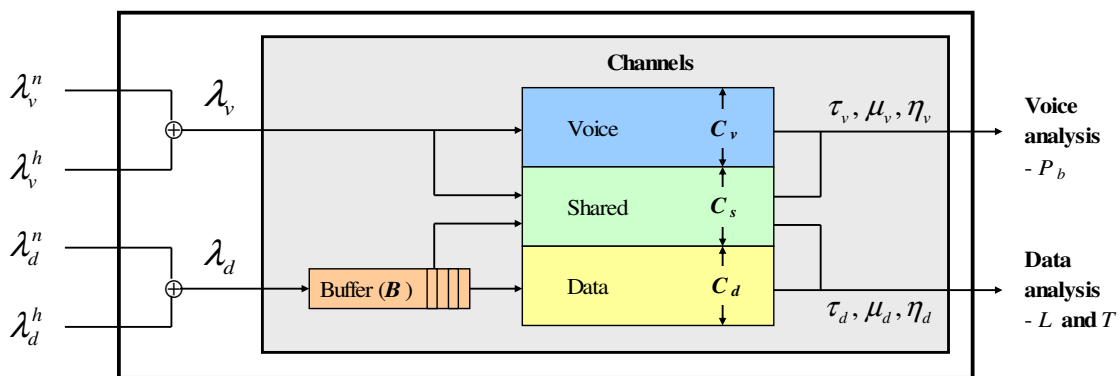


Figure 4.1 – Traffic model for the base station (adapted from [HaLH00]).

The number of physical channels for traffic, henceforth defined as C , corresponds to a scarce resource that needs to be shared among voice and data users. For this purpose, the available traffic channels are divided into three components: C_v channels exclusively dedicated to voice calls, C_d channels restricted to data packets, and $C_s = C - C_v - C_d$ channels to be shared between voice and data. The boundaries between these three components can be adjusted dynamically, aiming at an efficient utilisation of the available resources and satisfying the QoS requirements for both voice and data traffics. All channels are made available in a first-come first-served (FCFS) basis.

4. Traffic model

Instead of having a preset amount of C traffic channels per BS, it is necessary to convert this fixed parameter into a variable that is regularly updated to reflect UMTS characteristics, namely an interference balance based on the results of the coverage and capacity calculations. It may occur that the C traffic channels per BS are insufficient to serve all call attempts, thus, a finite buffer with size B is considered for data traffic, where packets are queued in case the available resources are busy. On the other hand, if the resources foreseen for voice calls are not available, the calls will simply not be admitted by the system, i.e., they will be blocked.

The unavailability of resources for voice leads to the inevitability to have calls blocked, which shall, for the sake of the network, be kept as small as possible. On the other hand, if data resources are all in use while new data packets are attempting to be transmitted, a limited amount of packets may be buffered, but delays or packet losses may occur.

Both voice calls and data packet transmissions need to be characterised through a statistical distribution. According to [HaLH00], voice and data traffic are assumed to follow a Poisson distribution. Voice call arrival rates, λ_v , including both new and HO calls, λ_v^n and λ_v^h , and data packets arrival rates, λ_d , including as well new and HO packets, λ_d^n and λ_d^h , are given by (4.1) and (4.2), respectively:

$$\lambda_v = \lambda_v^n + \lambda_v^h \quad (4.1)$$

$$\lambda_d = \lambda_d^n + \lambda_d^h \quad (4.2)$$

Moreover, it is assumed that the channel assignment to each of these types of calls is not distinguishable, i.e., the system uses a non-prioritised scheme for new and HO calls.

It is considered that voice and data traffic have an Exponential service time distribution, with means $1/\mu_v$ and $1/\mu_d$, respectively. The residence time in a cell for both, voice and data, does also follow an Exponential distribution, and its means are given by $1/\eta_v$ and $1/\eta_d$, respectively.

The channel occupancy time assumes as well an Exponential behaviour, with means given by (4.3) for voice and (4.4) for data, respectively.

$$\frac{1}{\mu_{cv}} = \frac{1}{\mu_v + \eta_v} \quad (4.3)$$

$$\frac{1}{\mu_{cd}} = \frac{1}{\mu_d + \eta_d} \quad (4.4)$$

It is first considered that the current cellular system has a homogeneous behaviour, leading to the fact that equal results are to be attained for every cell all over the network. Thus, the analysis done subsequently and the corresponding results are associated to a single cell. On a second stage, a heterogeneous scenario in terms of users' motion is considered, leading to an unequal flow of users into / out of a group of cells; the behaviour of the system under these circumstances is also evaluated and commented.

The C available channels per BS, divided in C_v voice, C_d data, and C_s shared channels, are used according to a FCFS scheme. When the resources are all given up, voice calls are simply lost, originating a blocking probability, P_b . On the other hand, data packets may still be kept on a buffer with length B , until it becomes full and cannot hold on any further packets; buffered data packets will, nevertheless, suffer a certain delay, leading to an emerging mean delay data, T . If data traffic increases more and more, and the buffer becomes completely filled up, packets start to be lost and a data loss probability, L , arises.

Summarising the results presented in [HaLH00], the voice call blocking probability, P_b , may be calculated through:

$$P_b = 1 - \left[Pi_0(1) + Pi_1(1) + \dots + Pi_{C_v-1}(1) + \sum_{i=C_v}^{C-C_d-1} \sum_{j=0}^{C-i-1} p_{ij} \right] \quad (4.5)$$

where:

$$Pi_i(z) = \sum_{j=0}^{\infty} p_{ij} z^j \quad (4.6)$$

Pi_i corresponds to the probability generating function of the distribution of data traffic, p_{ij} being the steady-state probability that there are simultaneously i voice calls and j data packets

4. Traffic model

in the cell under analysis, for $|z| \leq 1$ and $0 \leq i \leq C-C_d$, computed through (4.18), to be dealt with later.

The data loss probability, L , can be given by:

$$L = \sum_{i=0}^{C-C_d} q_{i,B} \quad (4.7)$$

with:

$$q_{ij} = \sum_{l=1}^{\infty} p_{i,j+l} \quad (4.8)$$

q_{ij} corresponds to the tail probability of the number of data packets when there are i voice calls in the cell.

Finally, the mean data delay, T , is obtained through:

$$T = \frac{\sum_{i=0}^{C-C_d} P i'_i(1)}{(\lambda_d^n + \lambda_d^h)(1-L)} \quad (4.9)$$

where $P i'_i(1)$ is obtained by differentiating (4.6):

$$P i'_i(z) = \sum_{j=1}^{\infty} j p_{ij} z^{j-1} \quad (4.10)$$

and then setting in (4.10) $z = 1$.

4.2 Adaptation of the model to UMTS

All UMTS aspects that were embedded in the traffic model under analysis are described hereafter, as well as any further simplifications required.

One of the crucial aspects in UMTS is the amount of channels, C , that may be offered to the user at any instant; there is here a huge difference between traditional 2G and the upcoming 3G systems, inherent to the technology chosen (TDMA vs. CDMA, respectively). The number of channels available per cell in a 2nd generation system results from a rather simple frequency planning activity, which requires, on one hand, the maximisation of channels per cell, but, on the other, the reduction to the maximum extend possible of adjacent- and co-channel interference, by increasing the re-use distance of channels. In UMTS, it is no longer possible to talk about a fixed amount of traffic channels; there are basically three matters that will impose restrictions to the system and, thus, limit the number of channels:

- The system load, which should not reach more than 50 % in the UL and 70 % in the DL;
- The BS power, that will be split among the users wishing to access the network, the power required to establish the connection being dependent on the location of the user, the type of service(s) he/she is requiring and the speed at which he is moving around;
- The existing DL codes.

The total number of voice and data channels available is, thus, dependent on instantaneous conditions. When implementing the traffic model, three test conditions are performed before the number of channels is estimated: if the UL and DL load limits are satisfied, by applying (3.5) and (3.8), if the BS power is enough to satisfy all users under the cell coverage, (3.7), and, finally, if the sum of codes required for all users, considering the service(s) under request, is lower or equal to the ones offered by the system. If either the UL / DL load, or the BS power, exceed the predefined values, the results from (3.5), (3.8) and (3.7) are considered to correspond to the totality of 256 DL codes and, thus, a proportional reduction on that value is carried out to pull down the parameter which exceeded its highest admissible value (Figure 4.2); e.g., assuming that the DL load would have reached 85 %, the system would allow only the use of 210 codes, according to:

4. Traffic model

$$Codes_{\{\eta_{UL}, \eta_{DL}, P_{Tx}^{BS}\}} = \frac{\{\eta_{UL}, \eta_{DL}, P_{Tx}^{BS}\} Limit}{\{\eta_{UL}, \eta_{DL}, P_{Tx}^{BS}\} ObtainedValue} \times 256 \quad (4.11)$$

On the other hand, if the number of required codes to satisfy all users is higher than 256, they will simply be truncated. After performing all tests, the final number of codes, corresponding in Figure 4.2 to the left hand side column, will be fixed on the minimum of $\{Codes_{\eta_{UL}}, Codes_{\eta_{DL}}, Codes_{P_{Tx}^{BS}}, 256\}$.

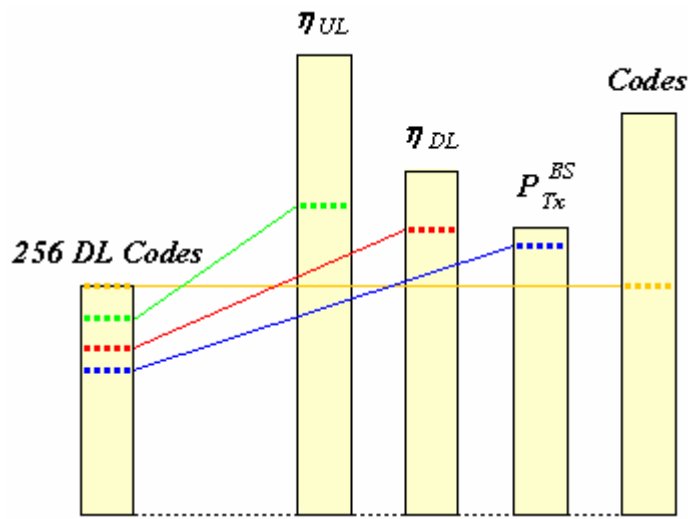
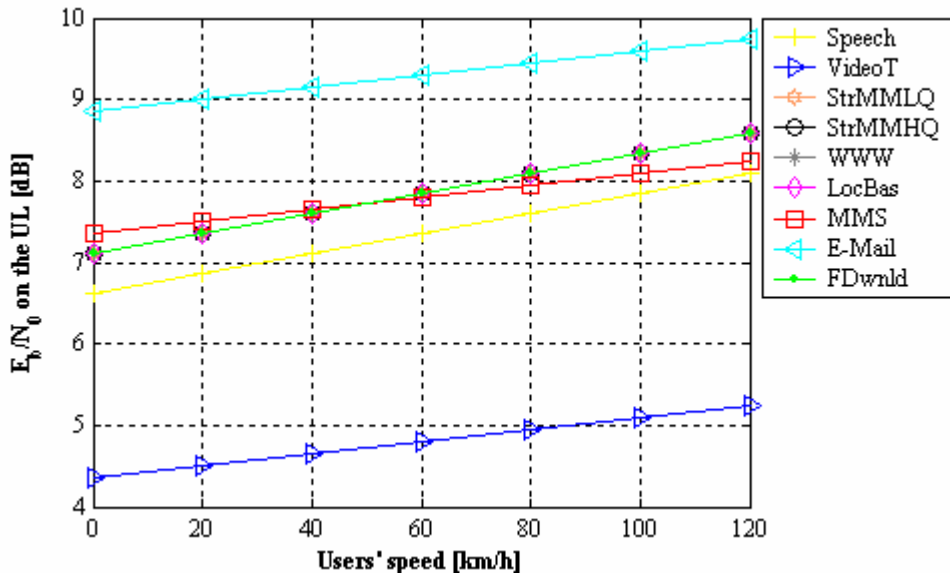


Figure 4.2 – DL code check.

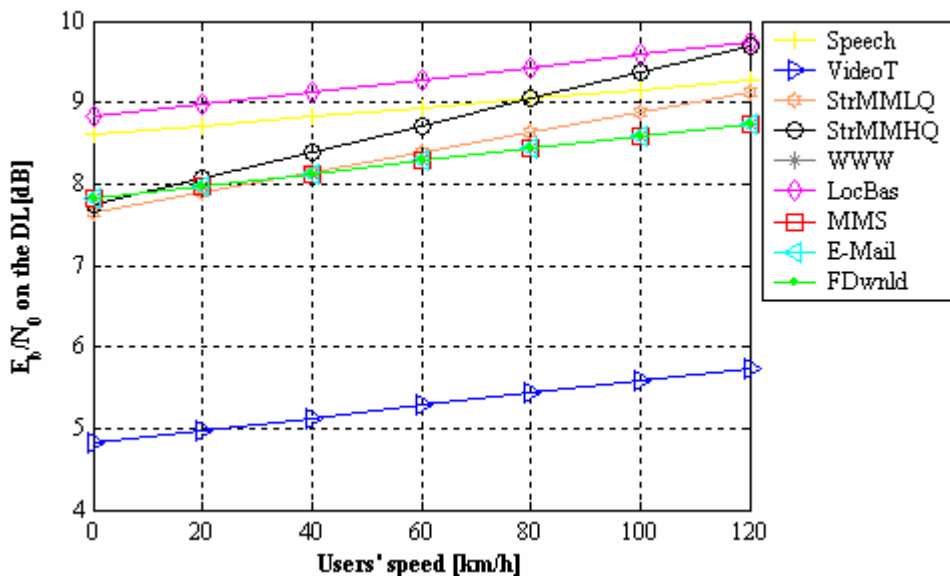
After knowing the exact number of DL codes that the system may handle, it is possible to determine the C channels, and corresponding voice and data users, that the system can support (as specified in Section 3.3). The conversion of a fixed number of channels in [HaLH00] into a variable one, as described, is the first adaptation done to the traffic model under study.

The first part of the model calculations, further presented in Section 4.3, requires values for E_b/N_0 ; namely, they are inputs to the UL and DL load estimation, and the BS transmission power calculation, and, consequently, influence the total number of channels on the system. E_b/N_0 values are usually obtained as a result of complex simulations, and, frequently, operators / vendors try to keep them confidential. The values that served as a basis for this thesis are the ones presented under [RFHL03]: as they reflect three particular situations in terms of users' speed, namely, static / pedestrian users at 3 km/h, vehicular up to 50 km/h and

up to 120 km/h, and in order to avoid any sharp disruption along any mobility analysis (users' speed between 0 and 120 km/h), a linear regression approach was used to predict, from the finite number of values, the remaining for the speed range under analysis, Figure 4.3.



(a) Uplink.



(b) Downlink.

Figure 4.3 – E_b/N_0 values (adapted from [RFHL03]).

4. Traffic model

It should be noted that there are some overlapped E_b/N_0 curves in Figure 4.3: StrMMLQ, StrMMHQ, WWW, LocBas and FDwnld on the UL, and WWW, MMS, E-Mail and FDwnld on the DL.

Higher values of E_b/N_0 lead to a more loaded system, both on UL and DL, and to an increase on the required BS power; consequently, higher values of this parameter may imply less overall channels.

The DL load estimation is as well affected by an orthogonal factor in the cell, α (Section 3.2). The values considered in the previous chapter correspond to 60 % for vehicular and 90 % for pedestrian users, as defined in [HoTo01]. Nevertheless, while studying the traffic model behaviour in terms of users' mobility, a smooth transition for the orthogonal factor is desirable all along the range of the speed variation; thus, a gradual reduction of the orthogonal factor is considered, assuming that the referred vehicular value is attained when the user reaches 60 km/h and is further kept up to 120 km/h, Figure 4.4.

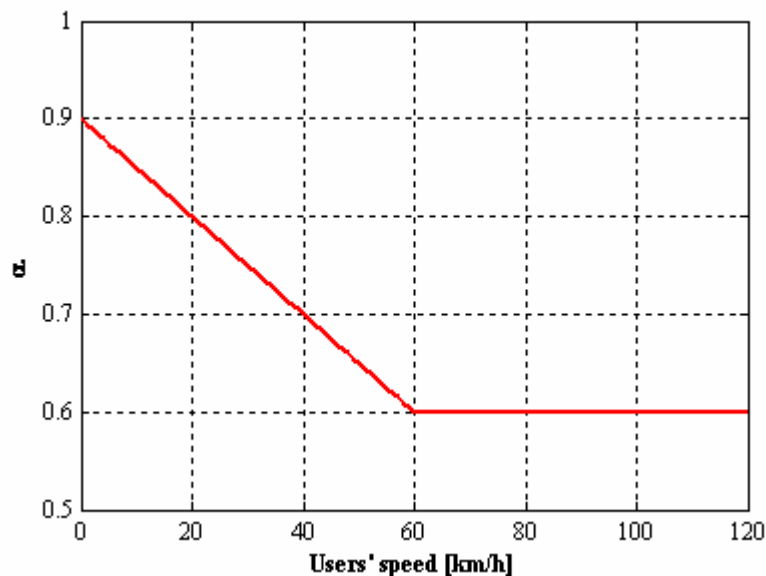


Figure 4.4 – Orthogonal factor as a function of users' speed.

Lower values of α lead, according to (3.8), to a higher DL system load; this means that when the orthogonal factor is smaller, the system delivers fewer channels to the users.

When the cell radius R is to be obtained via the characteristics of a reference scenario, a couple of other parameters, namely L_{in-car} , G_{SHO} and $M_{fast-fading}$, required for the estimation of the allowed propagation loss, need to be adapted as well, so that sharp transitions along the speed range, $[0, 120]$ km/h, are smoothed and results with discontinuities are avoided. The values as extracted from [HoTo01] are thus adapted in the way shown in Figure 4.5.

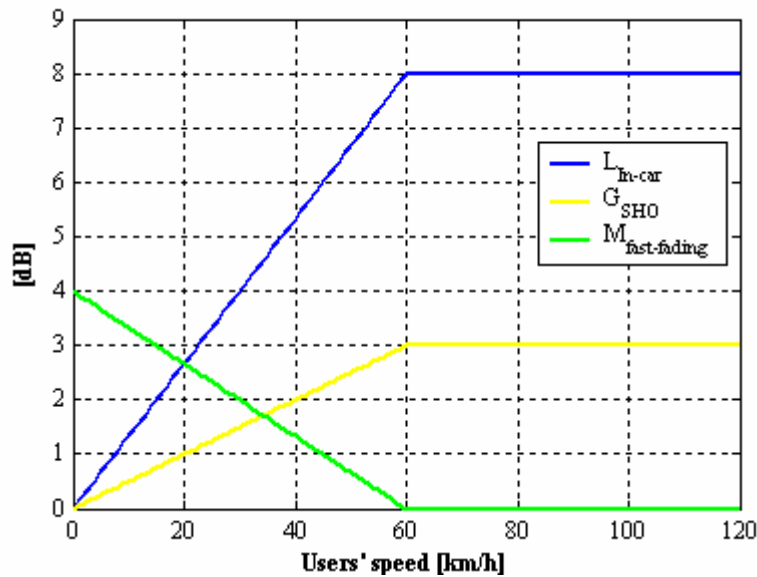


Figure 4.5 – Link budget parameters adapted to a varying users' speed.

The 8 dB L_{in-car} value will be assumed for users moving at speeds of 60 km/h or higher, whereas a smooth reduction until it reaches 0 dB for not-moving users is done:

$$L_{in-car}[\text{dB}] = \frac{(8-0)}{60} \times v_{[\text{km/h}]} \quad (4.12)$$

With respect to the G_{SHO} , the 3 dB value is as well assumed for 60 km/h and greater speeds; a gradual reduction of that value is also performed while speeds are decreased up to 0 km/h:

$$G_{SHO}[\text{dB}] = \frac{(3-0)}{60} \times v_{[\text{km/h}]} \quad (4.13)$$

The $M_{fast-fading}$ is applied to slow moving mobiles. Thus, the 4 dB margin will be decreased until it reaches 0 dB at 60 km/h, value to be further kept up to 120 km/h:

4. Traffic model

$$M_{fast-fading} \text{ [dB]} = \frac{(0-4)}{60} \times v_{\text{[km/h]}} + 4 \quad (4.14)$$

Higher values of L_{in-car} , obtained for users that move faster, lead to lower allowed propagation losses (3.1), and, consequently, smaller cell radii; on the other hand, G_{SHO} , which also increases while users' speed augments, leads to greater allowed propagation losses and the cell radii are positively influenced; with respect to the $M_{fast-fading}$, as it decreases with speed increase, the allowed propagation losses grow and cell radii expand as well, Table 4.1.

Table 4.1 – L_{in-car} , G_{SHO} and $M_{fast-fading}$ vs. number of channels.

$v \nearrow$	$L_{in-car} \nearrow$	$L_p \searrow$	$R \searrow$	$C \searrow$
$v \nearrow$	$G_{SHO} \nearrow$	$L_p \nearrow$	$R \nearrow$	$C \nearrow$
$v \nearrow$	$M_{fast-fading} \searrow$	$L_p \nearrow$	$R \nearrow$	$C \nearrow$

In order to proceed with the model calculations, it is required to find out the average voice and data call duration values, τ_v and τ_d . For PS, it is no longer correct to refer call duration in time units; nevertheless, the average DL session volume, as specified in Table 5.2, together with the channel bit rates, will enable to obtain equivalent data call duration values.

The traffic model will, for the time being, use an average value for data calls, instead of making the difference among each individual data service considered. In order to find out the resulting average data call duration, the duration of each individual service is weighed over the total number of users:

$$\tau_d = \frac{\sum_{i=1}^{TotDataServices} (Users_i \times \tau_i)}{\sum_{i=1}^{TotDataServices} Users_i} \quad (4.15)$$

If, for any reason, the selected scenario does not encompass any data user, a single average is applied:

$$\tau_d = \frac{\sum_{i=1}^{TotDataServices} \tau_i}{TotDataServices} \quad (4.16)$$

Another essential parameter used by the model is the voice and data call rates, λ_v and λ_d . Busy hour call attempt (BHCA) grids for 2005, provided by a mobile operator [Voda02], are used to obtain the required call rates. Basically, the total number of session calls per day and per customer segment (Business, SOHO and Mass-market) is first forecasted; part of these are made during the busy hour, originating then BHCA grids per service and customer segment (values provided per pixel). As the traffic model under analysis does not distinguish users among customer segments, these three different kinds of users will simply be grouped. A cell with a 100 m radius, and average high traffic intensity is considered, in order to extract the number of voice calls per second [Voda02]:

- $\lambda_{v100} = 0.015$ calls/s,
- $\lambda_{d100} = 0.01$ calls/s.

Afterwards, by knowing the exact radius, R , of the cell under analysis, voice and data call rates may be obtained:

$$\lambda_{v,d} = \left(\frac{R}{100}\right)^2 \cdot \lambda_{v100,d100} \quad (4.17)$$

It is important to point out that, by applying (4.17), users are assumed to be uniformly distributed in space and, consequently, the generation of calls within the operational environment is as well uniform; spatial and temporal users' behaviours will be neglected, in order to simplify the model analysis.

R is one of the parameters that may be either set up by the user each time the program is run, or obtained by calculating, for a pre-defined reference scenario, the maximum allowed propagation loss and, through a propagation model like COST231-Walfisch-Ikegami, the consequent maximum cell range is extracted.

4. Traffic model

When selecting the value of R for the cell under analysis, two aspects need to be looked upon: first of all, and it was seen earlier, voice and data call rates, λ_v and λ_d , depend directly on λ_{v100} and λ_{d100} ; the second aspect corresponds to the fact that, in queuing systems, stability is attained when the relation (3.31) is observed, i.e., $c\mu$ being the departure rate of the c server system, the call rate, λ , needs to be smaller to keep the system stable. When fixing the number of servers in 8, 16, 32 and 64, making λ_{v100} and λ_{d100} as specified earlier (rates used as well later in the program runs), and considering a voice and an equivalent data call durations of 120 and 150 s, respectively, a limitation in terms of the maximum cell radius arises, Figure 4.6.

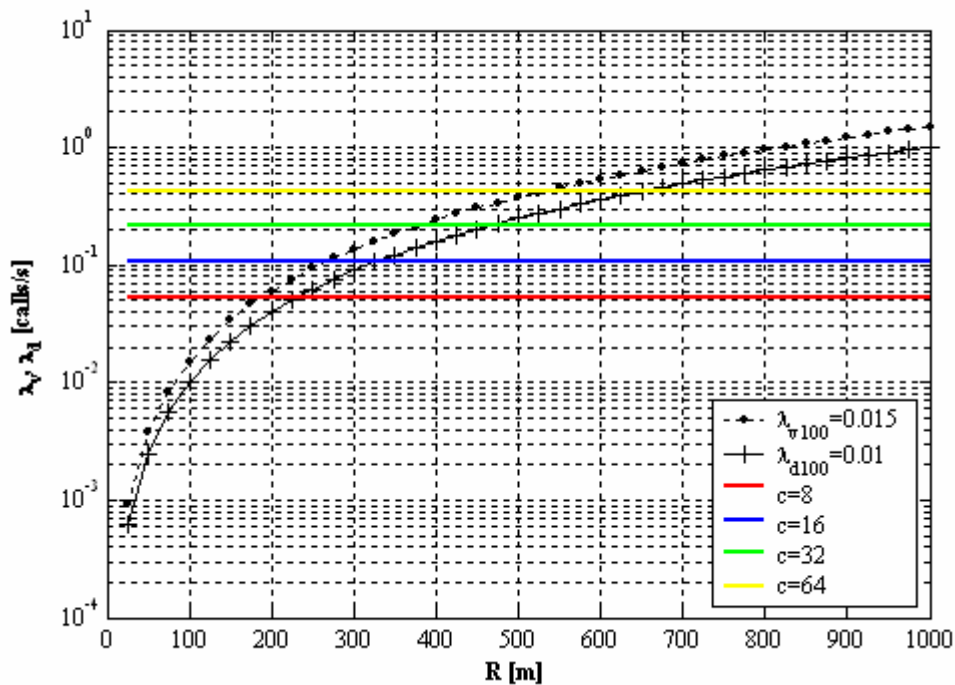


Figure 4.6 – Call arrival rate vs. cell radius.

The choice of adequate cell radii values will result from a compromise between the number of servers in the system (channels) and input parameters (namely, voice and data call rates and duration): if there are few channels, the cell radius cannot be increased much; on the contrary, when the system is able to deliver more channels, the limitations in terms of radio size tend to disappear; analysing this aspect the other way around, if the cell radius allowed is small, and considering the users uniformly distributed within the operational environment, the number of system channels decreases.

Neither the call rates, nor the call duration values, do influence the number of system channels, as it is clearly seen in the next section, where the flowcharts of the implemented algorithm are presented.

The steady-state probability that there are simultaneously i voice calls and j data packets in the cell, p_{ij} , is a fundamental input parameter of the traffic model that is obtained analytically. Assuming that voice and data events are independent [Meye84], it can be said that the probability of having at the same time i and j is given by:

$$p(i \cap j) = p_v(i) \cdot p_d(j) \quad (4.18)$$

This means that the p_{ij} matrix may be obtained after knowing the individual probabilities of each event, Figure 4.7.

		i (voice calls)					
		0	1	2	3	...	128
j (data packets)	0	$p_v(0) \cdot p_d(0)$	$p_v(1) \cdot p_d(0)$	$p_v(2) \cdot p_d(0)$	$p_v(3) \cdot p_d(0)$...	$p_v(128) \cdot p_d(0)$
	1	$p_v(0) \cdot p_d(1)$	$p_v(1) \cdot p_d(1)$				
	2	$p_v(0) \cdot p_d(2)$	$p_v(1) \cdot p_d(2)$				
	3	$p_v(0) \cdot p_d(3)$		\vdots	\vdots		\vdots
	4	$p_v(0) \cdot p_d(4)$	\vdots				
	\vdots	\vdots					
	128	$p_v(0) \cdot p_d(128)$	$p_v(1) \cdot p_d(128)$	$p_v(2) \cdot p_d(128)$	$p_v(3) \cdot p_d(128)$...	$p_v(128) \cdot p_d(128)$

Figure 4.7 – p_{ij} matrix.

$p_v(i)$ and $p_d(j)$ may be modelled by means of a discrete random variable, such as the Binomial, the Geometric or the Poisson one. According to [HaLH00], both voice and data calls are Poisson distributed; this assumption is considered as well for the traffic model under analysis.

It should be added that the range of variation from i and j in Figure 4.7 comes directly from Figure 3.4. Basically, 128 is the maximum number of users for voice and data, for particular scenarios where users do exclusively use Speech and LocBas, respectively, these being the less demanding services in terms of required number of codes. If other services are required by the users, the amount of customers that may be served reduces.

4. Traffic model

As the Poisson distribution is λ and τ dependent, the values assumed by both voice and data call rates and call durations have a strong influence in the probability matrix; this is basically seen in Figure 4.8 and Figure 4.9, where these parameters are set to a specific value and its double, respectively; (a) corresponds, in both figures, to the p_{ij} matrix, whereas (b) is the result of differentiating the coefficients of the matrix p_{ij} .

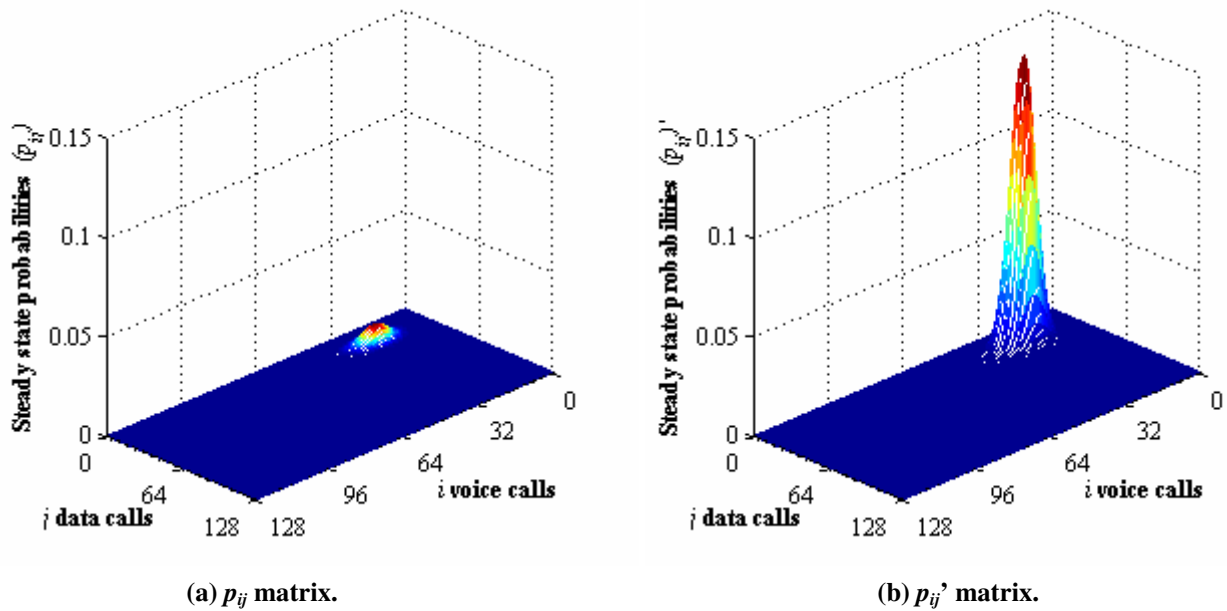


Figure 4.8 – Steady-states $[(\tau_v, \tau_d), (\lambda_v, \lambda_d)]$.

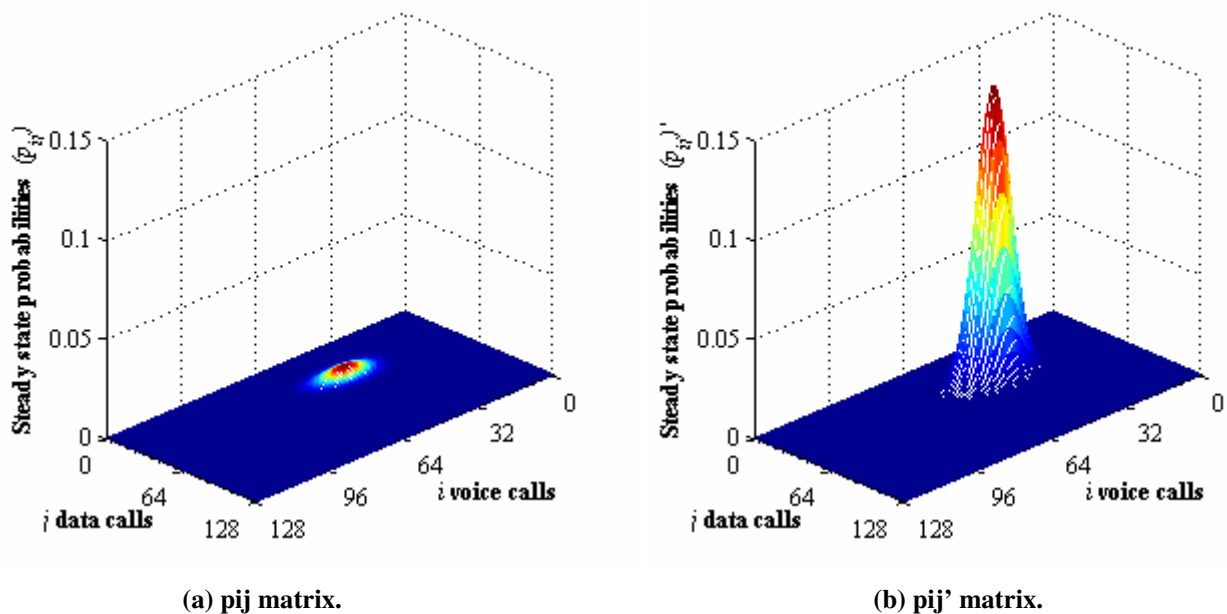


Figure 4.9 – Steady-states $[(2\tau_v, 2\tau_d), (\lambda_v, \lambda_d)]$ or $[(\tau_v, \tau_d), (2\lambda_v, 2\lambda_d)]$.

As it can be seen in Figure 4.8 and Figure 4.9, when increasing λ or τ , the circular area that encompasses the predominant p_{ij} and p_{ij}' elements is a little distended, but its value is smoothed (the sum of all p_{ij} matrix elements remains unitary); furthermore, the circular area is slightly pushed to the centre of the p_{ij} and p_{ij}' matrices; p_{ij}' elements are obtained by differentiating the p_{ij} matrix, meaning that the size of the predominant area is not changed with respect to p_{ij} , but the individual element values are amplified considerably. A variation of λ and/or τ implies an immediate change on the probability matrices, and, consequently, the behaviour of the traffic model is modified, as will be seen later on.

As previously referred, p_{ij} and p_{ij}' are modelled by a Poisson distribution, influenced by call rate and duration values; consequently, the probability matrices will not influence the number of channels made available by the system.

As the traffic model solely distinguishes between two types of services, i.e., voice and data, the particularities of each data service are lost when averaging it, as mentioned earlier in this section, to get a value to be used by the model. In order to have a better understanding on the behaviour of a real UMTS network, it would be desirable to adapt the model to account for the particularities of each key UMTS data service; namely, it would be worthwhile to distinguish between the average packet size of each service, and, consequently, its equivalent average call duration, as well as the specific data call rates. In order to do so, it would be necessary to consider an n -dimensional space, where s would be a vector containing the set of services, $s = (s_1, s_2, \dots, s_n)$, and $s \in \mathbb{R}^n$. The steady-state probabilities for the n number of services considered, $p_{1,2,\dots,n}$, would be a real-value function of n variables, $p_{1,2,\dots,n} = f(s_1, s_2, \dots, s_n)$.

The traffic model under study includes a buffer to store packets when the system resources are all unavailable; thus, the size B of this network element needs to be stipulated. It may be read from [ETSI01] that the maximum buffer size to store outstanding information shall be 24 320 in units of 16 octets. On the other hand, considering the DL session volume figures per service as specified in [FCXV03] and further listed in Table 5.2, the average DL session volume is close to 1 MB. As the reference value from ETSI is smaller than a session volume, the buffer size, for the purpose of the present analysis, will be settled to allow the storage of 20 messages with 1 MB average size, i.e., with a maximum size of 20 MB.

4. Traffic model

It is said, under Chapter 3, that new and HO calls are dealt with in the same way and that $P_{hf} = P_b$. This is basically valid if it is only seen from the perspective of lack of channels. Nevertheless, a HO process is usually a very complex action and does not have 100 % success; as mentioned in Section 2.3, there are three types of HOs in UMTS (hard, soft and softer) and the probability of having a system failure may not be totally ignored. Despite of that, and having in mind that technology evolves and the planning procedures become more accurate, the amount of calls that fail HO attempts is getting smaller and smaller, and do not depend so much on the system itself but on how the network is planned and on propagation conditions, any HO failure will be neglected for the purpose of the present work. Other reasons for having dropped calls, not related to lack of channels, will also simply be disregarded.

The instantaneous traffic variation, seen from the temporal side, was addressed in previous sections, focusing on parameters like call arrival rates and holding time. Meanwhile, there is another temporal traffic variation that was up to now not referred to: the traffic evolution over a certain period of time should not only account for daily variation, but also its behaviour along the days of a week. Taking into consideration the cellular philosophy of dimensioning networks for rush hour traffic, the traffic model under analysis will consider the worst case, pondering only peak instead of average values of call arrivals, so that rush hours do not destabilise system performance.

In order to simplify the traffic model under analysis, the users' density distribution is approximated through a statistical behaviour: a uniform distribution of users all over the cell is assumed, which corresponds to a very rude generalisation. In reality, the traffic density distribution is not uniform all over the cell, as it depends directly on the geographical characteristics of each area, and may vary along the day if, for instance, a typical business or residential area is depicted. The BS power consumption, as seen earlier, assumes different values depending on the users' location – when studying a real scenario, a specific analysis dedicated to the spatial distribution of users is essential.

Finally, when the cellular system reaches a steady-state, the incoming calls are considered to be equal to the outgoing ones. Such a homogeneous scenario leads to equal results in every

cell. The impact of hot-spot traffic on the system performance is going to be roughly analysed, when a heterogeneous scenario in terms of users' motion is considered, Figure 4.10.

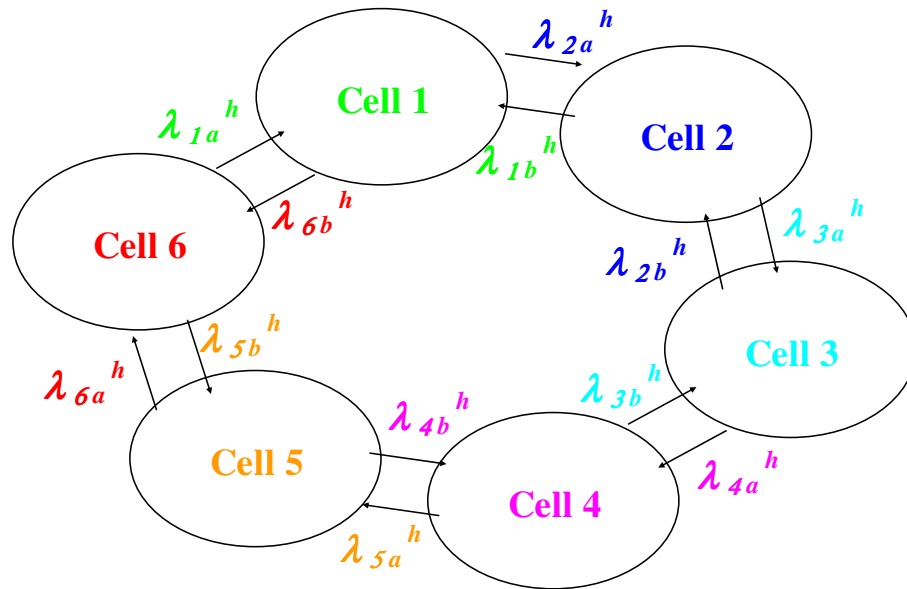


Figure 4.10 – Users' motion along a ring of six cells.

The incoming calls to cell k are split unequally between the two neighbouring cells:

$$\lambda_k^h = \lambda_{k_a}^h + \lambda_{k_b}^h \quad (4.19)$$

Thus, a six cell's ring is considered, where incoming and outgoing traffic per cell are no longer identical ($\lambda_{k_a}^h \neq \lambda_{k_b}^h$). A specific routing matrix is fixed and the system performance per cell evaluated.

4.3 The algorithm

The steps required to obtain P_b , L and T , that will structure the algorithm implemented, are presented hereafter; the approach as proposed under [HaLH00] is followed, despite of the fact that some further adaptations are introduced.

The following input parameters need to be given at the starting point of the calculations:

4. Traffic model

- *DL Codes*, the total number of DL codes that may be used;
- P_{Tx}^{BS} , the maximum BS transmitted power;
- η_{UL} , the maximum load allowed by the system in the UL;
- η_{DL} , the maximum load allowed by the system in the DL;
- B , the buffer size for data packets, to study the system behaviour in terms of users' speed;
- R , the cell radius;
- λ_{v100} , the new voice call arrival rate for a cell with 100 m radius;
- λ_{d100} , the new data packet arrival rate for a cell with 100 m radius;
- v , the speed at which an user will be moving around, to study the system behaviour in terms of buffer size;
- *Mscenario*, if not only a homogeneous scenario in terms of users' motion, along a set of cells, is to be considered, three different users' speeds are also introduced.

These input parameters may be specified by the user at the start of any run of the traffic model.

A file containing all services' parameters will be read when the traffic model program starts to run. Basically, the following information, per type of service, will be made accessible to the model:

- Average call duration;
- SF for both UL and DL;
- Number of codes required for the DL connection;
- Bearer service for both UL and DL.

Finally, a last file with the scenario that is to be studied is accessed by the program. The exact number of users per service type is specified there, and may be tailored as well for each program run.

The implementation of the traffic model is divided in 5 steps, corresponding to the gathering of all parameters required for the traffic model computation and the calculation of the system performance based on the traffic model under study.

Before really starting any calculation, **step zero** is to be performed by the program's user: it corresponds to the definition of the contents of files "input parameters", "services' parameters" and "users' scenario". These files are loaded before any further step is performed.

On the **first step**, the cell radius is set. If, in file "input parameters", the cell radius field is set to zero, this means that the program's user does not want to fix the cell radius, rather requiring that the program estimates that value; for this purpose, a specific function is called and run, where a reference scenario is read (by default, 50 % of UL load, bearer service of 384 kbps and 120 km/h users' speed), the corresponding allowed propagation loss is obtained and, through the application of the COST231-Walfisch-Ikegami model, the cell radius is extracted.

During the **second step**, three actions are performed:

- To obtain the UL and DL loads of the system, based on the scenario (number of users) defined by the program's user;
- To calculate the number of DL codes needed to serve all users in the system;
- To check the BS transmitter power to serve all users in the cell; the distribution of the system users inside the cell is required, thus, a pseudo-random function is used to determine the users' distance towards the BS (users are uniformly distributed between the BS and the cell edge); finally, the maximum allowed propagation loss per user is calculated.

If any of those results exceeds the maximum allowable values, the number of codes is reduced, so that the system works under the maximum specified limit.

In the **third step**, the number of channels, C , is calculated, as well as its split into voice, C_v , data, C_d , and shared channels, $C - C_v - C_d$, based on the results of step two; two ways of dividing the available channels among voice and data users are compared, Figure 4.11:

- The first option is to split the resources equally into voice, data and shared channels, which is designated by equitable;
- The second one is to provide channels proportionally to the users, having the scenario under analysis as a basis, any left resources being kept as shared channels, the proportional approach.

4. Traffic model

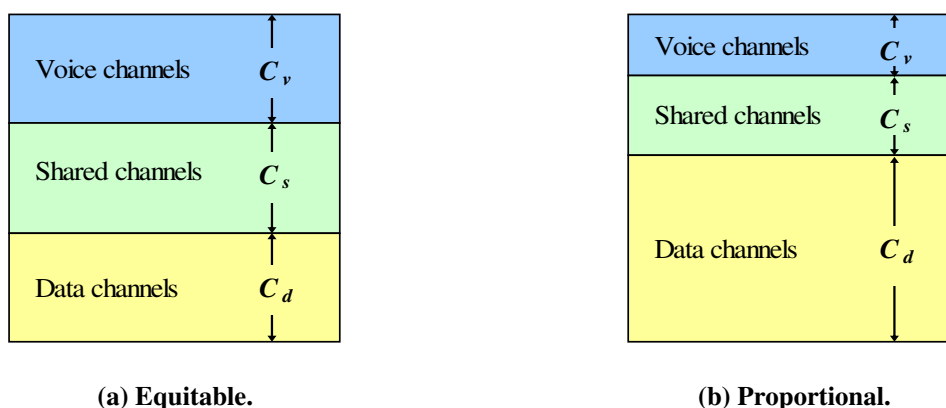


Figure 4.11 – Channel distribution.

In each of these two options, as the number of users' increases, more shared channels are used. If, at any instant, there is lack of resources, voice calls may be blocked and data packets lost or delayed.

The **fourth step** corresponds to the traffic model computation: the remaining input data is loaded; channel occupancy, handover rates and call rates are calculated; finally, P_b , L and T are evaluated.

If the program's user chose to study a heterogeneous scenario as well in terms of users' motion, the **fifth step** is performed; a pre-defined routing matrix is read, voice and data handover call rates per cell are calculated, and the consequent system performance measures obtained.

The described algorithm, presented also in the form of a flowchart, Figure 4.12, uses as a basis the model formulation in Section 4.1. It was implemented in the language C/C++, [KeRi88] and [MSDN03], and its results are then read and plotted in MATLAB [HaLi97].

Steps 2 and 4 from the main flowchart, Figure 4.12, are further complemented with other flowcharts; to be more specific, when the number of channels is being studied, Step 2, three tests are performed: system load verification, code verification and BS power verification.

The system load sub-routine, Figure 4.13, implements the verification of the load on both UL and DL. The recommended limits of 50 % and 70 %, respectively for UL and DL, shall be satisfied; thus, the scenario that is under analysis is set, the load for each individual user is

calculated and summed, and the thresholds are checked; in case any of these maximum allowed limits is exceeded, a reduction on the number of DL codes is performed.

The code sub-routine, Figure 4.14, implements the verification of the number of codes required to serve all users from the scenario under analysis; if the resulting value is below 256, no additional actions are undertaken; otherwise, the number of codes that is considered corresponds to that threshold.

The BS power sub-routine, Figure 4.15, implements the verification of the power delivered by the BS to the MTs. The first action required is the users' distribution within the cell radius; for that purpose, a pseudo-random function is called, and MTs are spread uniformly inside the cell coverage area. The allowed propagation loss is calculated through (3.1); afterwards, the BS power required to serve all users is summed and the results are compared with the threshold as defined by the program's user; again, if the required BS power is higher than the one that was set up in the system, then an adjustment on the number of codes is performed.

Finally, the traffic model computation, Figure 4.16, is carried out. The missing input parameters are read from input files prepared earlier, following the calculation of the probability matrix; other parameters, like channel occupancy, HO rates and arrival rate, are in the mean time computed as well. When all input parameters are known, one sole task remains: the calculation of the three system behaviour parameters, namely, P_b , L and T .

Two particular scenarios are studied in Chapter 5, the corresponding results being presented in Annexes C and D; in particular, the traffic model behaviour is first loaded with more voice than data, and then an almost symmetrical scenario is analysed. Several considerations with respect to the traffic model are drawn along the next chapter.

4. Traffic model

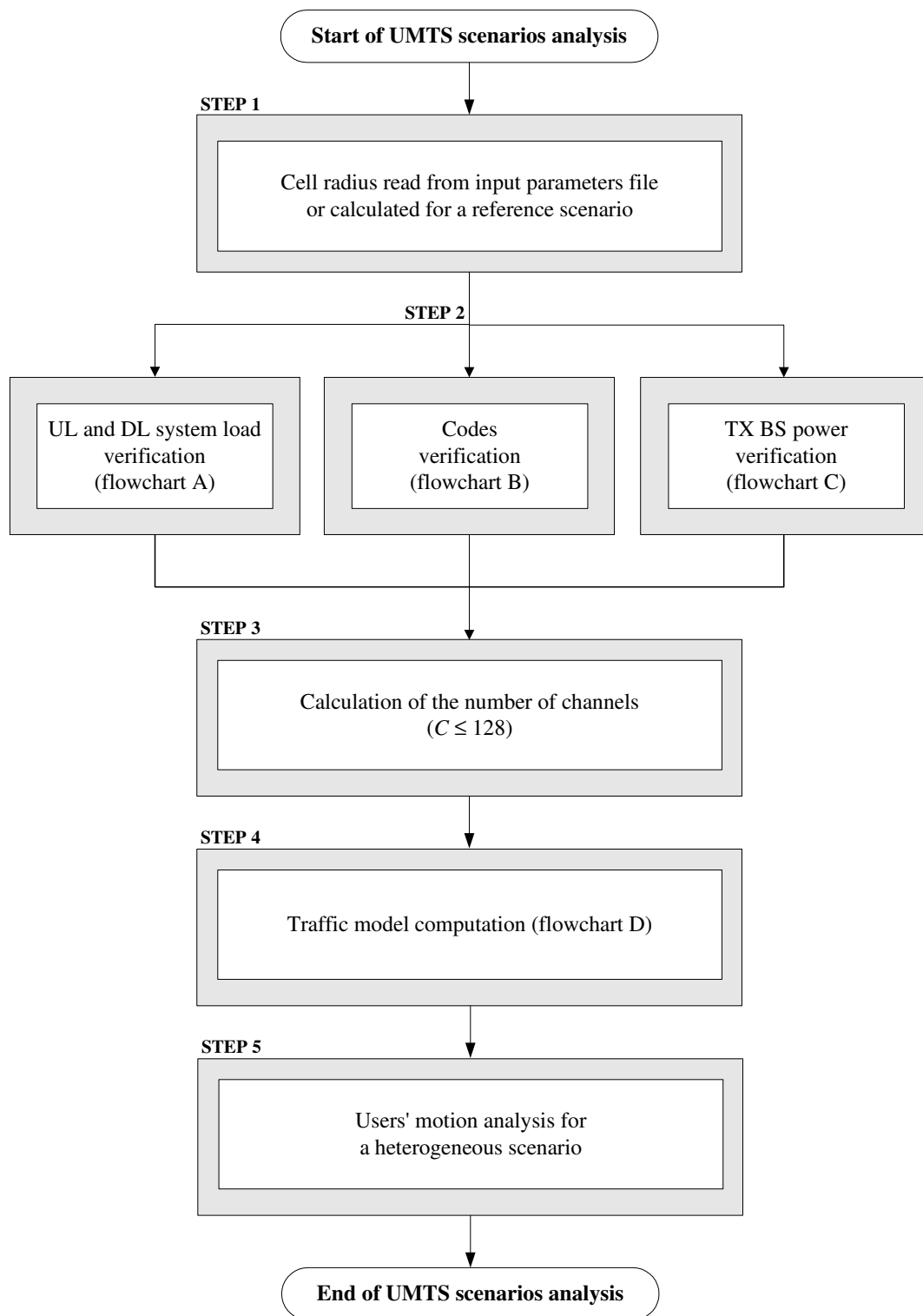


Figure 4.12 – Traffic model algorithm, main flowchart.

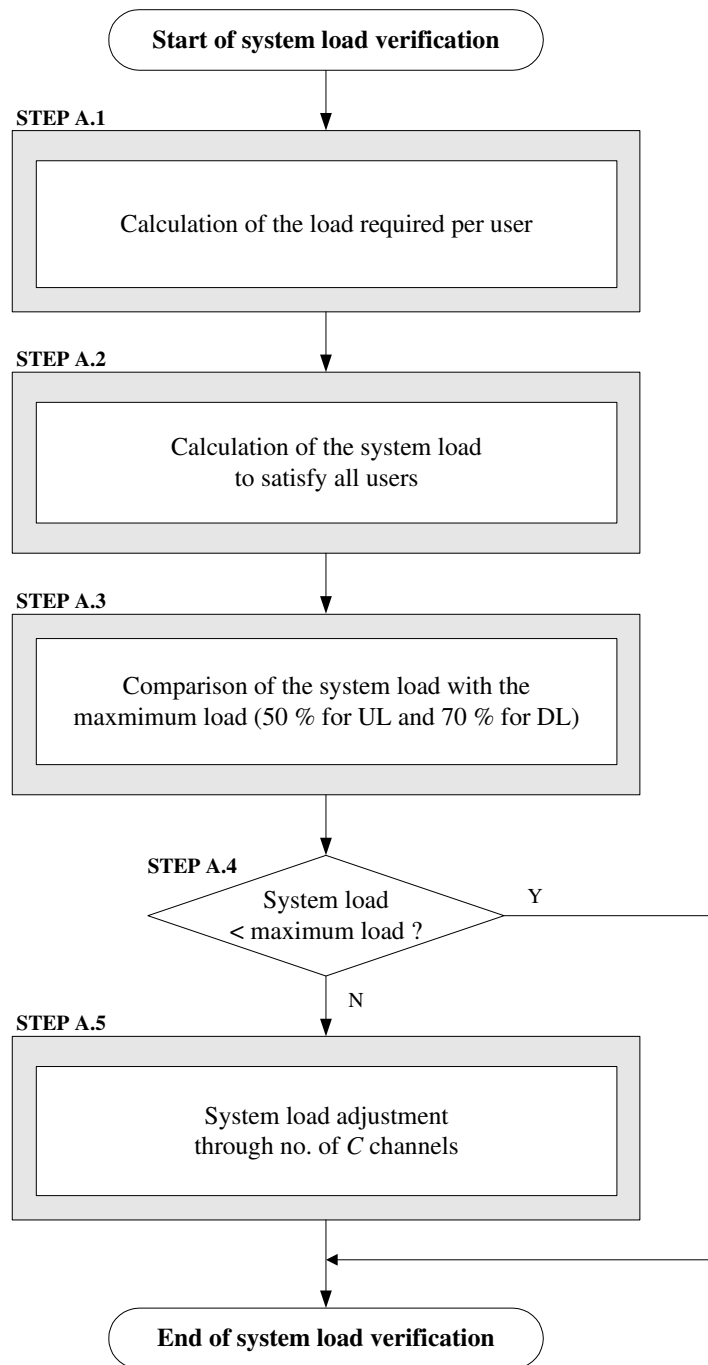


Figure 4.13 – System load verification, flowchart A.

4. Traffic model

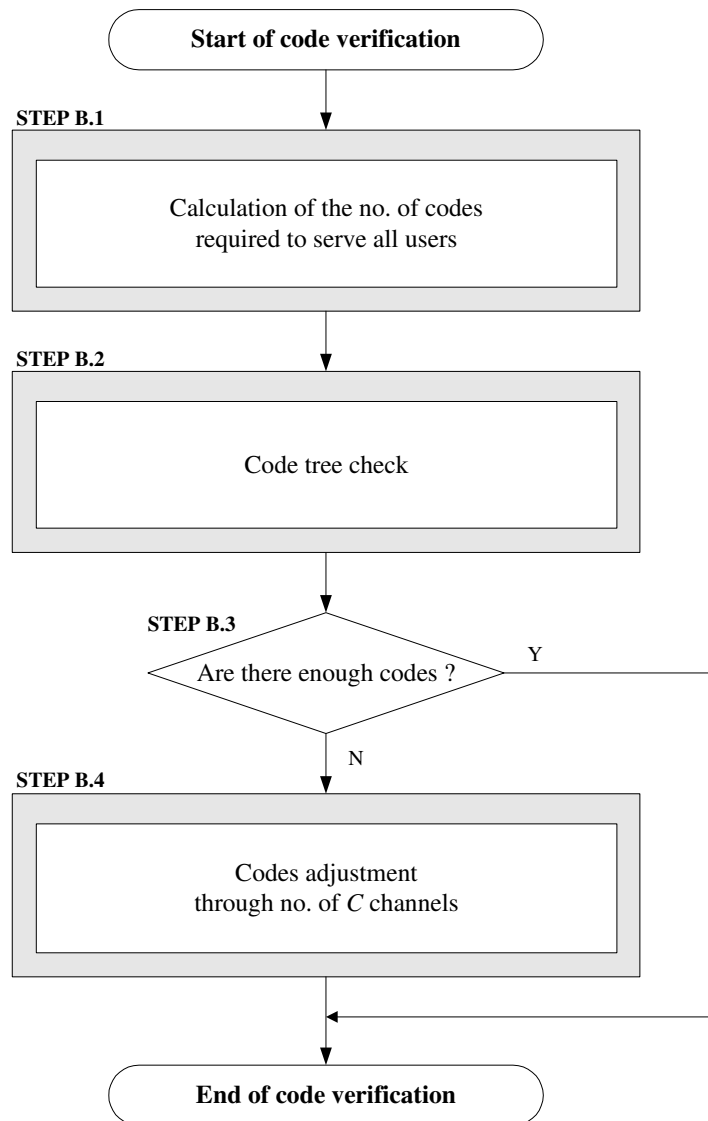


Figure 4.14 – Code verification, flowchart B.

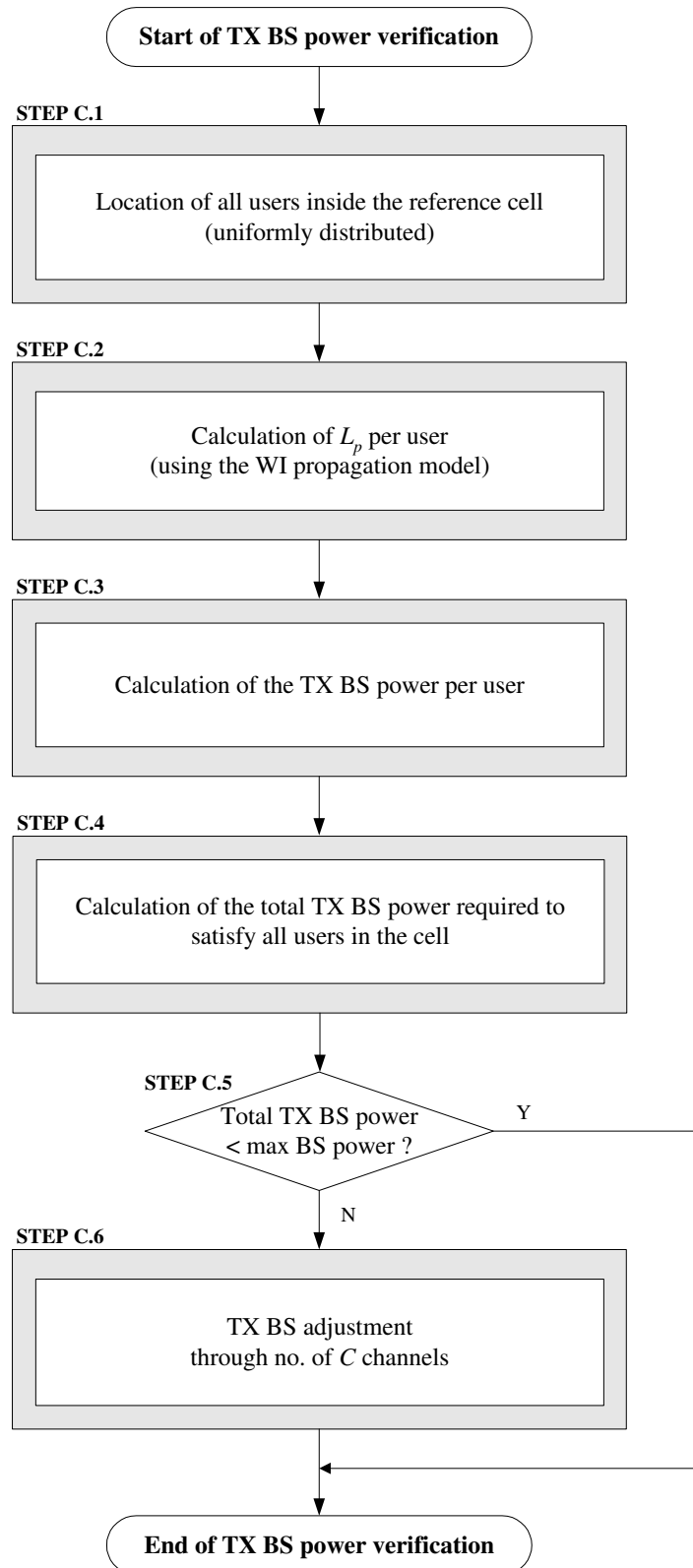


Figure 4.15 – BS power verification, flowchart C.

4. Traffic model

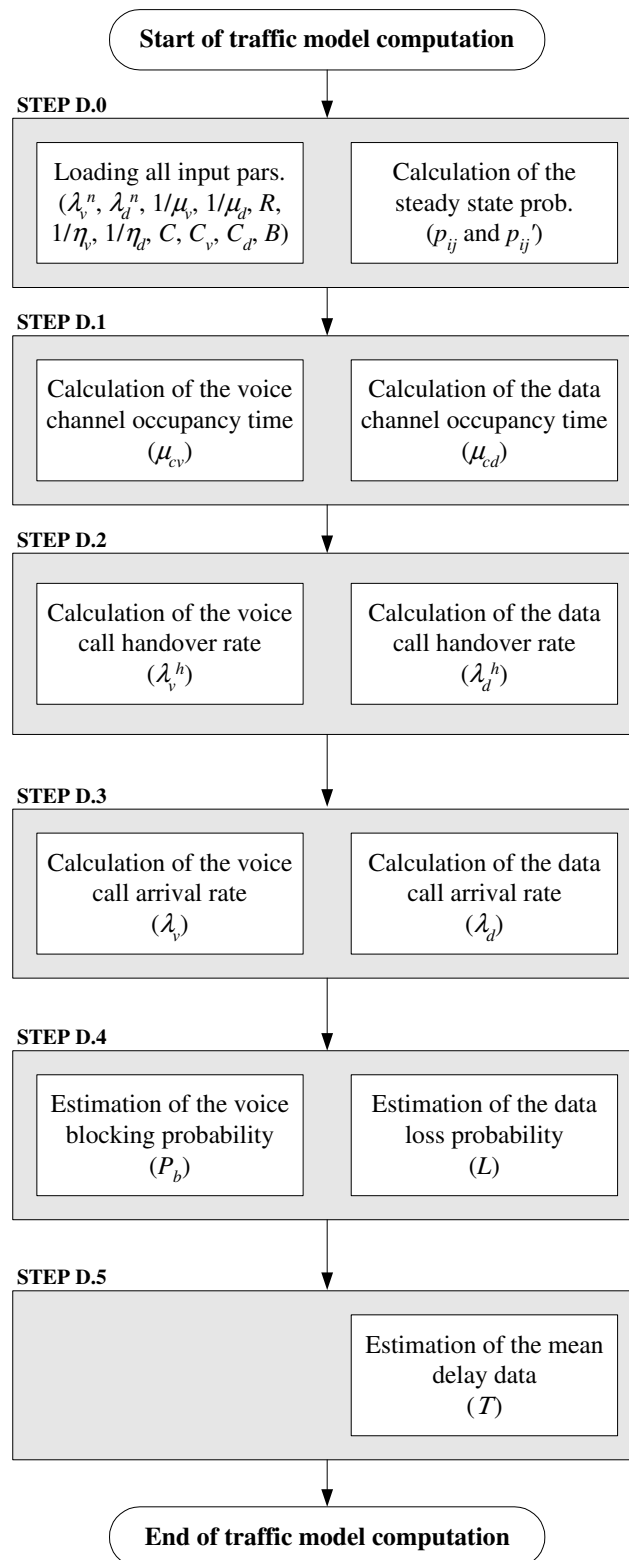


Figure 4.16 – Traffic model computation, flowchart D.

5 Analysis of results

5.1 Description of scenarios under study

Two different scenarios are analysed in this chapter, Table 5.1: one that weighs mainly a considerable amount of voice users and scarce data users, Scenario A, and another where the system load due to voice users is not as predominant as the one due to data users, Scenario B.

Table 5.1 – Number of users forming Scenarios A and B.

	Scenario A		Scenario B	
	UL	DL	UL	DL
Speech	80	80	10	10
VideoT	10	10	2	2
StrMMLQ	0	0	2	2
StrMMHQ	0	0	2	2
WWW	1	1	5	5
LocBas	1	1	2	2
MMS	2	0	5	0
Email	0	2	0	5
FDwnld	1	1	5	5

The traffic model is run for the number and type of users as specified, aiming at analysing the system performance in terms of voice call blocking probability, P_b , data loss probability, L , and mean data delay, T . The output of the model is provided as a function of the user's motion, between 0 and 120 km/h, and as a function of the buffer size, up to 20 MB. When the users' speed is under analysis, two different buffer sizes will be used: 20 MB and half of it, 10 MB; on the other hand, when the buffer size is the object of analysis, two different users' speeds are set: 15 km/h and 60 km/h.

Other parameters will be set to different input values at the start of the program, in order to study further the performance of the traffic model, e.g., the cell radii and the channel

5. Analysis of results

distribution among voice and data users (either equitable or proportional, as defined in Section 4.3).

Aiming at presenting results that may have similarities with UMTS networks at their launch, i.e., which will use essentially low bit rate bearer services, the DL channel bit rates to be applied will be based on the probability that the service is mapped onto particular bearers, namely 16, 32 and 64 kbps rather than 128 and 384 kbps, as suggested in [FCXV03]. Further basic services' characteristics (average voice call duration, average DL session volume, DL bearer rate and equivalent data call duration) are presented in Table 5.2; as it was mentioned in Section 4.2, the equivalent call duration for PS is obtained by knowing the average DL session volume and the channel bit rate, or, as an alternative to this last parameter, the SF and the relation (3.10).

Table 5.2 – Services characteristics (adapted from [FCXV03]).

Service	Average call duration [s]	Average DL session volume [kB]	DL bearer rate [kbps]	Equivalent data call duration [s]
Speech	120	-	32	-
VideoT	120	-	64	-
StrMMLQ	-	2250	64	300
StrMMHQ	-	2250	64	300
WWW	-	1125	32	300
LocBas	-	22.5	16	18
MMS	-	60	32	16
E-Mail	-	10	32	3
FDwnld	-	1000	64	133

The remaining input parameters, i.e., those that are kept equal in every program run, are presented in Table 5.3.

Two different cell radius values are used, aiming at studying the model behaviour with respect to this parameter. In order to find out the adequate values for cell radii, preliminary runs were performed for a reference radius of 200 m. Bearing in mind that this analysis is being done for a typical urban environment, the number of channels that is considered to find

the appropriate cell radius corresponds to those obtained for an average users' motion of 30 km/h, Table 5.4.

Table 5.3 – Input parameters common to Scenarios A and B.

Parameters	Values
DL codes	256
BS transmitted power [dBm]	43
Maximum UL load [%]	50
Maximum DL load [%]	70
Maximum buffer size [MB]	20
λ_{v100} [calls/s]	0.015
λ_{d100} [calls/s]	0.01

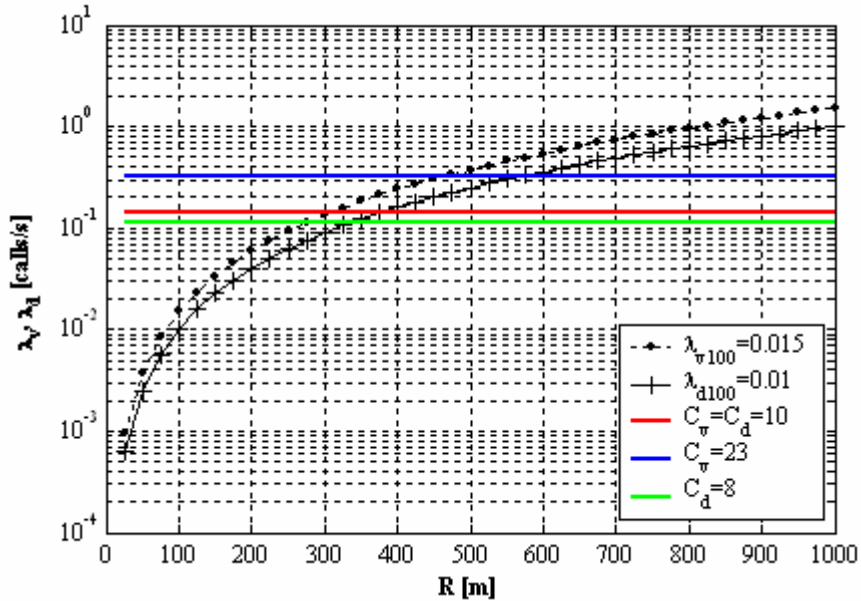
Table 5.4 – No. of codes for $R = 200$ m at 30 km/h, Scenarios A and B.

	Equitable distribution	Proportional distribution
Scenario A	$\tau_v = 120$ s and $\tau_d = 69.9$ s	
Total	63	63
Voice	21	47
Data	21	16
Shared	21	0
Scenario B	$\tau_v = 120$ s and $\tau_d = 134.5$ s	
Total	59	59
Voice	19	13
Data	19	46
Shared	21	0

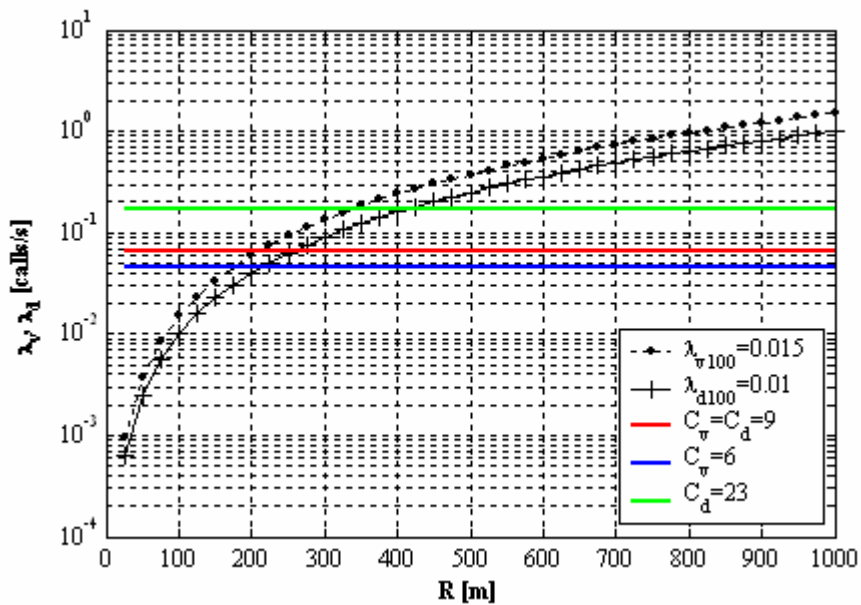
With the number of codes, the call rates and corresponding average duration, it is possible to define the cell radius values more accurately, as specified earlier in Section 4.2; the range of possible values is shown in Figure 5.1. Considering Scenario A, for an equitable distribution of channels, the cell radius may reach 300 m for voice and 400 m for data (red line); for a proportional distribution of channels, voice goes beyond 450 m (blue line), but data only allows a maximum of 350 m radius (green line). For Scenario B, the equitable distribution of

5. Analysis of results

channels allows voice at 225 m distance and data at 275 m, but the proportional distribution restricts voice to 175 m distance. The two values of cell radii to be chosen should be below or equal to 175 m; nevertheless, as this seems to be an extremely low limit and, Scenario A being the most probable one for the first years, the two cell radii values that are used henceforth are 150 m and 250 m.



(a) Scenario A.



(b) Scenario B.

Figure 5.1 – Possible cell radii.

5.2 Analysis of the number of channels

The number of codes obtained by simulating Scenarios A and B, for both 150 and 250 m cell radius, are presented in Figure 5.2 and Figure 5.3, respectively.

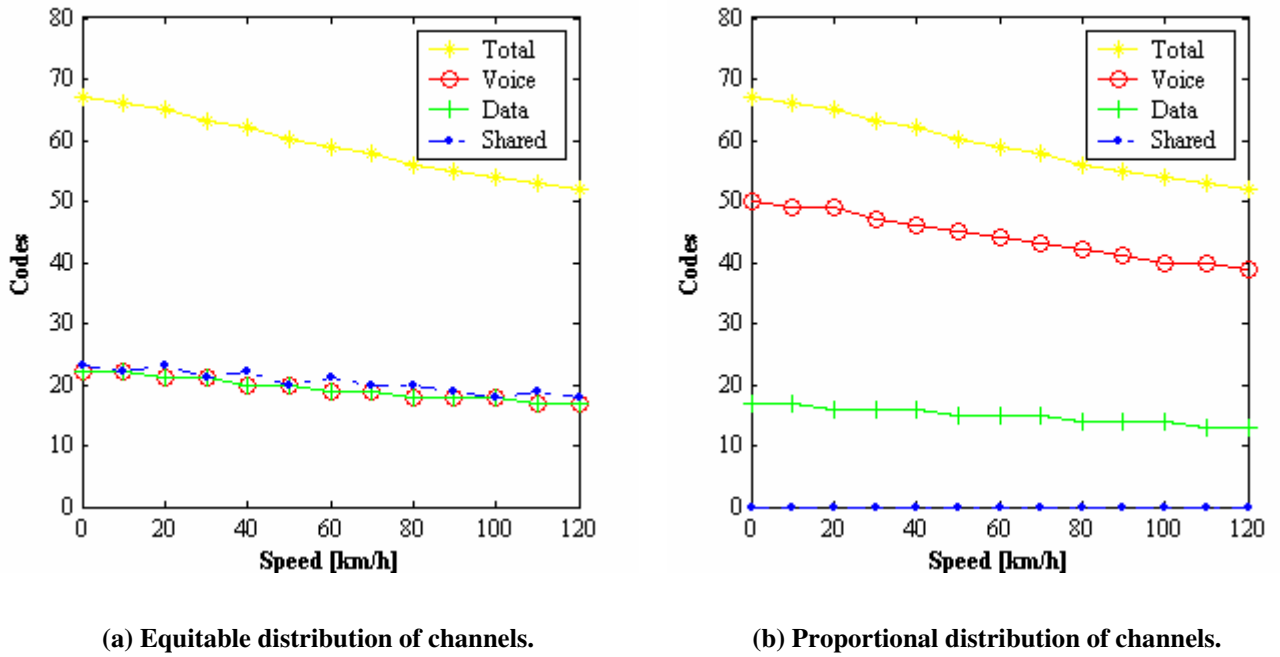


Figure 5.2 – Number of codes for Scenario A.

For Scenario A, the proportional distribution of channels, Figure 5.2 (b), shows that the majority of the available codes are devoted to voice users. On the other hand, it can be seen that in Figure 5.3 (b) the most important bandwidth will be provided to data users, those who are loading the system more. The proportional distribution of channels reflects better the real load of each service type, leading, as it will be seen later, to a better overall system performance than the equitable distribution.

Another additional comment arises concerning Figure 5.2 and Figure 5.3: as the users' speed increases, it is possible to observe that the number of channels provided by the system gets smaller. It is seen in Section 4.2 that the overall channels vary as a function of many factors: the system load on both UL and DL, the BS transmitted power and the number of DL codes; these parameters are dependent as well on other variables (e.g., E_b/N_0 , bit rate, orthogonal factor, losses, gains and other margins). The global tendency of the system results,

5. Analysis of results

considering all these varying parameters, corresponds to a decrease on the number of channels with a growing average users' speed.

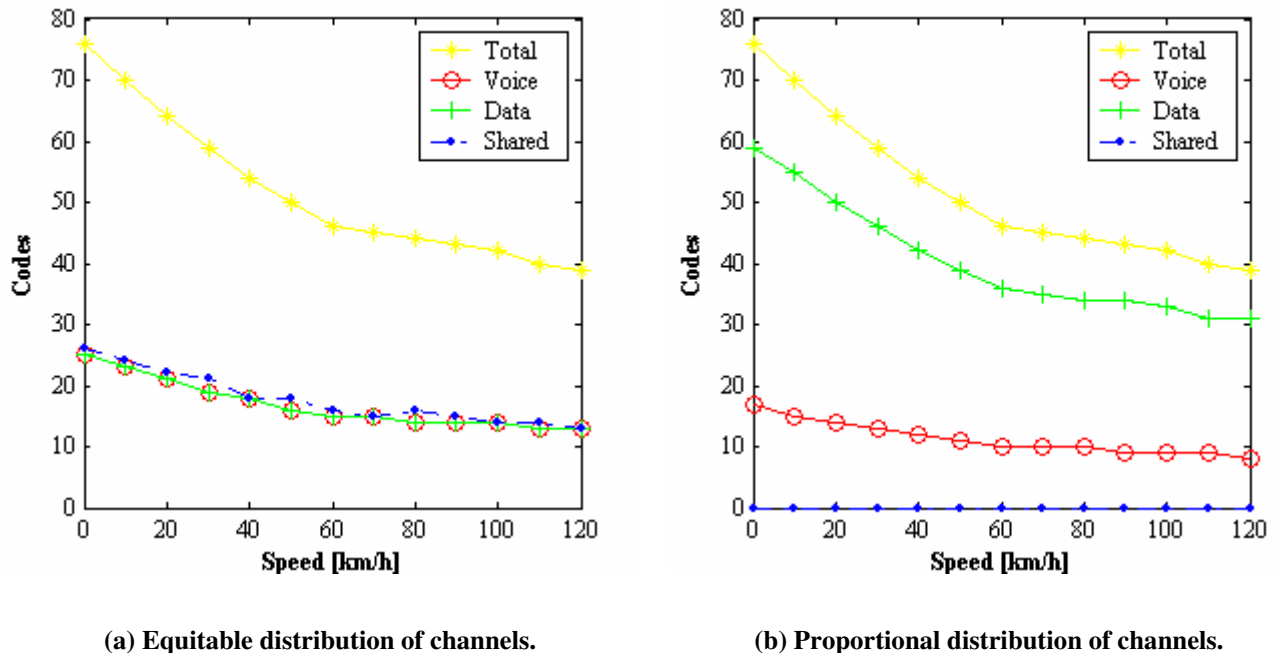


Figure 5.3 – Number of codes for Scenario B.

It has to be pointed out that, when applying radii of 150 and 250 m, the same numbers of codes as those shown in Figure 5.2 and Figure 5.3 are obtained for the corresponding scenarios; this is basically due to the fact that the system is exceeding the allowed load limits, 50 % on UL and 70 % on DL, whereas the BS power required to satisfy all users does not go beyond the limit of 43 dBm; if the BS transmitted power would correspond to the most severe limiting system factor, and as it depends on the position of the MTs with respect to the BS, the number of channels for two cells with different sizes would be distinct.

The channels in UMTS are not equally sized: the number of codes required per service, which is a direct result of the DL SFs, which, in turn, depends on the channel bit rates, will determine the size and quantity of the UMTS channels; considering a real scenario, with different users / services popping up, the instantaneous number of channels may present a discontinuous variation.

5.3 Comparison of traffic model results with known models

There are essentially two ways to validate the traffic model results: either by looking into real data and comparing it with the model output, or to use well known traffic models that may, for particular situations, represent accurately the reality. The level of development of network elements and terminals, achieved up to date, does not allow following either one or the other suggested approaches, *per se*, as they are not enough to test and certify the accuracy of the present traffic model.

There are currently very few UMTS networks in operation around the world; moreover, the amount of UMTS terminals already in the market is so small and their prices are still so high, that the current users do not yet represent on average the overall population and its behaviour; thus, the analysis of real data needs to be postponed for a later point in time, when some actual and reliable UMTS traffic information is made available.

As far as the comparison of known traffic models against the present one is concerned, it is also not a straightforward task. There are currently no models that allow simultaneously multi-service traffic, thus, with diverse characteristics. Consequently, it was decided to separate voice from data and compare only the voice call blocking probabilities obtained with the results of the Erlang-B model; due to the UMTS characteristics embedded in the model, e.g., the variable number of channels as a function of instantaneous environment conditions, it is not expected that the traffic model results match completely the Erlang-B ones. With respect to data services, and as none of the known models present similarities with the nature of the traffic model under analysis, no comparison in terms of data losses and delays aiming at validating the traffic model behaviour for data is possible.

As said in Chapter 3, the Erlang-B model does not have capability to store any call that cannot be served due to lack of resources, meaning that users willing to enter the system while there are no available channels are simply lost (blocked calls are cleared); this is basically what happens with voice users emulated through the traffic model, as no buffering for this kind of calls is foreseen.

The blocking probability for an Erlang-B model is given by (3.25), and, by varying the amount of traffic, A , between 1 and 100 Erlang, for systems with, e.g., 8, 16, 32 or 64 voice

5. Analysis of results

channels, is given by Figure 5.4. When the number of channels becomes smaller, it is visible that the blocking probabilities, for the same amount of traffic, increase.

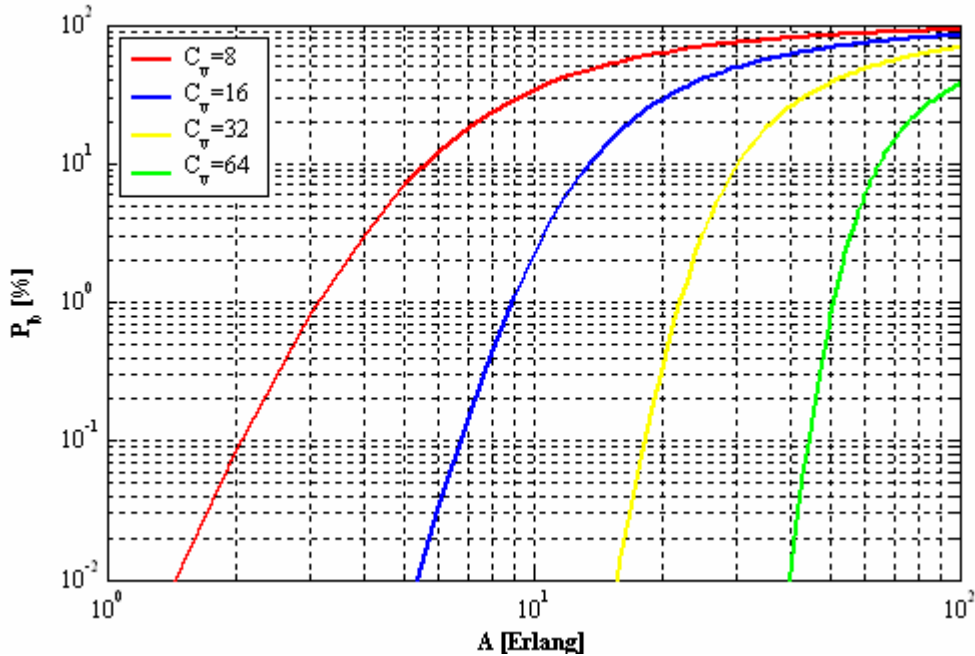


Figure 5.4 – Blocking probability for Erlang-B model.

To obtain the exact number of voice channels, C_v , for each scenario under analysis, the first block of the traffic model algorithm is implemented (steps 0 to 3, as specified in Chapter 4); the resulting values are plotted in Figure 5.5; these will be used in the Erlang-B model to calculate the traffic.

It should be pointed out that the call rates used for Scenarios A and B, for the purpose of comparing the traffic model results with other known traffic models, correspond to the ones obtained by considering a 250 m cell radius; both new and HO calls are accounted for.

The blocking probabilities, obtained through the traffic model, Figure 5.6, and the Erlang-B model, Figure 5.7 and Figure 5.8, are plotted for users' speeds of 30, 60, 90 and 120 km/h.

Scenario A being a predominant voice users' scenario, and, knowing that voice does not load extremely the system, the model does not lead to reflect any probability of blocking, i.e., it is below 10^{-2} %. With respect to Scenario B it is the other way around, as there is much more

load due to data than voice calls, especially for the proportional distribution of resources; while the number of channels for voice users decreases, it imposes an increase on the blocking probability when obtained through the current traffic model; this is visible in Figure 5.6 for the proportional distribution of channels, where few resources are left for voice; with respect to the equitable distribution of channels, and, as can be seen, only for very high average speeds, e.g., 120 km/h, a blocking probability greater than 10^{-2} % is experienced.

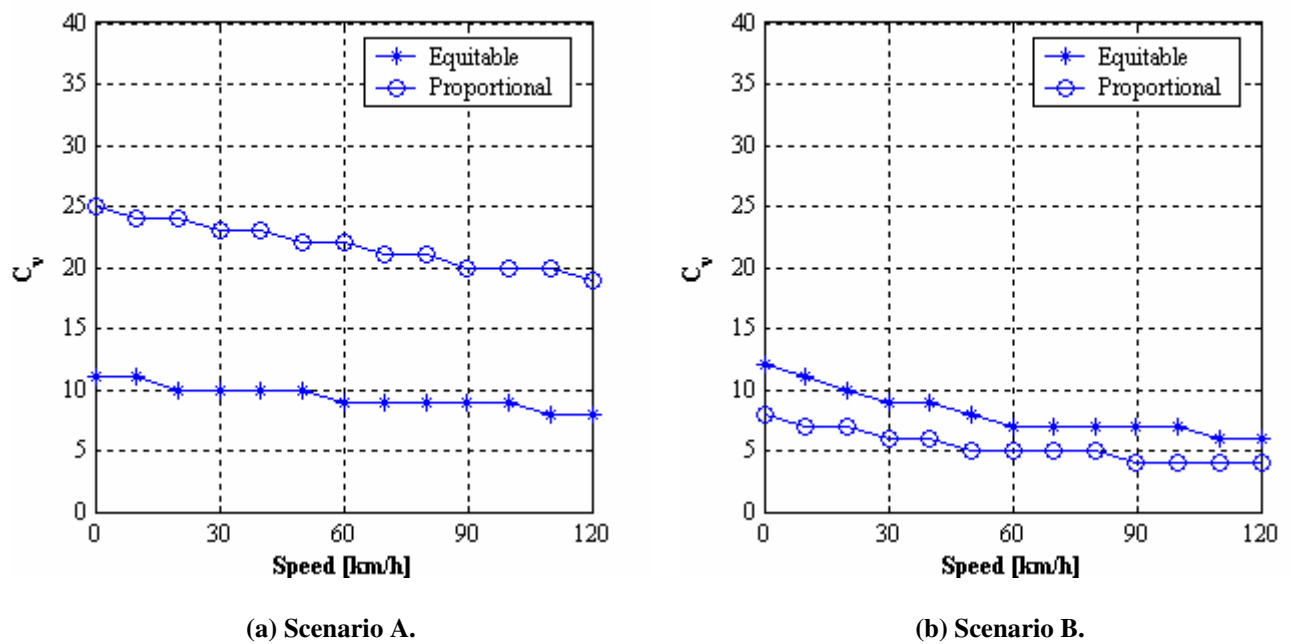


Figure 5.5 – Available voice channels versus users' speed.

A clarification needs to be done with respect to the Erlang-B calculations, to perform the comparison with the traffic model: the speeds for which the models' results are to be compared (the ones mentioned earlier), are converted into a specific number of channels, plotted in Figure 5.5; those numbers of channels are used to obtain the amount of traffic through (3.17); afterwards, by applying the Erlang-B model, one obtains the corresponding blocking probabilities. Figure 5.7 and Figure 5.8 show the resulting P_b for Scenarios A and B.

It is possible to observe in Figure 5.7 (a) and Figure 5.8 (a) that the results for the equitable distributions from the two scenarios are similar, as a consequence of the number of voice channels, which is almost equal, Figure 5.5.

5. Analysis of results

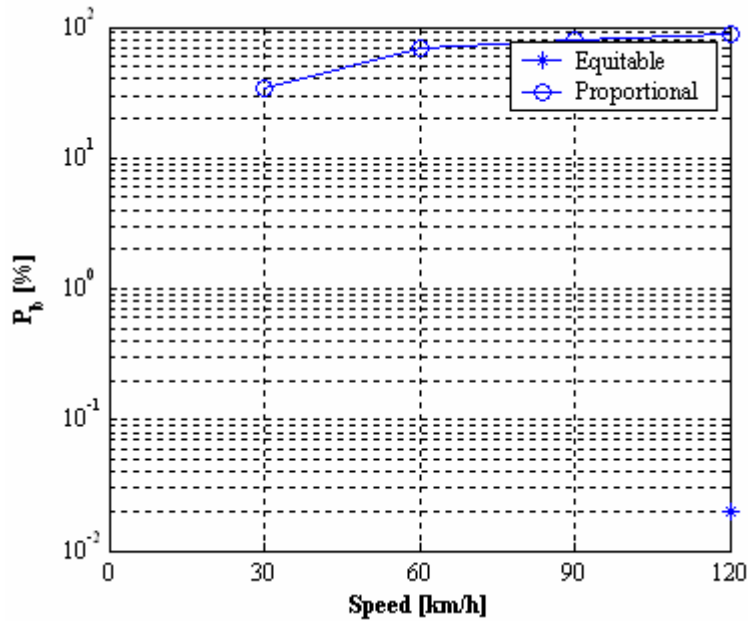
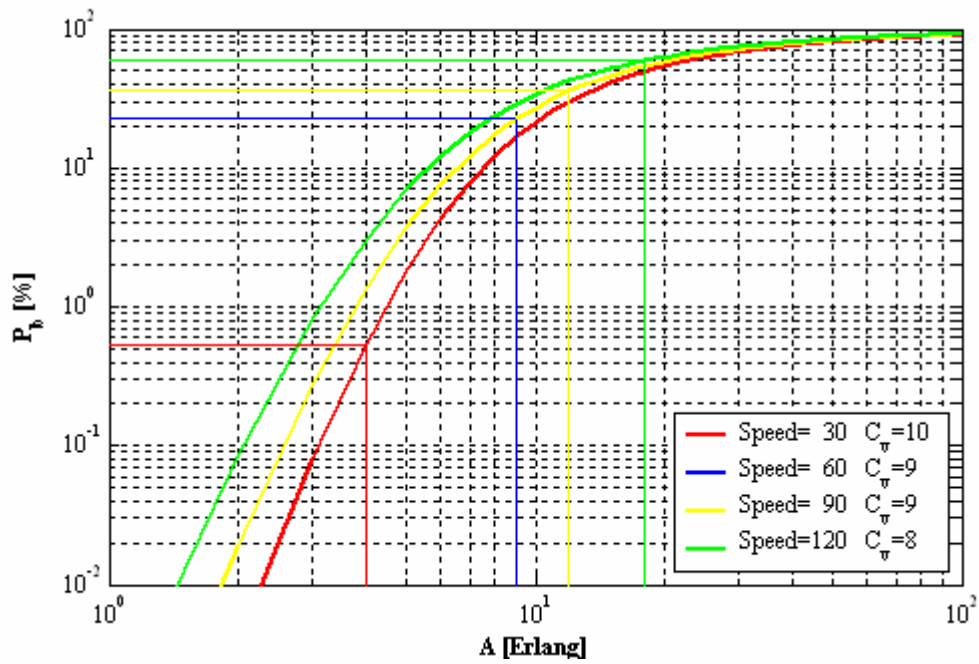


Figure 5.6 – Traffic model blocking probability for Scenario B.

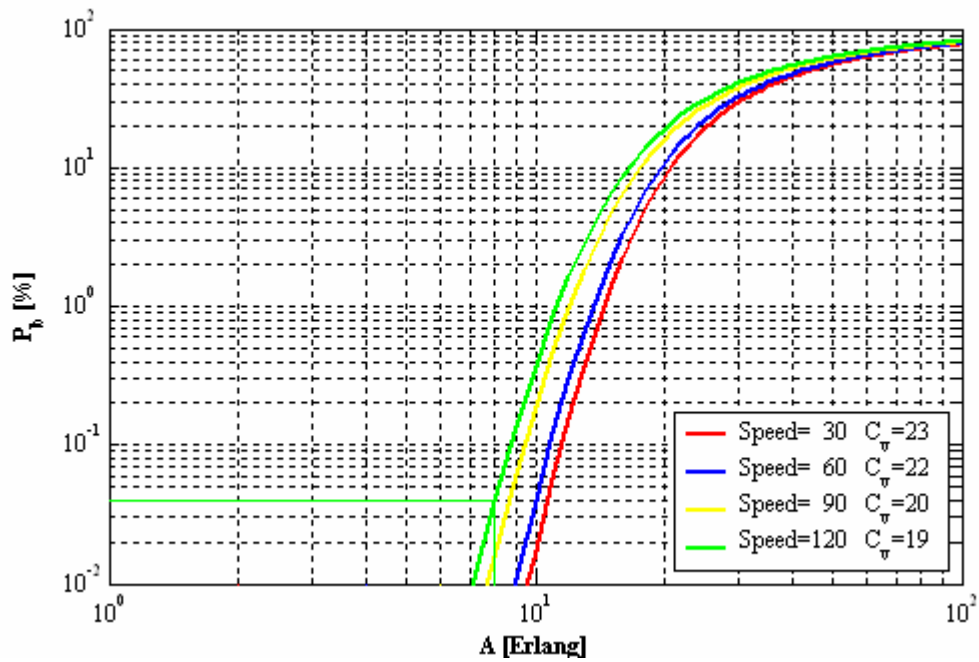
Another aspect that should be noted is the fact that in Figure 5.7 (a) and in Figure 5.8 (a) and (b), there are some overlapped curves; this happens when the number of channels does not change for different users' speeds, Figure 5.5, leading the corresponding blocking probability curves, obtained through the Erlang-B model, to be overlapped.

It becomes clear from Figure 5.6, Figure 5.7 and Figure 5.8 that, for the same amount of channels, the Erlang-B model presents higher blocking probabilities than the traffic model under analysis, being the attained values rather significant, not negligible. Additionally, it is possible to note that, when the system delivers relatively few channels for voice, the two models present very similar results: the curves for the proportional distribution of channels in Figure 5.6 and Figure 5.8 (b) show visibly this analogous behaviour; in contrary, when the amount of voice channels increases, the results from the two traffic models no longer agree, the Erlang-B model showing, as known, to be a conservative traffic model.

It has to be mentioned that all the modifications required to adapt the model of [HaLH00] to a UMTS network model, as detailed in Section 4.2, made it rather complex; quite many security margins were introduced all over the planning steps (e.g., $M_{log-normal}$, $M_{fast-fading}$, η_{UL} , η_{DL} , and others), while defining parameters and calculating partial results; it is clear that the model needs further refining, after real data is available, to tune it into a realistic and trustful model.



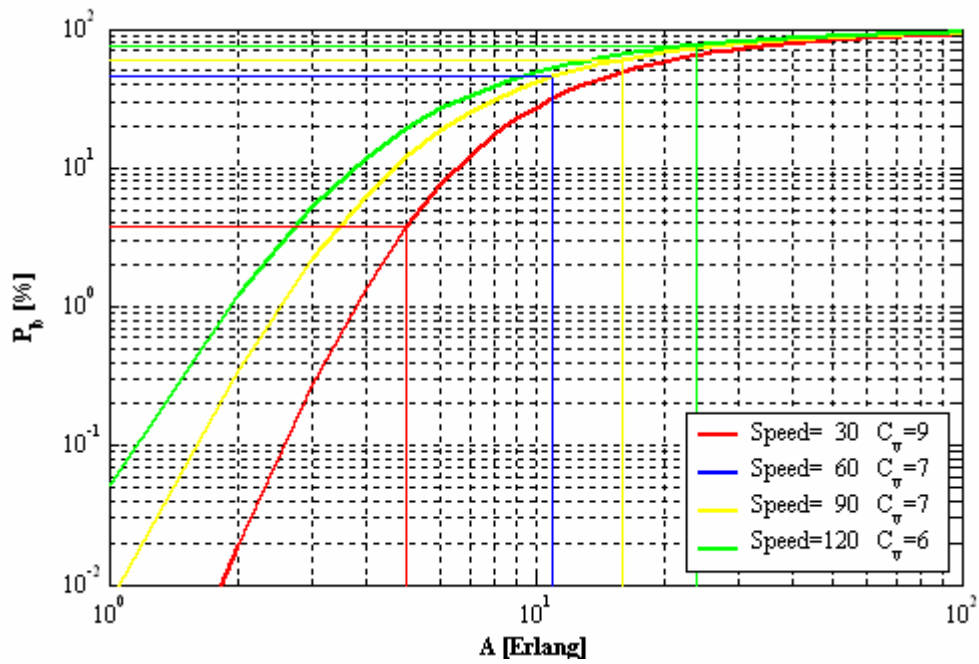
(a) Equitable distribution of channels.



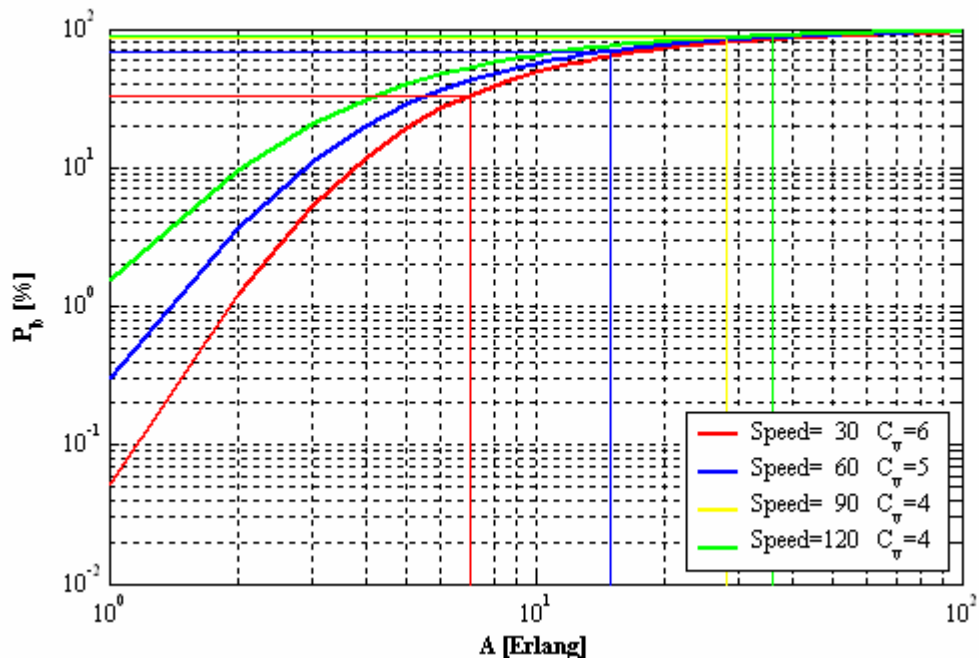
(b) Proportional distribution of channels.

Figure 5.7 – Erlang-B model blocking probability, Scenario A.

5. Analysis of results



(a) Equitable distribution of channels.



(b) Proportional distribution of channels.

Figure 5.8 – Erlang-B model blocking probability, Scenario B.

5.4 Results for a single cell

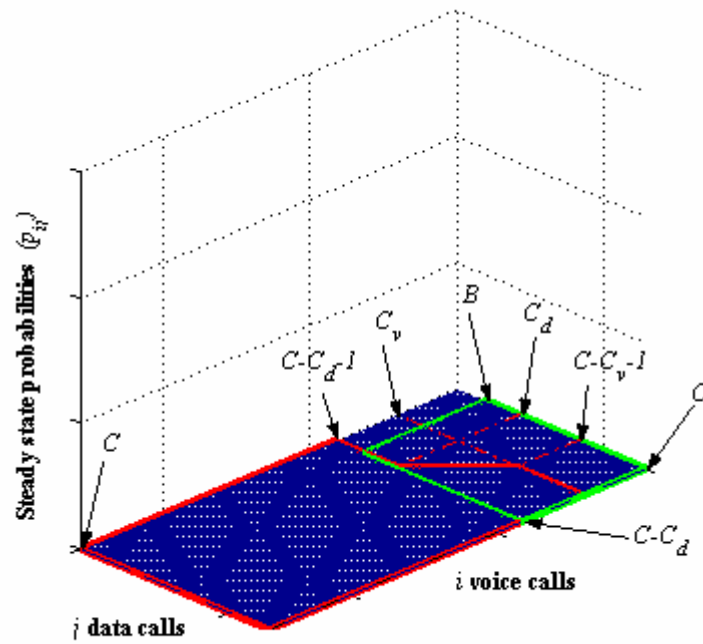
Voice and data call rates, λ_v and λ_d , obtained by knowing the effective cell radius and the reference rates listed in Table 5.3, together with the (equivalent) average call duration considered in Table 5.2, τ_v and τ_d , and weighed against the number of users, fix the amount of traffic in the system. The model is forced to support a specific amount of traffic, $[(\tau_v, \tau_d), (\lambda_v, \lambda_d)]$, and two times that quantity, $[(2\tau_v, 2\tau_d), (\lambda_v, \lambda_d)]$ or $[(\tau_v, \tau_d), (2\lambda_v, 2\lambda_d)]$.

Before going into a more detailed analysis of the traffic model results, it is worthwhile to provide an explanation on the behaviour of the three parameters that are under discussion: voice call blocking probability, P_b , data loss probability, L , the mean data delay, T .

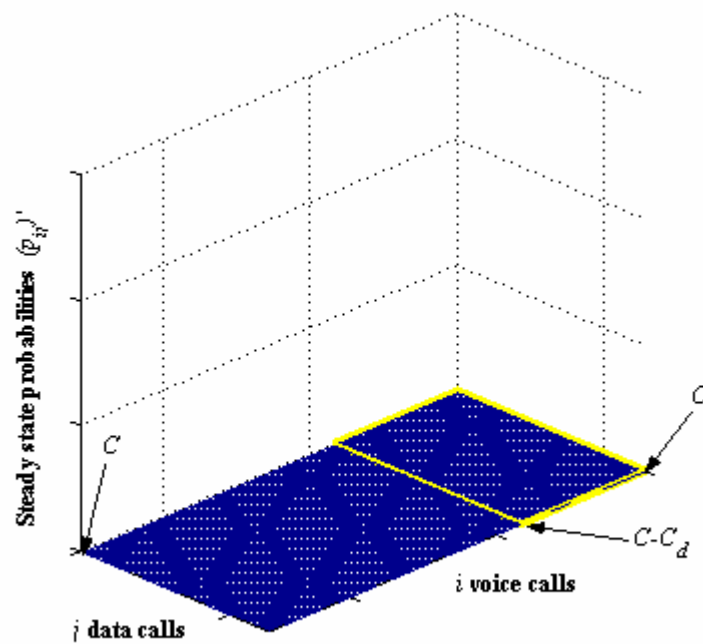
According to the principles of the traffic model, P_b is calculated through (4.5), meaning that its resulting value corresponds to the sum of a number of p_{ij} elements, and depends on the number of channels available. If the condition $C_v \leq C - C_d - 1$ is satisfied, those p_{ij} fall inside some red delimiters as drawn in Figure 5.9 (a) (e.g., when the total amount of channels is equitably distributed between voice and data users); otherwise, these boundaries may be represented as in Figure 5.10 (a) and Figure 5.11 (a) (e.g., when the available channels are proportionally distributed to the users that compose the scenario under analysis; in case there are more voice users than data, Figure 5.10 applies; for more data users, Figure 5.11 is a better illustration of the situation). It is clear from those figures that P_b is smaller when there are a large number of channels devoted to voice users; if, contrariwise, there are very few voice channels, the P_b influence area gets more extended and further voice calls get blocked.

L is also dependent on p_{ij} , and on the size of the buffer, B ; the data loss probability is, for the purpose of the current traffic model, obtained through (4.7). Similarly to P_b , L does have an influence area as well, graphically delimited through the green frames from Figure 5.9 (a), Figure 5.10 (a) and Figure 5.11 (a). Undoubtedly, the greater the number of data channels, C_d , and B , the smaller the area inside the green borders; consequently, L decreases. If either the buffer is small or the data channels are reduced, that same influence area increases and more packets may get lost.

5. Analysis of results

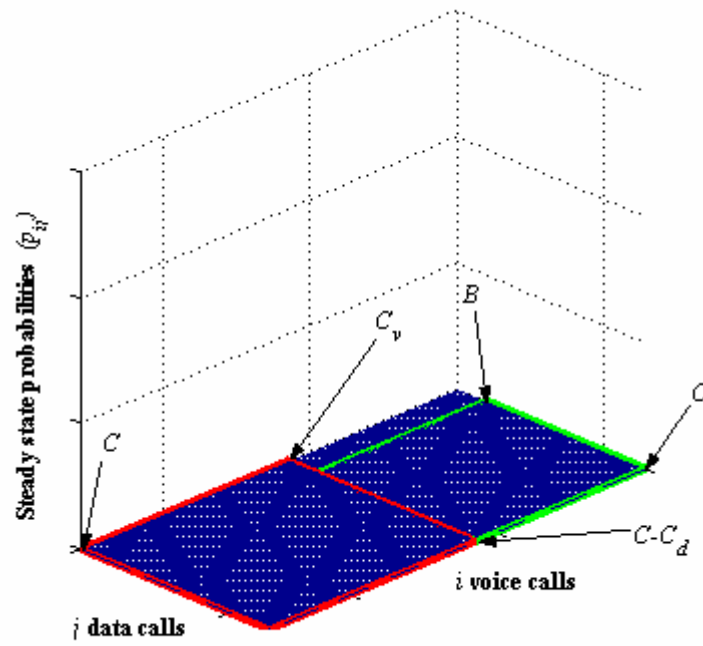


(a) p_{ij} matrix.

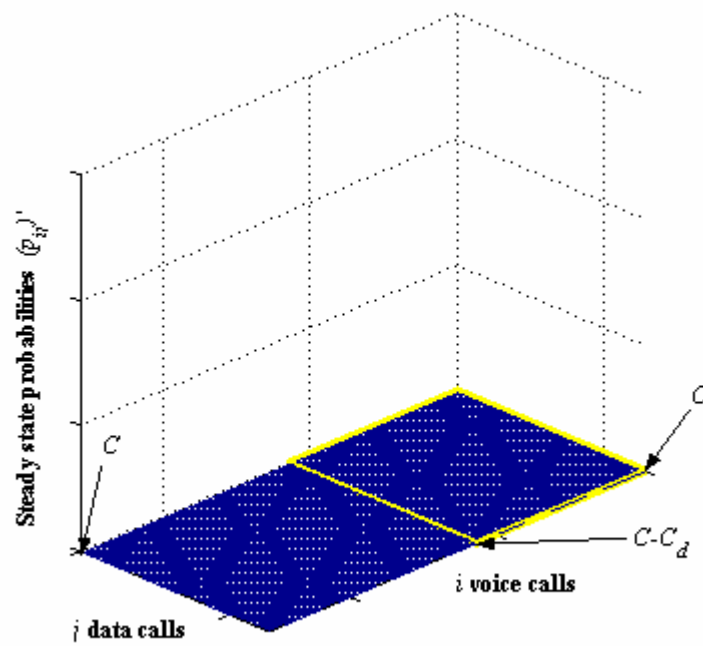


(b) p_{ij}' matrix.

Figure 5.9 – Equitable distribution of channels.



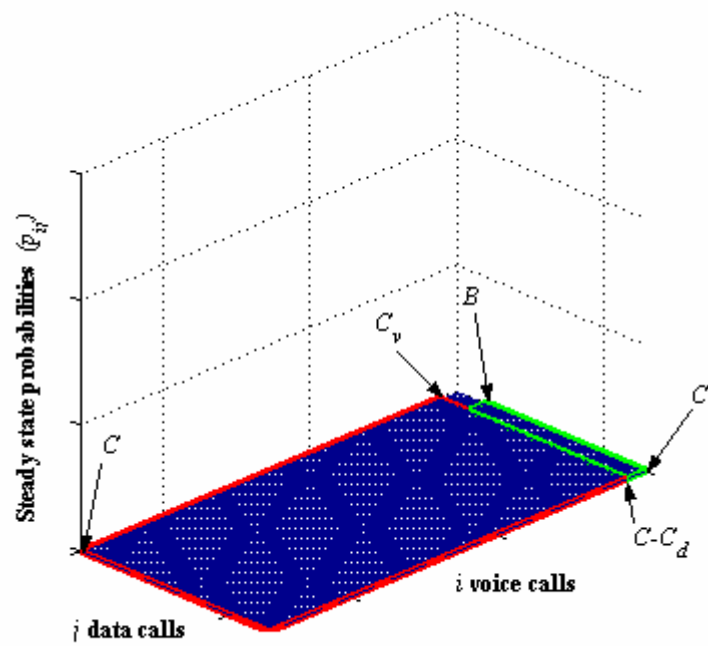
(a) p_{ij} matrix.



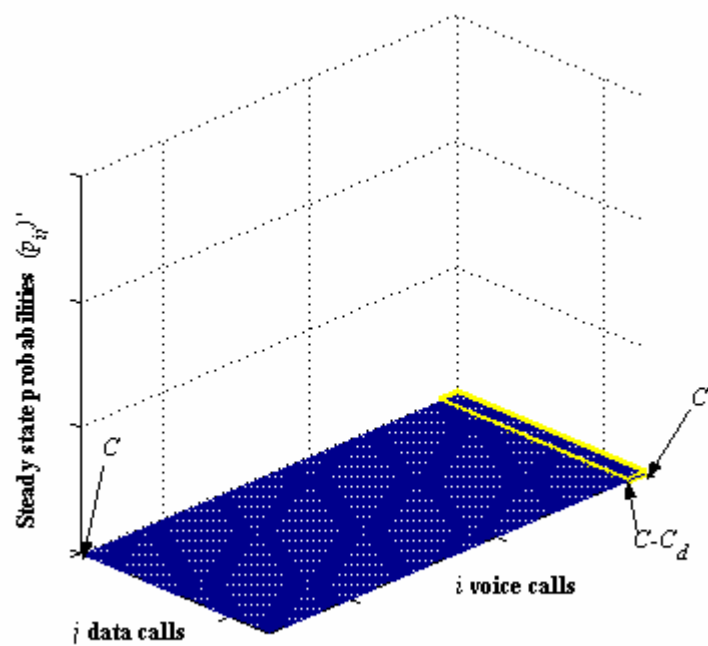
(b) p_{ij}' matrix.

Figure 5.10 – Proportional distribution of channels, predominant voice users.

5. Analysis of results



(a) p_{ij} matrix.



(b) p_{ij}' matrix.

Figure 5.11 – Proportional distribution of channels, predominant data users.

Finally, the tendency of the last system parameter, the mean data delay, shall be analysed. From (4.9), a non-straightforward behaviour of T is to be expected: there are three variables that influence the final result, namely, the differentiation of the probability matrix p_{ij} , hereafter referred to as p_{ij}' matrix, the data call rates, λ_d^n and λ_d^h , and the data loss probability, L . The p_{ij}' influence area is shown in Figure 5.9 (b), Figure 5.10 (b) and Figure 5.11 (b), for the distribution of channels mentioned earlier; it becomes visible from those figures that the number of p_{ij}' elements that contribute to T is higher when data channels are reduced. T varies inversely with the data call rates (new and handover), and, as it was already referred earlier, there is a straightforward connection between cell radius and data call rates, as well as users' speed and handover call rates; considering simply the aspects that affect data call rates, another conclusion is reached: T decreases for higher radii and for higher users' speeds. The third aspect that influences T is L : as L rises, T tends to follow that behaviour. These three aspects assume, for specific values, rather different weights: one or the other becomes predominant or irrelevant, depending on the various inputs that are being given to the traffic model, instead of assuming a clear tendency.

The complete results of the traffic model behaviour for Scenarios A and B is presented in Annexes C and D, respectively. Some important and determinant aspects are nevertheless addressed in what follows.

The traffic model is forced to react to the variation of four basic system parameters:

- average speed at which users' move around;
- cell radius for which the analysis is being performed;
- buffer size;
- channels' distribution between voice and data users.

As expected, the average speed at which users move around influences decisively the results of the traffic model. A first aspect that justifies this comment is the number of channels supported by the system when users' speed varies; when adapting the traffic model under analysis to UMTS (Section 4.2), the number of channels is made dependent on three system aspects: UL/DL loads, BS transmission power and available DL codes. UL/DL loads, as well as the BS transmission power, depend, among others, on E_b/N_0 values, which are strictly

5. Analysis of results

connected to the users' speed. A reduction on the amount of channels made available by the system with an increase on the users' speed is clearly visible in Figure 5.2 or Figure 5.3, as well as on the complete sets of results presented in Annexes C and D.

When there is a reduction on the number of channels with speed increase, the voice call blocking probability will be affected: the top limit of the P_b influence area (red borders) gets closer to the beginning of the probability matrix and more p_{ij} elements are thus summed up. Figure 5.12 shows clearly this tendency, especially for higher traffic values, $[(2\tau_v, 2\tau_d), (\lambda_v, \lambda_d)]$ or $[(\tau_v, \tau_d), (2\lambda_v, 2\lambda_d)]$; the input data corresponds to Scenario B with a cell radius of 250 m, a 20 MB buffer size and channels distributed equitably among users.

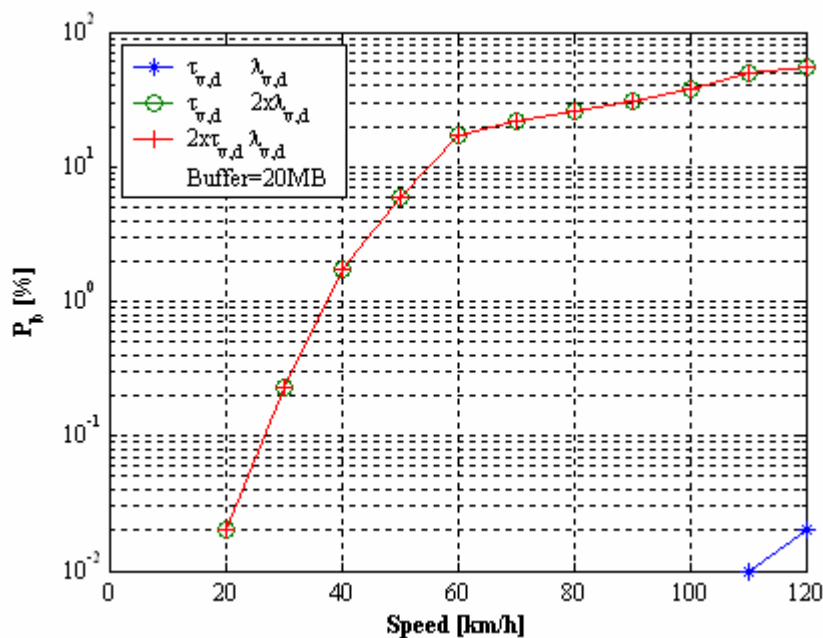


Figure 5.12 – Blocking probability as a function of users' speed.

Both the green and the red curves are overlapped in Figure 5.12; this results directly from the fact that when either the call duration or the call rates are doubled, the consequence is the same and corresponds to doubling the amount of traffic in the system. The blocking probabilities for $[(\tau_v, \tau_d), (\lambda_v, \lambda_d)]$ are, for any speed up to 120 km/h, kept at a rather negligible value; in contrary, when the amount of traffic in the system doubles, the blocking probabilities assume, for average speeds higher than 60 km/h, values above 2 %, beyond the acceptable threshold commonly used in GSM.

With respect to L , and considering solely the channel number aspect (the buffer effect will be analysed later on), it can be said that reducing channels in general means approximating the bottom limit of the L influence area (green boundary) to the beginning of the probability matrix; clearly, less p_{ij} elements will count for L when users' speed is increased, Figure 5.13.

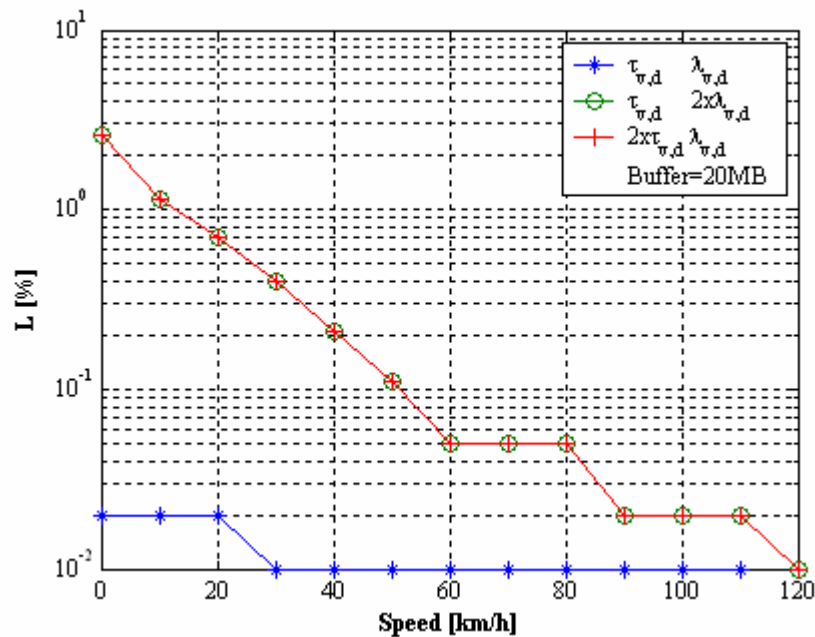


Figure 5.13 – Data loss probability as a function of users' speed.

These results were obtained for Scenario B, considering a cell with 250 m radius, 20 MB of buffering capability and channels distributed proportionally among voice and data.

It is visible in Figure 5.13 that the red and the green curves are overlapped, due again to the fact that the p_{ij} matrices coincide for these two situations. For lower traffic amounts, e.g., the blue curve, the effect of an increase on speed is smoother than for higher traffic values; the p_{ij} influence area is, in this case, more distant from the green borders, meaning that an increase on the users' speed does not push straight away the relevant p_{ij} elements out of the boundaries that determine L , as is the case – when the amount of traffic in the system is high.

Increasing users' speed means, thus, less channels and the p_{ij} ' influence area decreases as well; the overall data call rates also augment with speed; finally, as mentioned earlier, L gets smaller with higher speeds, leading to a decrease of T . These three variables will altogether

5. Analysis of results

impose its tendency on T , yielding its decrease with speed increase, Figure 5.14; the input values are equal to those from Figure 5.13.

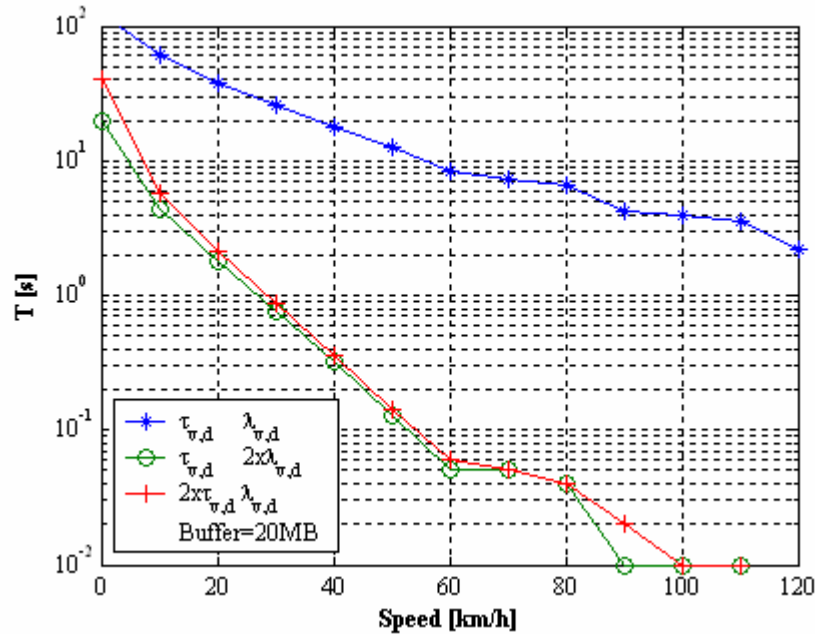


Figure 5.14 – Mean data delay as a function of users' speed.

The mean delays obtained for $[(2\tau_v, 2\tau_d), (\lambda_v, \lambda_d)]$ and $[(\tau_v, \tau_d), (2\lambda_v, 2\lambda_d)]$ do not coincide, as they do not depend exclusively on the p_{ij} ' elements falling inside the yellow borders; as seen earlier, the call rates and loss probabilities play also a role in the overall result of T .

Two additional results observable in Figure 5.14 shall be pointed out: an increase on the users' speed and on the amount of traffic leads to a reduction on the mean delays. Augmenting the users' speed means that the cell cross-over rate grows (3.11), and, as a consequence, the HO call rates, (3.24), and overall call rates, (3.16), increase; as a result, the predominant p_{ij} ' elements are pushed out of the yellow influence area, leading T to decrease. When, on the other hand, there is an increase on the traffic amount, the same occurs to the p_{ij} ' elements and T gets smaller as well. This behaviour is opposite to what is to be expected: as there is an increase on the amount of traffic in a system, it is more likely that the mean delays increase than the other way around, as the system has to deal with more information. Thus, despite of the fact that the traffic model formulation imposes this tendency [HaLH00], it does not seem to be adequate to reflect in a correct way the users' mobility and variation on the

traffic amount. It is important to refer that this is a point where a tuning of the model is clearly required, to correct this abnormal behaviour with respect to the data packet mean delays.

When forcing the traffic model to react to the variation of the cell radius, further conclusions are reached. When augmenting the cell radius, the call rates increase and, consequently, the predominant p_{ij} elements may slightly shift to the centre of the probability matrix. The red delimiters, influencing P_b , encompass more matrix elements; for this particular buffer size, the p_{ij} elements falling inside the green borders turn also to be higher; thus, the voice blocking and the data loss probabilities grow, Figure 5.15 and Figure 5.16. In contrast, the yellow borders, which are not influenced directly by the buffer size, contain less predominant p_{ij} elements and T could decrease; on the other hand, as L grows, T may as well rise up; finally, increasing the call rates leads T to get reduced; the final tendency of T is not very straightforward, but results from weighing these three components and identifying which one(s) impose its behaviour at each instant.

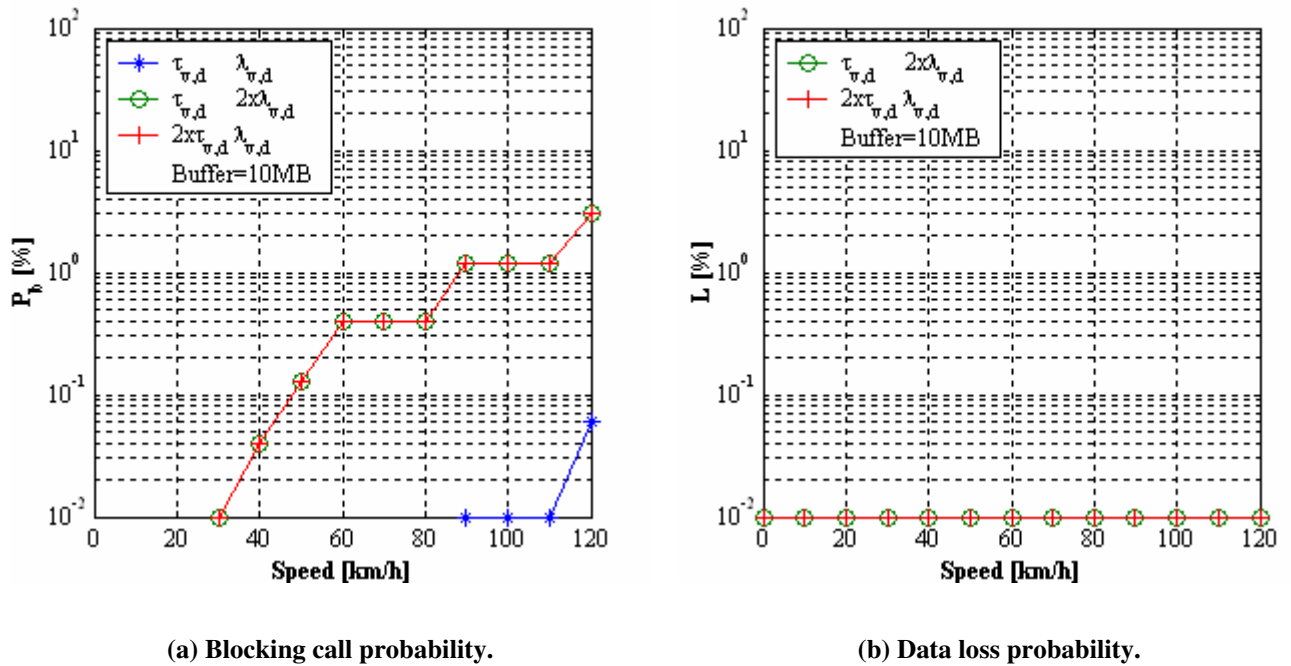


Figure 5.15 – P_b and L as a function of the users' speed, for $R = 100$ m.

Figure 5.15 and Figure 5.16 result from running the traffic model for Scenario B with a 10 MB buffer, considering a proportional distribution of channels, and the cell radius being set to 100 and 200 m, respectively.

5. Analysis of results

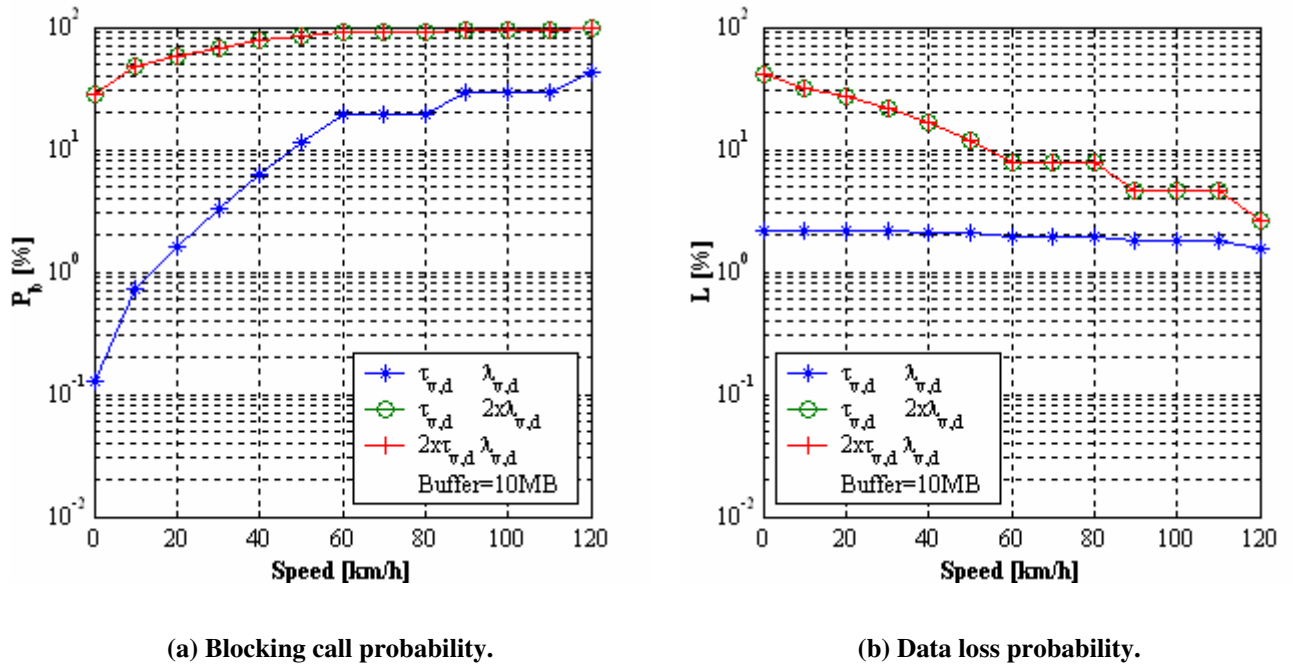


Figure 5.16 – P_b and L as a function of the users' speed, for $R = 200$ m.

It has to be pointed out that for a 10 MB buffer and a 100 m radius, Figure 5.15 (b), the data loss probabilities assume rather very small values, for the scenario under analysis: for high traffic, it only reaches 10^{-2} % and the users' speed does even not influence L .

There are two tendencies that may additionally be observed in Figure 5.15 and Figure 5.16: first, when increasing the users' speed, P_b increases and L gets stationary or decreases, as seen earlier; the second aspect is the fact that, when augmenting the cell radius, P_b keeps that tendency to increase with speed, whereas L tends to decrease; this tendency of L is especially verified for high traffic, $[(2\tau_v, 2\tau_d), (\lambda_v, \lambda_d)]$ or $[(\tau_v, \tau_d), (2\lambda_v, 2\lambda_d)]$; the reason for this behaviour is the fact that the p_{ij} influencing area is initially outside the green borders, i.e., for small radii or low traffic, and then, it enters the L influence area and, finally, starts going beyond the limits for higher traffic values.

If, in addition, it happens that the increase on the cell radius leads the system to get limited by the BS transmitted power, then a reduction on the number of channels is to be expected in conjunction to the extension of the cell radius. Thus, its effect will affect, in a cumulative form, the system parameters.

Analysing now what happens to the results of the traffic model when the buffer size, B , is changed, it is possible to conclude, as expected, that voice calls are neither positively, nor negatively, affected by that system element. Contrariwise, L is directly influenced by the size of the buffer: as seen in Figure 5.9 (a), Figure 5.10 (a) and Figure 5.11 (a), one of the quadrilateral sides of the green shape is formed by B , leading to the conclusion that the greater the buffer is the smaller L gets; as a consequence, T tends to decrease.

The fourth system parameter that requires to be analysed is the channels' distribution between voice and data users: it is definitively one of the parameters that influences most the behaviour of the traffic model. The equitable distribution of channels between voice and data users, keeping the remaining channels as spare for any user type, brings more disadvantages to the majority of the users when the system becomes heavily loaded; the proportional distribution of channels between voice and data users, as a function of the scenario under analysis, seems to be a more realistic approach and, without any doubt, more fair for the majority of users. When a scenario with many voice users is under analysis, like Scenario A, the equitable distribution of channels will benefit data users, as they receive, *a priori*, more than one third of the resources; on the other hand, when talking about a scenario that encompasses fundamentally data users, Scenario B, the equitable distribution of channels favours a little the voice users, making the blocking probability much smaller due to a "possible" over-dimension of the number of channels kept for voice.

The major conclusions related to the system behaviour are summarised in Table 5.5.

Looking into the complete results of Scenarios A and B, presented in Annexes C and D, respectively, the expected tendencies of P_b , L and T , are confirmed: the results agree *ipso facto* with the summary presented in Table 5.5.

There are, nevertheless, aspects on the performance of the traffic model that may be analysed and, why not, turned into points to be further enhanced; some comments on this direction are presented in the last chapter.

5. Analysis of results

Table 5.5 – System tendency due to the traffic model.

Average users' speed, $v \in [0, 120]$ km/h										
v	\nearrow	\Rightarrow	C	\searrow	P_b	\nearrow	L	\searrow	$T(p_{ij}')$	\searrow
									$T(\lambda_d)$	\searrow
									$T(L)$	\searrow
Cell radius, $R \in \{150, 250\}$ m										
R	\nearrow	\Rightarrow	λ_d	\nearrow	P_b	\nearrow	L	\nearrow	$T(p_{ij}')$	\searrow
							(L)	\searrow	$T(\lambda_d)$	\searrow
									$T(L)$	\nearrow
R	\nearrow	\Rightarrow	C	\searrow	P_b	\nearrow	L	\searrow	$T(p_{ij}')$	\searrow
									$T(\lambda_d)$	\searrow
									$T(L)$	\searrow
Buffer size, $B \in [5, 20]$ MB										
B	\nearrow				P_b	$=$	L	\searrow	T	\searrow
Cannel distribution										
Equitable, voice > data					P_b	\nearrow	L	\searrow	T	\searrow
Equitable, voice < data					P_b	\searrow	L	\nearrow	T	\nearrow
Proportional, voice > data					P_b	\searrow	L	\nearrow	T	\nearrow
Proportional, voice < data					P_b	\nearrow	L	\searrow	T	\searrow

5.5 Results for multi-cells

Before closing the current chapter, it seems to be the right point in time to introduce a brief explanatory note on the consequences of considering a heterogeneous scenario, e.g., users from Scenario B, inside a cell with 250 m radius and the system buffer being equal to 20 MB, are no longer considered to behave homogeneously in terms of motion. Thus, it is assumed that those users' displacement is limited to a ring of six cells (as mentioned under Section 4.2). The following routing matrix models the users' movement:

$$R_{ij} = \begin{bmatrix} 0 & 1/2 & 0 & 0 & 0 & 1/2 \\ 2/5 & 0 & 3/5 & 0 & 0 & 0 \\ 0 & 1/4 & 0 & 3/4 & 0 & 0 \\ 0 & 0 & 1/2 & 0 & 1/2 & 0 \\ 0 & 0 & 0 & 4/5 & 0 & 1/5 \\ 1/3 & 0 & 0 & 0 & 2/3 & 0 \end{bmatrix} \quad (5.1)$$

Each r_{ij} element of this matrix corresponds to the routing probability from cell i to cell j ; the non-zero values on row k represent the outgoing traffic from Cell k (equal to unity in steady-states), the non-zero values on column k being the incoming traffic to that same cell; e.g., Cell 3 delivers 25 % of its traffic to Cell 2 and 75 % to Cell 4, whereas the incoming traffic in that same cell results from Cell 2 (60 % of its traffic) and from Cell 4 (50 % of its traffic).

In this heterogeneous scenario, and bearing in mind that the system is in steady-state, i.e., the overall traffic in the system does not grow, the exchange of traffic between two cells may be unbalanced, leading to a higher amount of incoming handover traffic in some cells (Cells 3, 4 and 5) and a lower one in the others (Cells 1, 2 and 6).

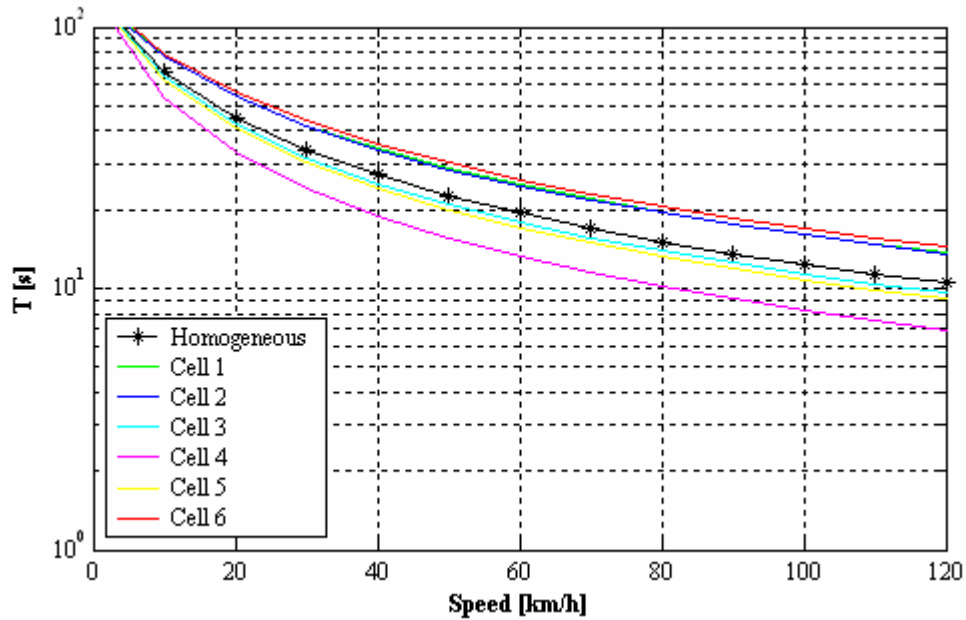
With respect to the system parameters, and bearing in mind (4.5), (4.7) and (4.9), that, respectively, provide P_b , L and T for the current traffic model, it is expected a variation on the results obtained only for the mean data delays, as it corresponds to the unique parameter directly influenced by handover rates. As the program results confirm this expectation, the figures presented hereafter will only mention the mean data delay.

Figure 5.17 shows the mean data delay for each of the six cells considered in a heterogeneous scenario, for both types of channel distributions (equitable to voice / data and proportional to the number of users from each type); the curve for a homogeneous scenario is plotted as well, in order to serve as a comparison.

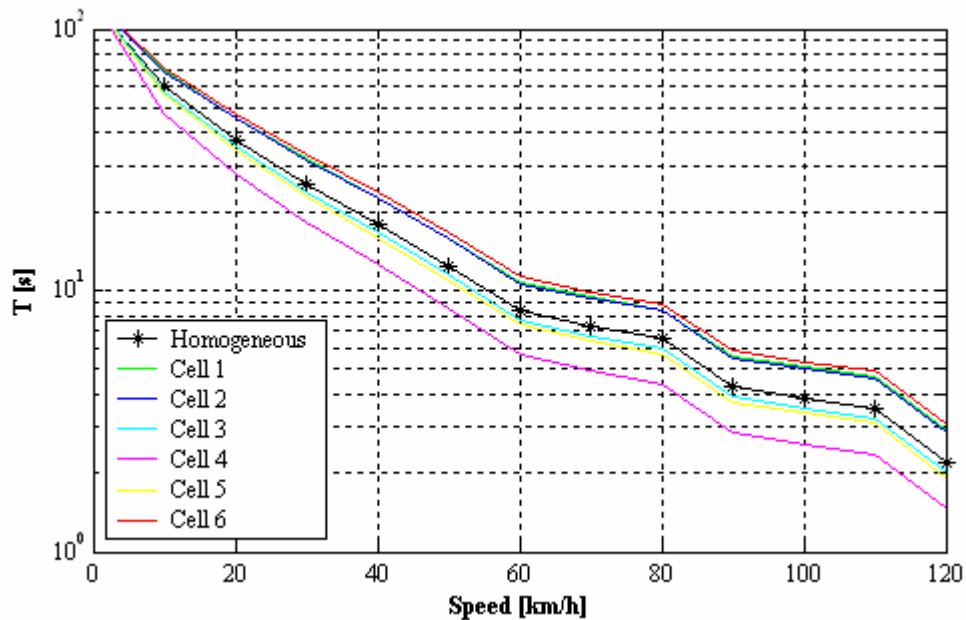
According to (4.9), it is expected that the cells with higher incoming HO traffic provide lower mean data delays: as new and handover call rates are inversely proportional to the mean data delay, when more traffic is coming into the cell, less delays are observed. The results plotted in Figure 5.17 agree with this expectation: the curves resulting from Cells 3, 4 and 5 are below the one from the homogeneous scenario, where incoming and outgoing traffic from one to another cell are equal; Cells 1, 2 and 6, in contrary, show to have a worse behaviour, as the

5. Analysis of results

mean delays are higher than the obtained for the homogeneous scenario; Cell 4 presents the highest handover rate and Cell 6 the lowest one (5.1), and, through Figure 5.17, those correspond to the cells that encompass less and more delays, respectively.



(a) Equitable distribution of channels.

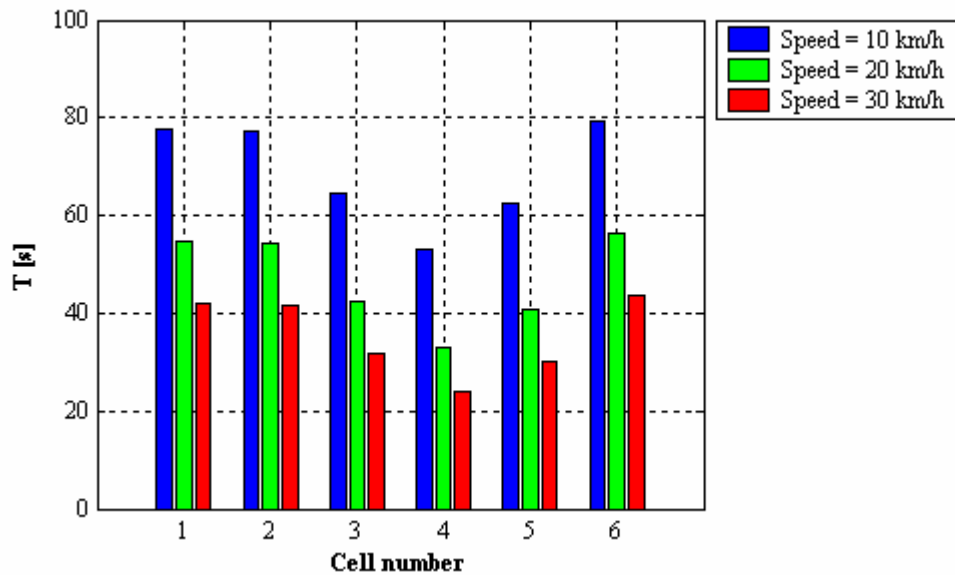


(b) Proportional distribution of channels.

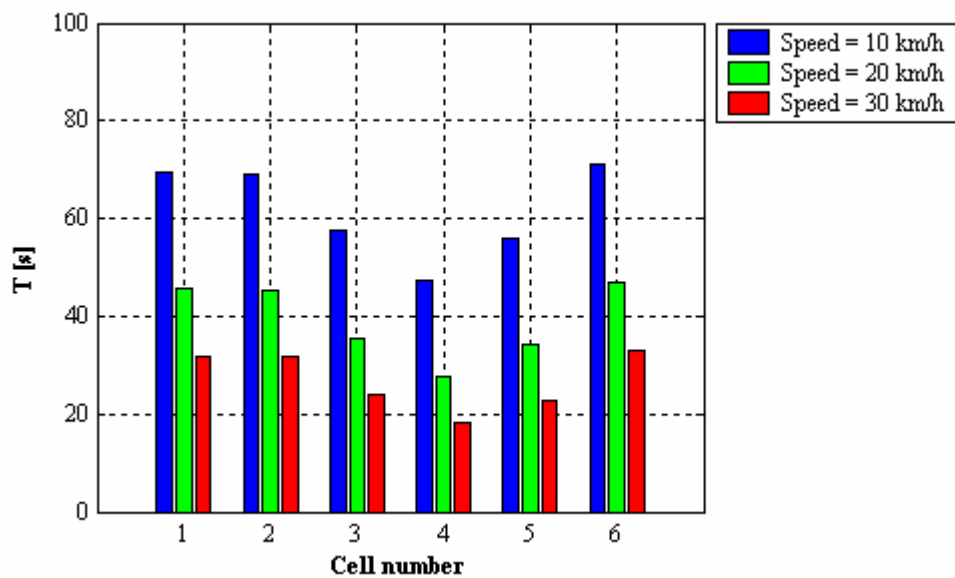
Figure 5.17 – Mean data delay vs. speed for a heterogeneous scenario.

The homogeneous curve equals the one presented in Figure D.3 as expected, as the input parameters are the same.

When setting now three different speed values, namely, 10, 20 and 30 km/h, the corresponding delays are shown for each cell in Figure 5.18.



(a) Equitable distribution of channels.



(b) Proportional distribution of channels.

Figure 5.18 – Mean data delay per cell for a heterogeneous scenario.

5. Analysis of results

It is clearly observed through Figure 5.18 that an increase on speed leads, for every cell, to a decrease on the corresponding delays. Additionally, when comparing the cells among each others, it is possible to remark which ones have more / less incomer users, according to the lower / higher delays presented. Finally, it should be noted that for the equitable distribution of channels, the delays are greater than the proportional distribution (for the scenario under analysis, which takes into consideration more load due to data users rather than voice); as seen earlier, this behaviour is justified by the number of channels that each of these distributions allocates to voice / data users.

6 Conclusions

This thesis presents a traffic model that considers scenarios with voice and data users, mixing up, in the same infrastructure, different services and applications. Many UMTS aspects are built in the model, so that the performance of a UMTS network, in terms of voice call blocking probabilities, data loss probabilities and mean data delays, is estimated.

The large amount of parameters that need to be addressed and the many environments that can be visited by a 3G user, turn the task of gathering all details into a single traffic model rather difficult to achieve. As a consequence, some simplifications had to be proposed and implemented in the model, aiming at reducing its complexity.

The traffic model that was studied, like any other models, e.g., Erlang-B or Engset models, has a limited scope of applicability. It is referred, along the previous chapters, the simplifications that are done in order to allow the use of this model to study the traffic behaviour of a UMTS network; some of the simplifications challenge the accuracy of the model a little bit, as the particularities of the scenarios, service characteristics, etc., get smoother or lost with all the simplifications done; nevertheless, the results achieved are in line with the original expectations. Some comments in terms of the results obtained through this traffic model may thus be drawn.

The total amount of channels that, at any time, the system is making available to the users, keeping in mind that the traffic model is analysing the behaviour of a number of users under the coverage of one BS, corresponds to the most critical aspect in UMTS. Rather few simultaneous users may be served if one considers the number of codes that need to be employed per user and per service; however, it has to be said that all the results were obtained using one single carrier frequency, and that, e.g., in Portugal, 3G mobile operators were awarded 4 carriers in FDD mode; when more traffic is to be expected, one or two carriers can additionally be put on service per BS, although care has to be taken in order to control any interference that may occur. The low number of channels is due to the fact that many security margins are considered when performing the various steps that precede the calculation of the number of channels; the majority of the tested scenarios showed that the system is limited by

6. Conclusions

the DL load (the way the traffic model is handling interference). As long as real data cannot be measured, any tunings may be useless.

When analysing the two ways of distributing channels between voice and data users, it becomes clear from the results that allocating channels on a proportional form is better for the majority of users than distributing them equitably between voice and data users. If, in addition, the interoperability between networks becomes effective, some calls may be served by other networks that provide overlapped coverage, e.g., GSM, releasing the resources for more demanding services; the sole problem is whether the terminals will be able to cooperate with diverse networks and technologies.

The radii obtained through the assumptions as specified in Chapter 4 seem to fit UMTS purposes. When they augment, the performance of the system shows some degradation (especially in terms of blocking voice calls and often by losing data packets; in contrast, the delays on packet deliveries get smaller). Broader areas under UMTS coverage will thus involve high investment, in order to provide many cells with small radii. 3G operators will certainly have as first targets the coverage of hot-spot areas, focusing first on high density business areas and residential areas with medium to high incomes, where those users that can afford to pay UMTS services, which will not be offered for free, are to be found. In the mean time, and as other networks and technologies may offer global coverage, some services will be provided by alternative networks.

In addition, high radii make the system sensitive to the traffic amount, which requires vigilance in order to keep the system capacity below maximum allowable limits. It is important to say that the call rate values, on which basis the traffic figures were obtained, correspond to estimates for the year 2005; initially, the UMTS launch was foreseen to occur during 2001, meaning that these figures could correspond to the 4th year of operation. Shifting these values along with the UMTS delays, it is possible that, as the traffic augments and reaches those estimations, some system improvements did already occur (new HW and SW releases), and that the system performs already better.

Considering now the values of the blocking probabilities for Scenario A (voice users predominant with respect to data), and, focusing only on the proportional distribution of channels, the traffic amount for 2005 leads to blocking probabilities below 1 % for a cell

radius of 250 m and average speeds up to 120 km/h. On the other hand, when Scenario B is considered, data weighing more than voice, 2 % are attained for 40 – 50 km/h speeds when the radius is 250 m; decreasing the radius to 150 m, the blocking tends to be negligible. Bearing in mind that in 2G a 2 % blocking probability is a quite common threshold, the results of the traffic model seem to be acceptable.

The packet losses obtained for any of the scenarios depends mainly on the buffer size. Increasing B to 15 or 20 MB, the losses are below 0.1 % for any users' speed, for the amount of traffic expected in 2005. Any further increase on the buffer size, does not ameliorate the system performance, but, instead, make it more costly. The tolerable losses depend on the specific type of data service; on average, knowing that there is yet no priority scheme implemented in the model, these global results are considered to be satisfactory.

In terms of delays suffered by packets before being delivered to end-users, they reach 1 to 2 minutes for low speeds in Scenario A, but reduce drastically when one moves quicker; on the other hand, Scenario B shows in general to influence positively the system performance. Again, each type of data service will have its demands in terms of delays: if one thinks that an e-mail message may easily take 10 minutes to arrive at the destination, and none will remark it effectively, an internet download should not leave the user to wait for more than half a minute; the acceptable values depend enormously on the service type. It is important that the traffic model works with the particularities of each data service, as the averaged values may, sometimes, be meaningless.

Being aware that the first UMTS cells will appear in high dense urban areas, the average speeds expected will certainly not be very high. In addition, it is not practical to use some services at very high speeds (e.g., when one needs to read much and is not sitting in a high speed train, where stability is absolutely required); others may be tailored to be used inside cars (e.g., location based services); the users' speed tendency, either high or low, is, once more, a particularity that is essentially service dependent.

QoS guarantees are still not implemented in the traffic model. It is nevertheless important to proceed in that way, as, out of the services' list that will be offered, some may require any kind of guarantee in terms of minimum transmission rates, maximum average delays, or even

6. Conclusions

no data losses (or imperceptible); there will be some 3G users that do not mind to pay, but that want to receive from their operator such guarantees.

While analysing separately the results that were obtained, it can be verified that, despite of the current model formulation, totally different from known traffic models, partial results are comparable to “typical” ones in non-3G environments. However, the traffic model showed to be a little conservative.

Finally, it should be reinforced that it is extremely important to confront any traffic model results with measurements done in real UMTS networks, in order to perform further adjustments and tunings to some system parameters. Nevertheless, it is still too early to do so, as the first UMTS networks in Portugal, as well as all over the World, did not yet reach a mature deployment; on the other hand, there are still few commercially available terminals, meaning that the mass market did not yet have access to this new technology.

Despite of the fact that some results are presented in this thesis, it does not mean that the traffic model that was the object of a detailed analysis is completely studied. There are always more and more variables or parameters that may be added, or even any changes in terms of input parameters that can still be tested, making the model analysis some more complex, but, possibly, closer to a real UMTS scenario.

While the present work was still under preparation, several alternative options that could be implemented in the traffic model were kept on hold; as part of those are believed to provide more conclusions in terms of the current traffic model behaviour, they will be put together in a list of actions to be deployed in a later stage, as future work:

- To obtain the probability matrix according to the methodology presented in [HaLH00], and implement it, as an alternative, in the traffic model;
- To test the traffic model using another probability matrix, where voice and data users would be modelled by different statistical distributions;
- To avoid averaging all data services, since much information in terms of data service particularities is lost; the joint probabilities would require to be entirely rephrased, as a two dimensional matrix would no longer apply;

- To implement a different priority scheme than the FCFS; instead of serving all users in the same order as the sequence of their arrival, they would additionally be distinguished according to their UMTS traffic classes, aiming at respecting distinct QoS requirements;
- To study different users' motion possibilities; the current routing matrix allows a user to move in two different directions, but, in reality, it is common that a cell is surrounded by more than two neighbours;
- To adequate the traffic model in such a way that the blocking probabilities and the data losses would as well be directly affected by mobility, when the scenario is no longer homogeneous;
- To analyse what kind of adjustments need to be done to the traffic model in order to validate it for the UMTS unpaired spectrum (TDD mode of operation);
- To compare, as soon as there is information available, the traffic results with real UMTS traffic figures.

These aspects are considered to preserve the aim of this thesis and the purpose of the traffic model that served as a basis for the current analysis, namely voice and data integration on a finite-buffer mobile system.

Annex A

COST231-Walfisch-Ikegami Model

The COST231-Walfisch-Ikegami propagation model [DaCo99] is adequate to analyse scenarios with urban characteristics, as it considers data that may model this type of environments: building heights and separation, road widths and orientation with respect to the direct radio path. It makes the distinction between direct paths with line-of-sight or with non line-of-sight.

The COST231-Walfisch-Ikegami model was based on measurements performed in Stockholm, combined with some results of the Ikegami and the Walfisch-Bertoni models [Corr99]. It is a mixture of an empirical model with a deterministic one, and typical values that characterise the environment are inserted, based on topographical building databases.

Figure A.1 specifies the parameters used in the COST231-Walfisch-Ikegami model.

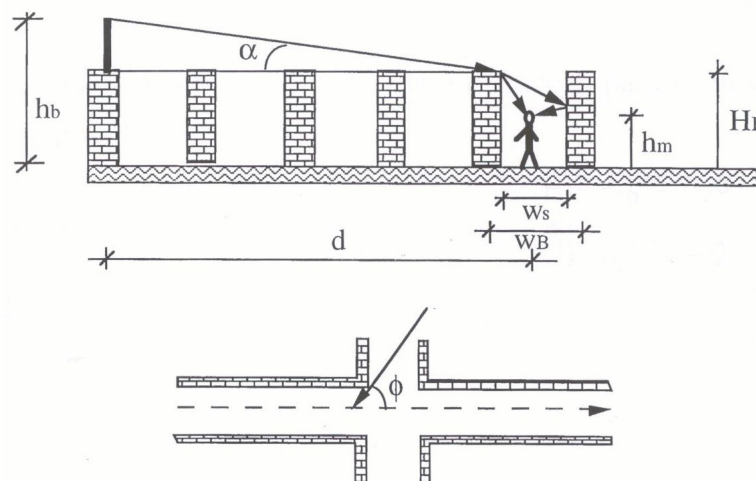


Figure A.1 – Parameters used in the COST231-Walfisch-Ikegami model (extracted from [Corr99]).

If there is line-of-sight between MT and BS, the propagation losses are obtained through:

$$L_p[\text{dB}] = 42.6 + 26\log(d_{[\text{km}]}) + 20\log(f_{[\text{MHz}]}) \quad \text{for } d \geq 0.02 \text{ km} \quad (\text{A.1})$$

If the line-of-sight is obstructed, the path loss estimation is given by the following equation:

A. COST231 – WI Propagation Model

$$L_p[\text{dB}] = \begin{cases} L_0[\text{dB}] + L_{rts}[\text{dB}] + L_{msd}[\text{dB}] \\ L_0[\text{dB}] \end{cases} \quad \text{for } L_{rts} + L_{msd} \leq 0 \quad (\text{A.2})$$

where each of these components reflect:

- L_0 free space loss
- L_{rts} roof-top-to-street diffraction and scatter loss
- L_{msd} multi-screen loss

The free space loss is given by:

$$L_0[\text{dB}] = 32.4 + 20\log(d_{[\text{km}]}) + 20\log(f_{[\text{MHz}]}) \quad (\text{A.3})$$

The roof-top-to-street diffraction and scatter loss is obtained through:

$$L_{rts}[\text{dB}] = -16.9 - 10\log(w_{s[\text{m}]}) + 10\log(f_{[\text{MHz}]}) + 20\log(H_{B[\text{m}]} - h_{m[\text{m}]}) + L_{ori}[\text{dB}] \quad (\text{A.4})$$

where:

$$L_{rts}[\text{dB}] = \begin{cases} -10 + 0.354 \phi_{[^\circ]} & \text{for } 0^\circ \leq \phi < 35^\circ \\ 2.5 + 0.075 (\phi_{[^\circ]} - 35) & \text{for } 35^\circ \leq \phi < 55^\circ \\ 4.0 - 0.114 (\phi_{[^\circ]} - 55) & \text{for } 55^\circ \leq \phi \leq 90^\circ \end{cases} \quad (\text{A.5})$$

The multi-screen loss may be calculated via:

$$L_{msd}[\text{dB}] = L_{bsh}[\text{dB}] + k_a + k_d \log(d_{[\text{km}]}) + k_f \log(f_{[\text{MHz}]}) - 9\log(w_{B[\text{m}]}) \quad (\text{A.6})$$

where:

$$L_{bsh}[\text{dB}] = \begin{cases} -18\log(1 + h_{b[\text{m}]} - H_{B[\text{m}]}) & h_b > H_B \\ 0 & h_b \leq H_B \end{cases} \quad (\text{A.7})$$

$$k_a = \begin{cases} 54 & h_b > H_B \\ 54 - 0.8 \times (h_{b[\text{m}]} - H_{B[\text{m}]}) & d \geq 0.5 \text{ km and } h_b \leq H_B \\ 54 - 1.6 \times (h_{b[\text{m}]} - H_{B[\text{m}]}) \times d_{[\text{km}]} & d < 0.5 \text{ km and } h_b \leq H_B \end{cases} \quad (\text{A.8})$$

$$k_d = \begin{cases} 18 & h_b > H_B \\ 18 - 15 \times \frac{h_b[m] - H_B[m]}{H_B[m]} & h_b \leq H_B \end{cases} \quad (\text{A.9})$$

$$k_f = \begin{cases} -4 + 0.7 \times \left(\frac{f_{[\text{MHz}]}}{925} - 1 \right) & \text{for medium sized cities and suburban} \\ & \text{centres with moderate tree density} \\ 5 \times \left(\frac{f_{[\text{MHz}]}}{925} - 1 \right) & \text{for metropolitan centres} \end{cases} \quad (\text{A.10})$$

In case the data on the structure of the buildings and roads is unknown, it is recommended to use the following values:

- Building separation (w_B) \in [20, 50] m
- Widths of roads (w_s) $w_s = 0.5 \times w_B$
- Heights of buildings (H_B) $H_B = 3 \times \{\text{number of floors}\} + H_{roof}$
- Roof height (H_{roof}) $H_{roof[m]} = \begin{cases} 3, & \text{pitched} \\ 0, & \text{flat} \end{cases}$
- Road orientation with respect to the direct radio path (ϕ) $\phi = 90^\circ$

The validity ranges of the COST231-Walfisch-Ikegami model correspond to:

- Frequency (f) \in [800, 2000] MHz
- BS height (h_b) \in [4, 50] m
- MT height (h_m) \in [1, 3] m
- Distance (d) \in [0.02, 5] km

Random variables arise in many applications, the sequence of incidents being commonly non-correlated events. The occurrences of these variables reflect often models of fundamental mechanisms that lie behind a random behaviour. Two statistical distributions, namely Poisson and Exponential, which were referred along this thesis, are presented hereafter.

For the message arrival process the most common description is given in terms of Poisson statistics. Poisson statistics are based on a discrete distribution of events, as presented in Figure B.1.

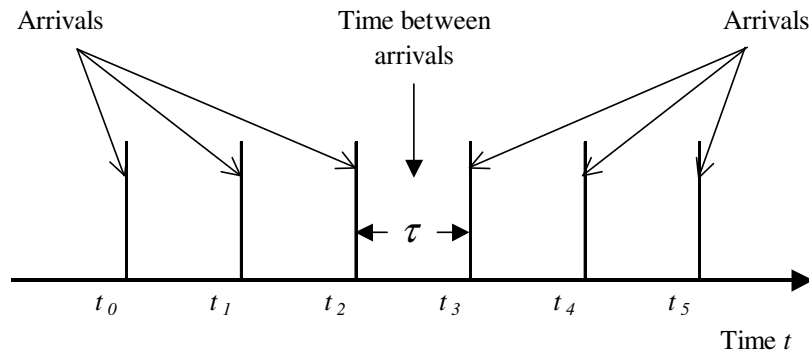


Figure B.1 – Discrete distribution of events (extracted from [Keis89]).

The messages arrive at the system at times t_0, t_1, t_2, \dots where $t_0 < t_1 < t_2 \dots < t_n$.

Taking into consideration an infinite source number (i.e., there is a large number of independent users), the probability $P_n(t)$ of exactly n users arriving during a time interval of length t , according to Poisson's distribution, is given by [Keis89]:

$$P_n(t) = \frac{(\lambda t)^n e^{-\lambda t}}{n!} \quad (\text{B.1})$$

where:

- $n = 0, 1, 2, \dots$
- λ mean call arrival rate
- t time interval in which the call arrives

B. Statistical distributions

The Poisson distribution is frequently used to model call arrival times. The average or expected number of arrivals in the time interval T is thus:

$$E[N] = \sum_{n=0}^{\infty} n P_n(t) = \lambda \cdot T \quad (\text{B.2})$$

The expected number of arrivals in the time interval $(0, T)$ is equal to $\lambda \cdot T$.

Considering that users enter the queuing system at times $t_0, t_1, t_2, \dots, t_n$, the random variables $\tau_n = t_n - t_{n-1}$ are called the inter-arrival times, that can be assumed to form a sequence of independent and identically distributed random variables. Letting τ represent an arbitrary inter-arrival time having a probability density function $f(t)$, it can be said that Poisson arrivals generate an exponential probability density:

$$f(t) = \lambda e^{-\lambda t} \quad (\text{B.3})$$

It is further assumed, when considering the traffic model analysed along this thesis, that the service time distribution, $S(t)$, is given by (B.4):

$$S(t) = \mu e^{-\mu t} \quad (\text{B.4})$$

where:

- μ service rate

The service time varies in a statistical way because the messages themselves vary randomly in length.

Annex C

Scenario A, Program results

Scenario A takes into account the number of users referred in Table 5.1: a considerable amount of voice calls and rather few data. The program is first run for a cell with 150 m radius; average speeds of 15 km/h and 60 km/h and buffer sizes of 20 and 10 MB are applied in particular situations. The program is run a second time for a cell with 250 m radius.

The numbers of codes obtained are presented in Figure C.1:

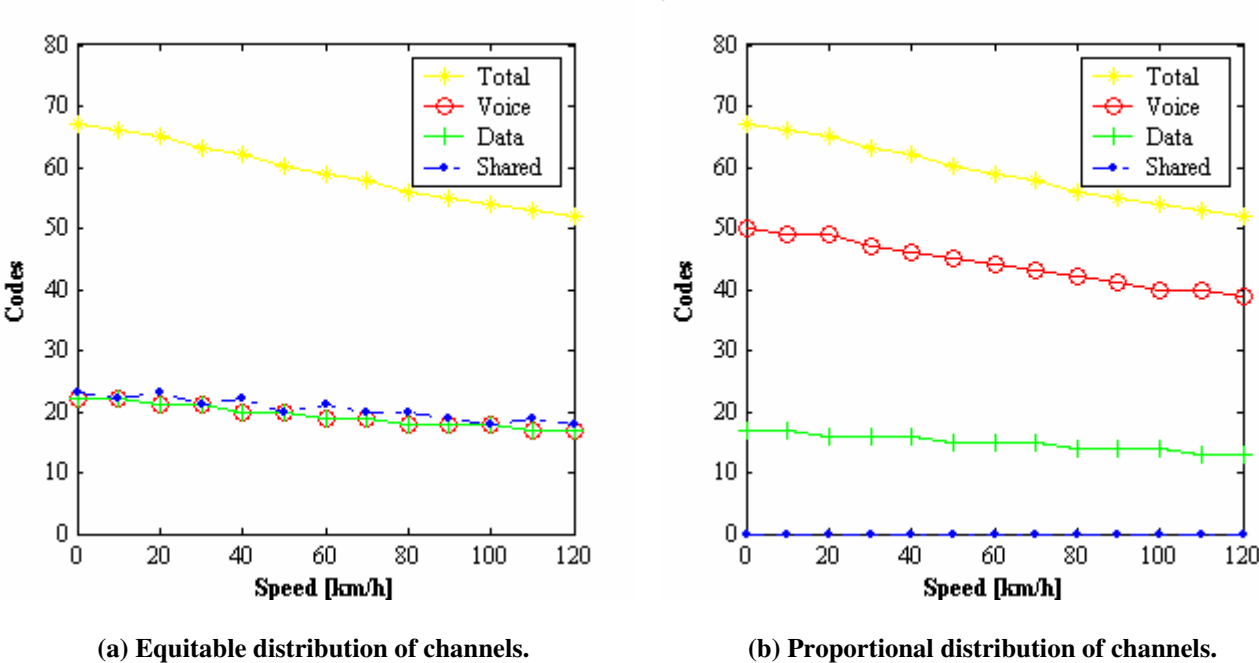
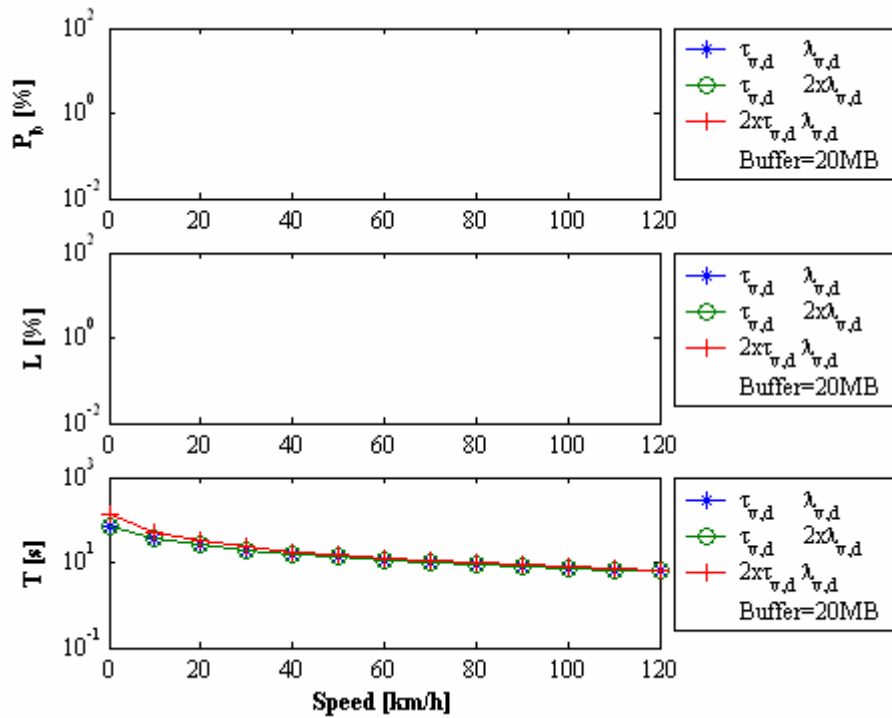


Figure C.1 – Number of codes for Scenario A with a 150 and 250 m cell radius.

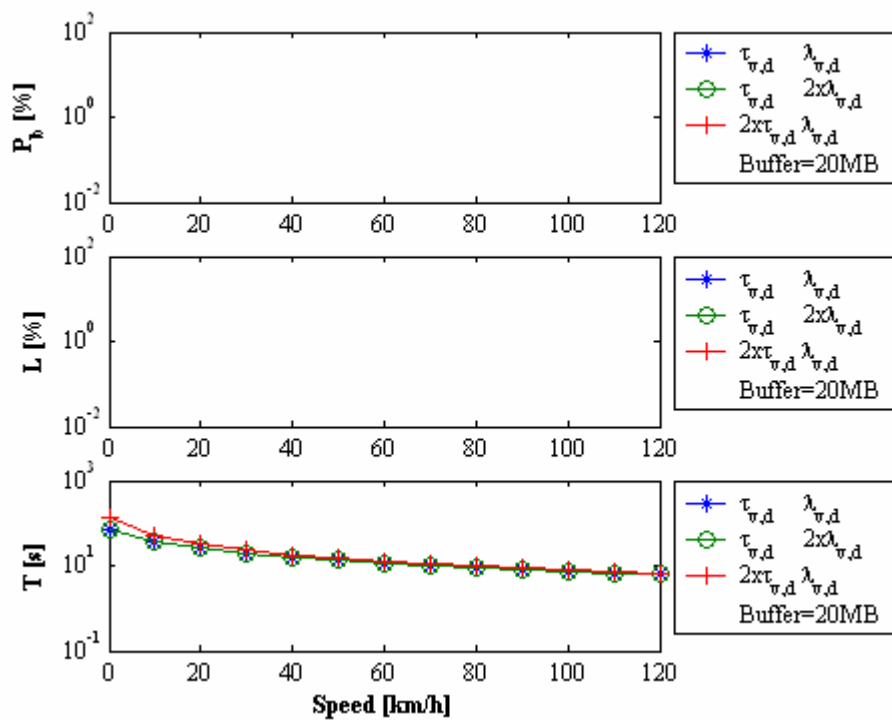
The performance results, as a function of users’ speed, are presented in Figure C.2 to Figure C.5, and as a function of the buffer size, correspond to Figure C.6 to Figure C.9.

Figure C.10 to Figure C.13 show the p_{ij} and p_{ij}' matrices for a cell with 150 m radius, whereas the results for a 250 m cell are presented in Figure C.14 to Figure C.17.

C. Scenario A, Program results

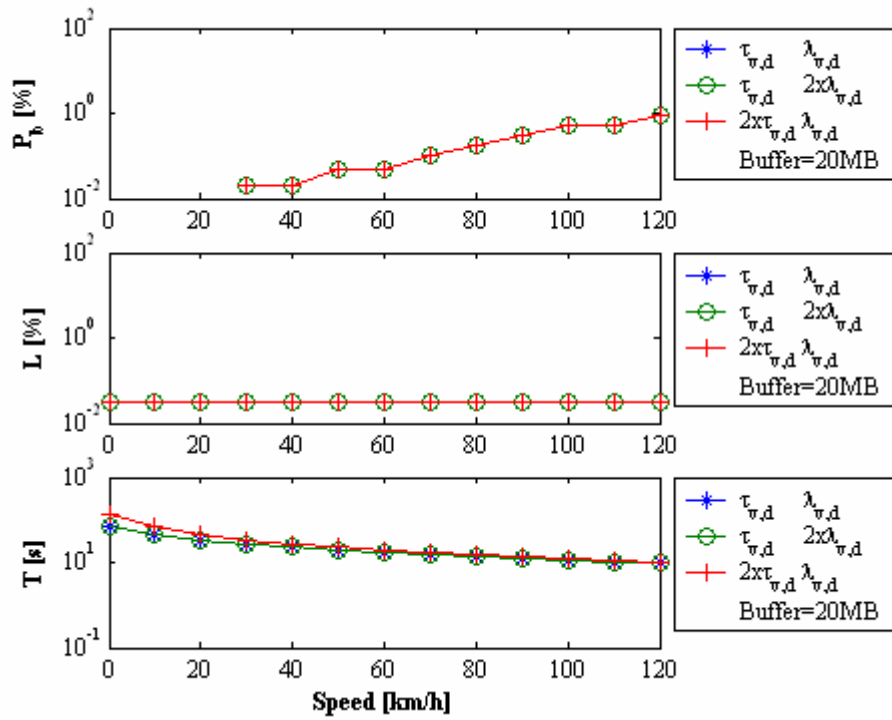


(a) Equitable distribution of channels.

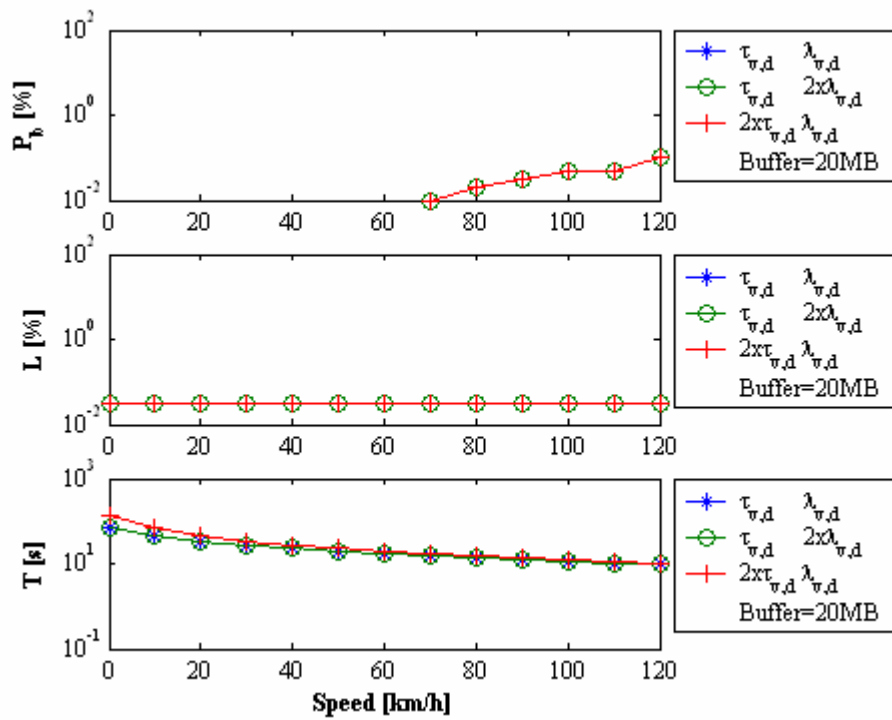


(b) Proportional distribution of channels.

Figure C.2 – System performance versus users' speed (150 m cell radius; 20 MB buffer size).



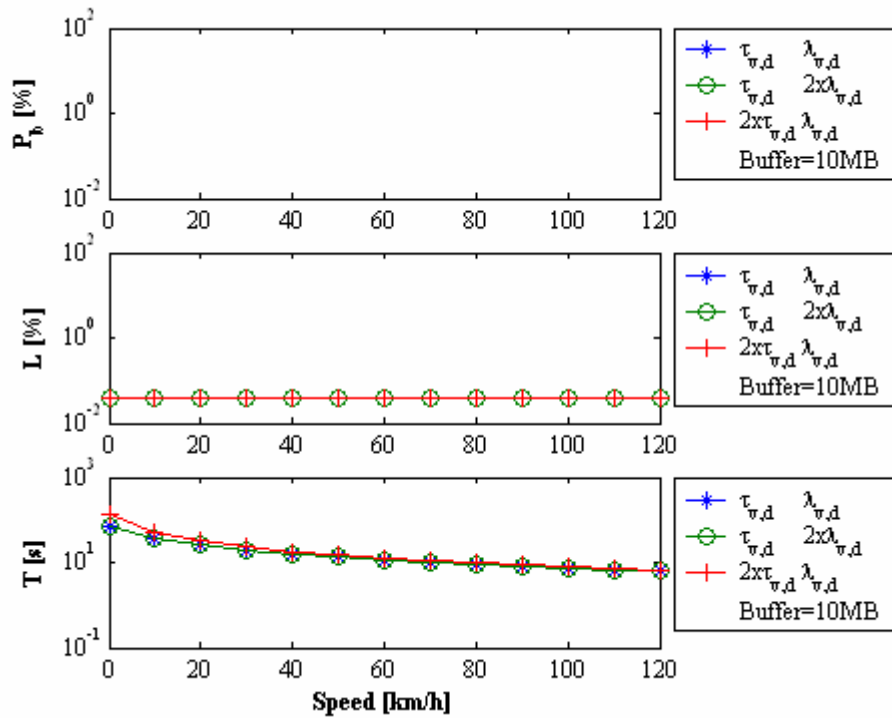
(a) Equitable distribution of channels.



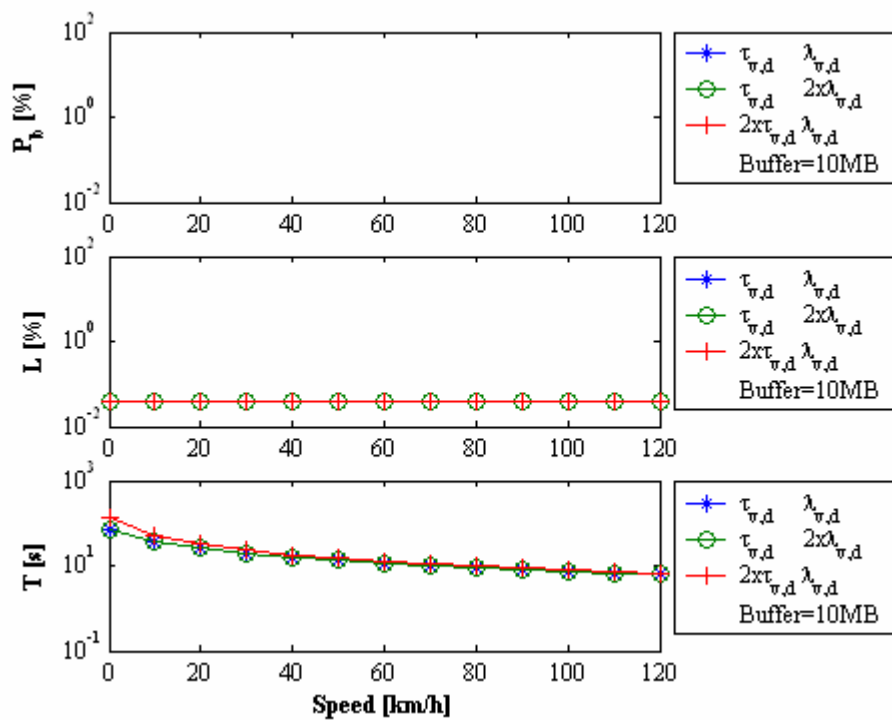
(b) Proportional distribution of channels.

Figure C.3 – System performance versus users’ speed (250 m cell radius; 20 MB buffer size).

C. Scenario A, Program results

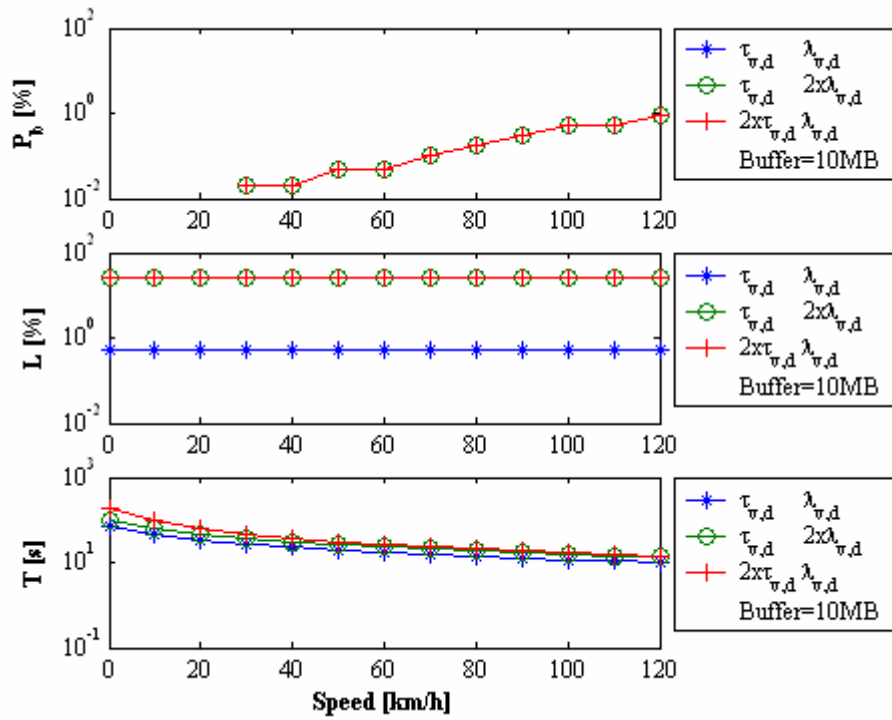


(a) Equitable distribution of channels.

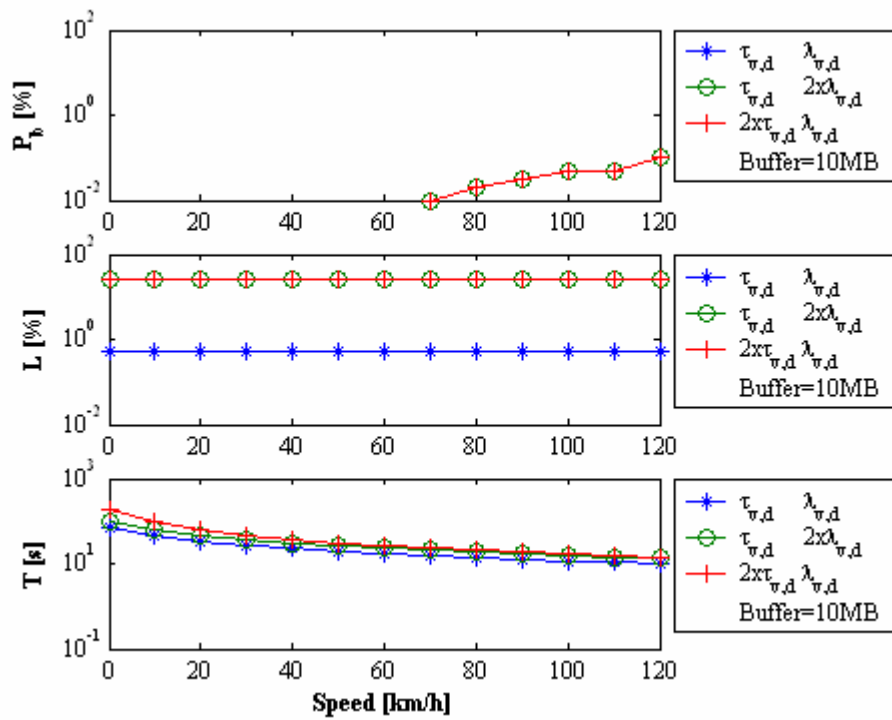


(b) Proportional distribution of channels.

Figure C.4 – System performance versus users' speed (150 m cell radius; 10 MB buffer size).



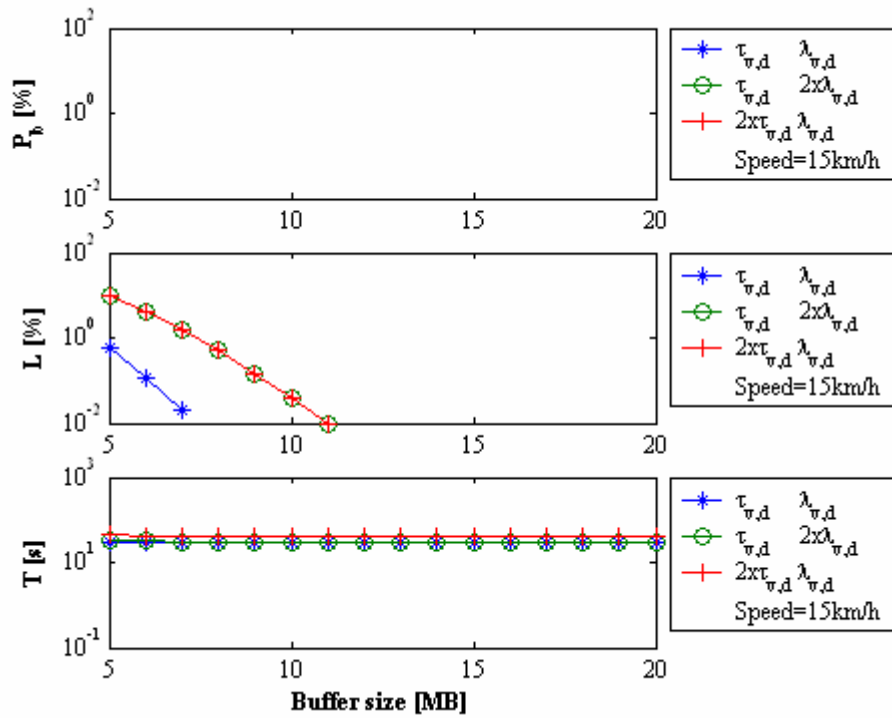
(a) Equitable distribution of channels.



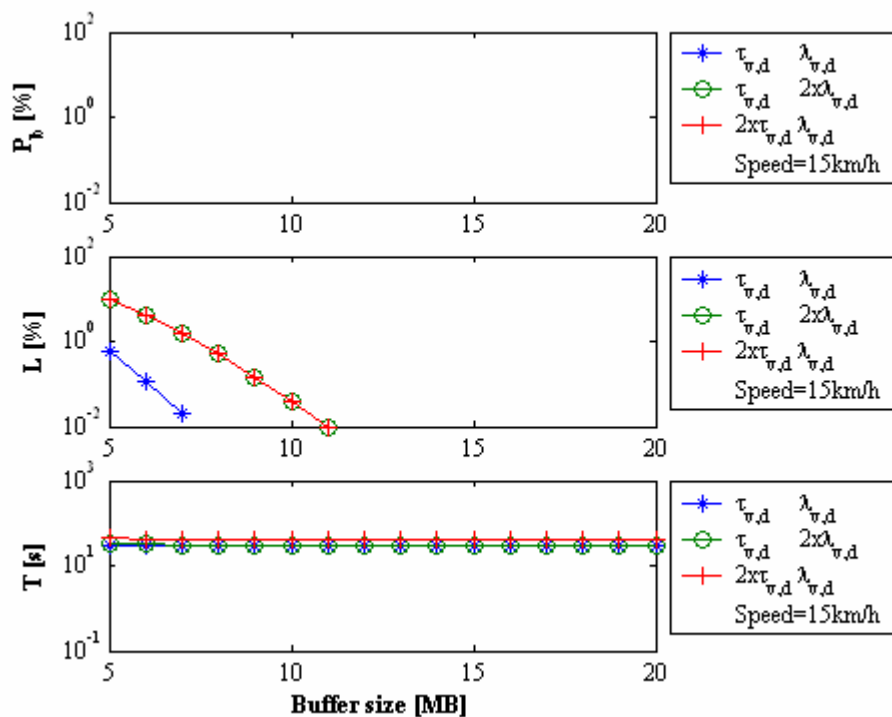
(b) Proportional distribution of channels.

Figure C.5 – System performance versus users’ speed (250 m cell radius; 10 MB buffer size).

C. Scenario A, Program results

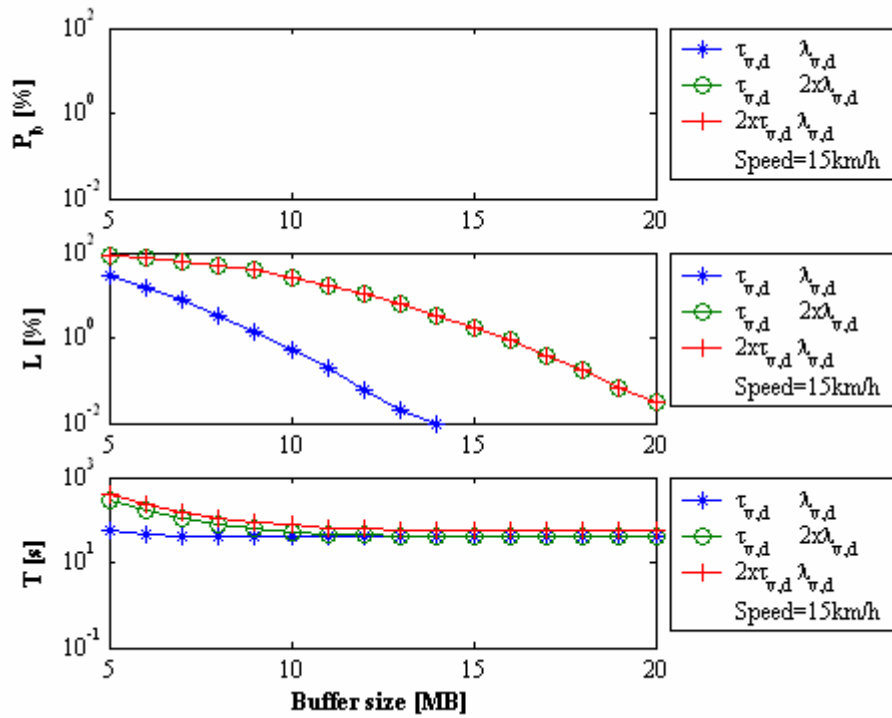


(a) Equitable distribution of channels.

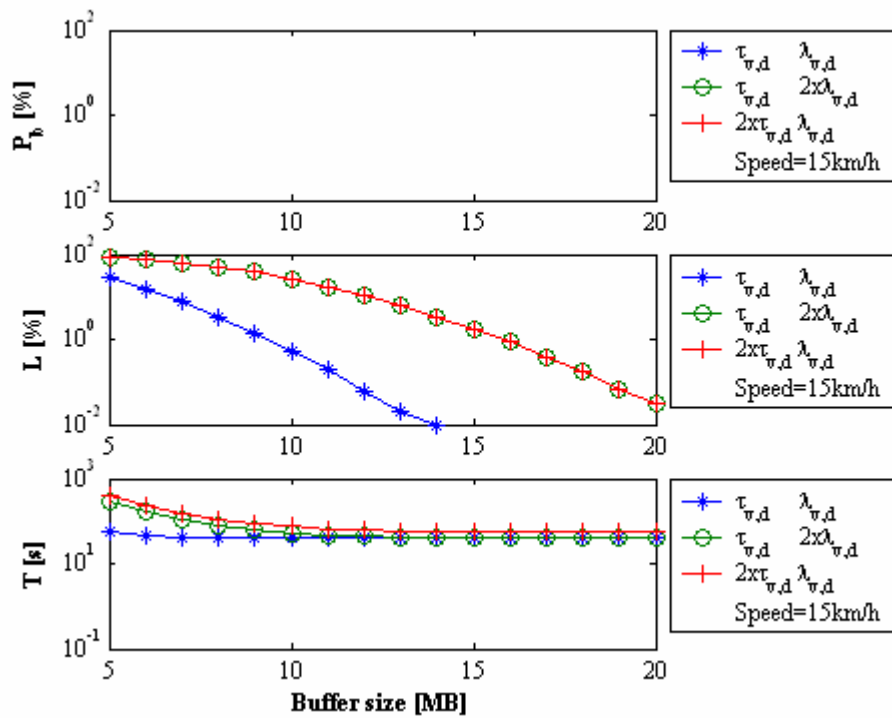


(b) Proportional distribution of channels.

Figure C.6 – System performance versus buffer size (150 m cell radius; 15 km/h average speed).



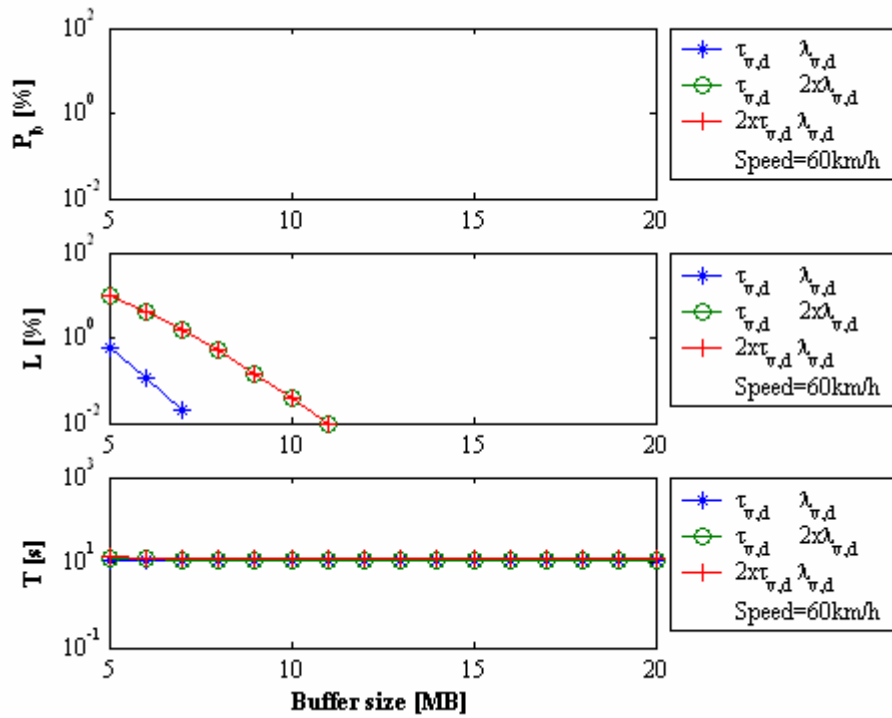
(a) Equitable distribution of channels.



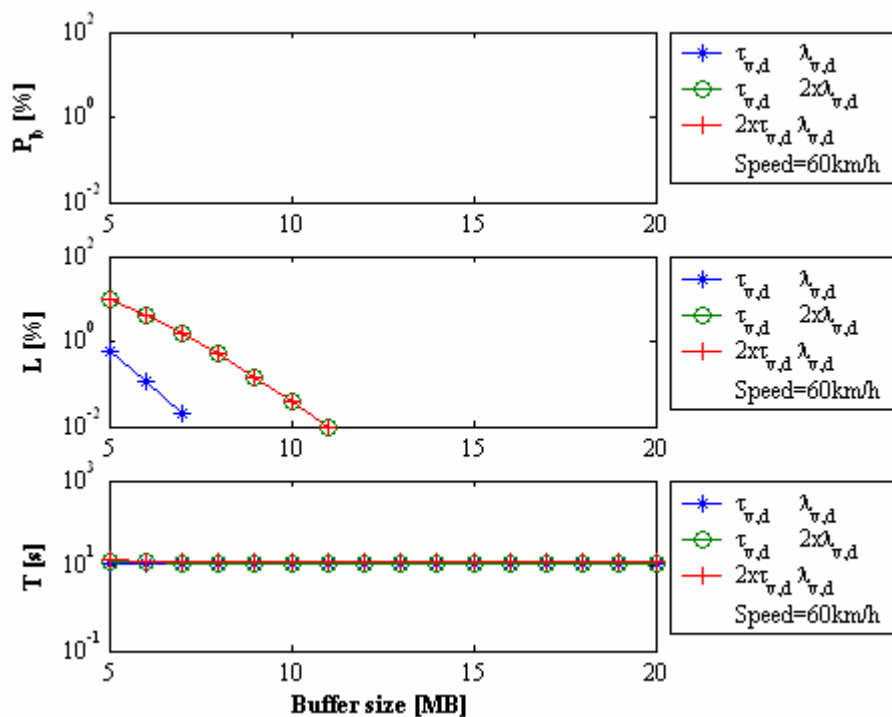
(b) Proportional distribution of channels.

Figure C.7 – System performance versus buffer size (250 m cell radius; 15 km/h average speed).

C. Scenario A, Program results

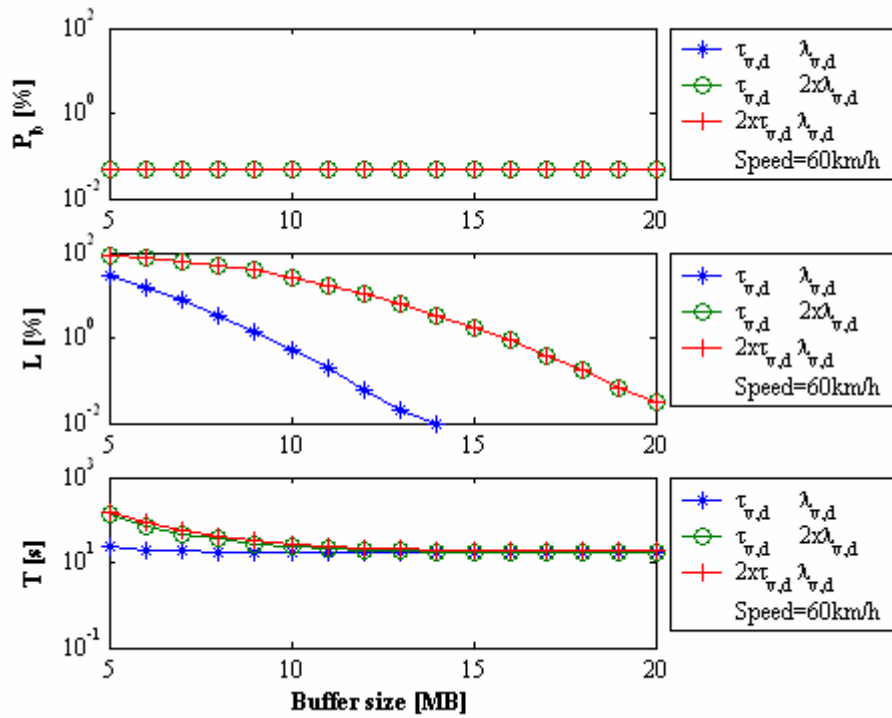


(a) Equitable distribution of channels.

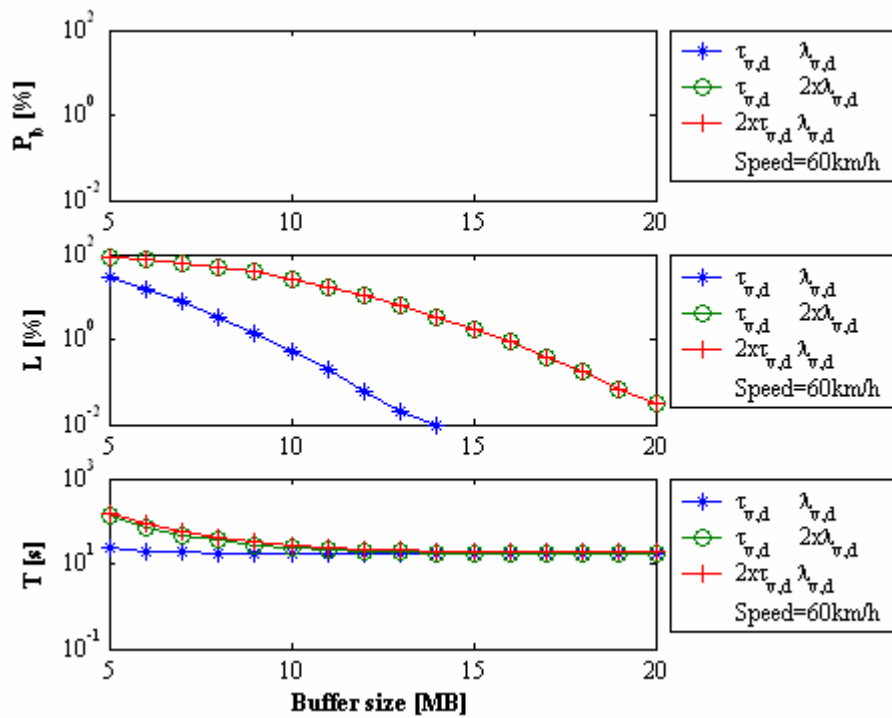


(b) Proportional distribution of channels.

Figure C.8 – System performance versus buffer size (150 m cell radius; 60 km/h average speed).



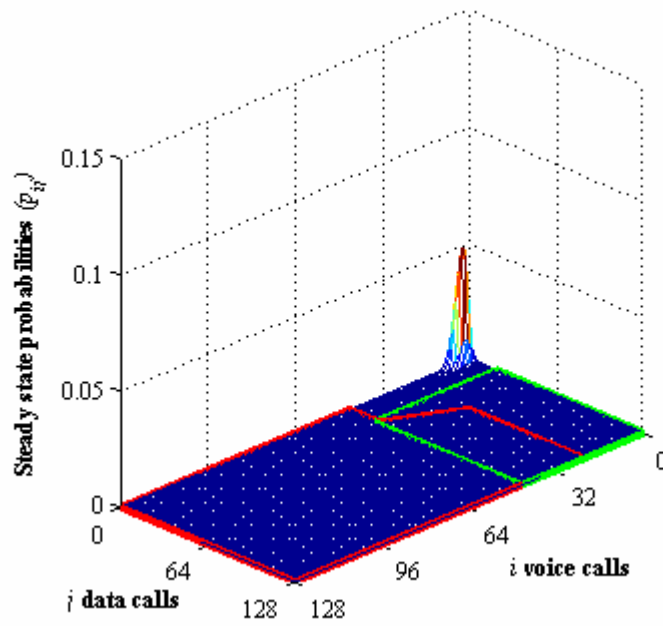
(a) Equitable distribution of channels.



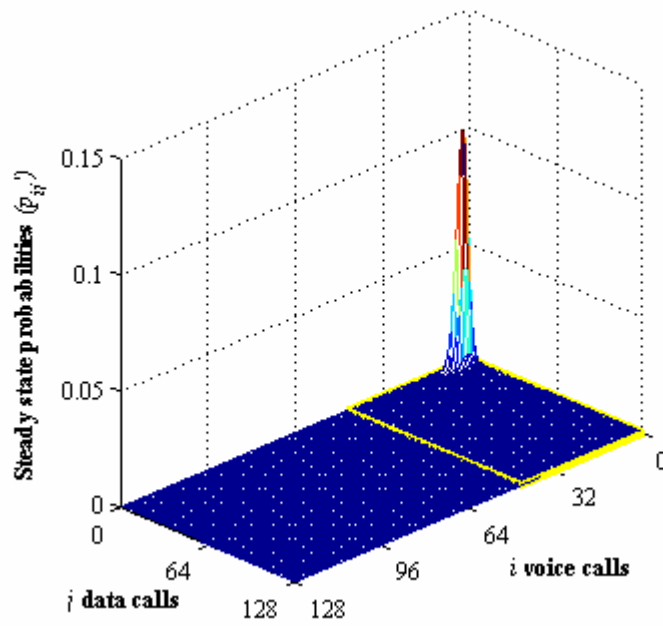
(b) Proportional distribution of channels.

Figure C.9 – System performance versus buffer size (250 m cell radius; 60 km/h average speed).

C. Scenario A, Program results

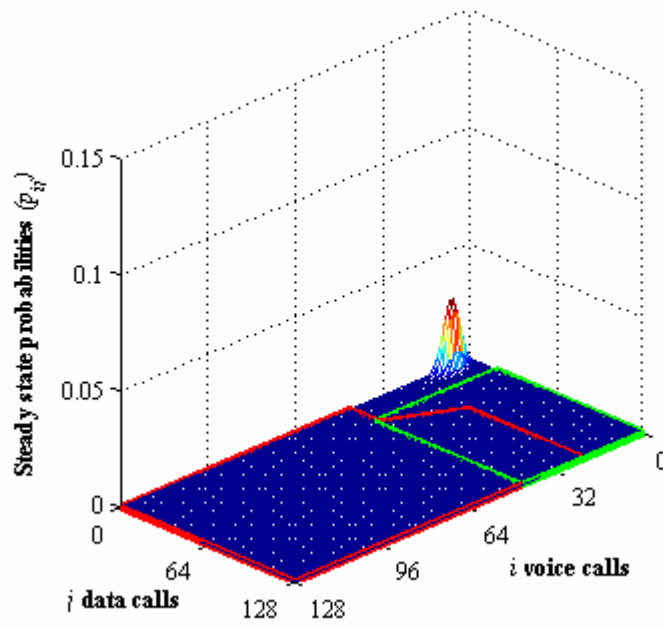


(a) p_{ij} for an equitable distribution of resources.

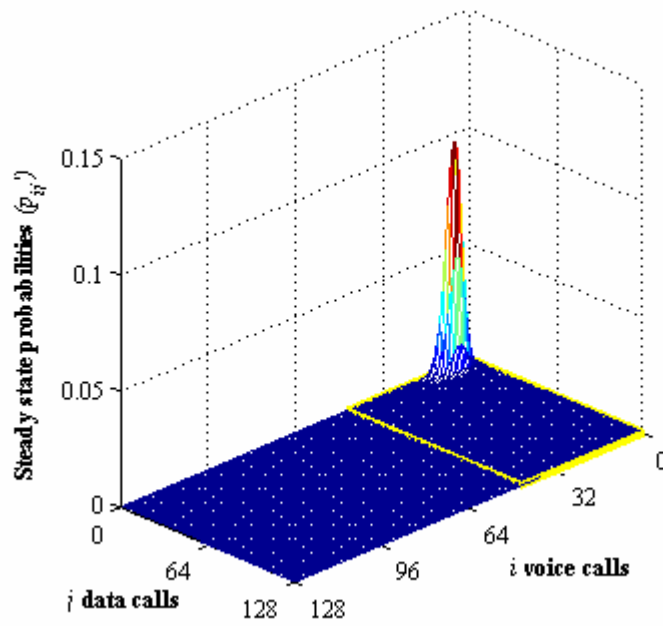


(b) p_{ij}' for an equitable distribution of resources.

Figure C.10 – Steady-states $[(\tau_v, \tau_d), (\lambda_v, \lambda_d)]$, equitable distribution of resources and 150 m cell radius.



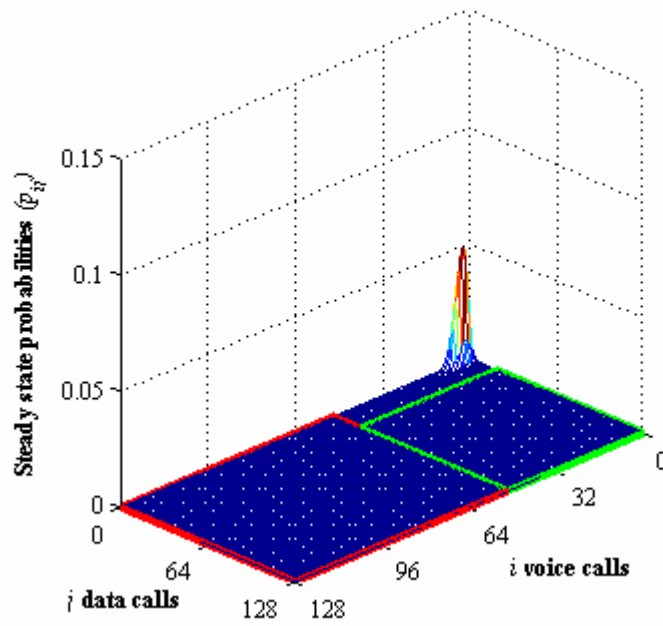
(a) p_{ij} for an equitable distribution of resources.



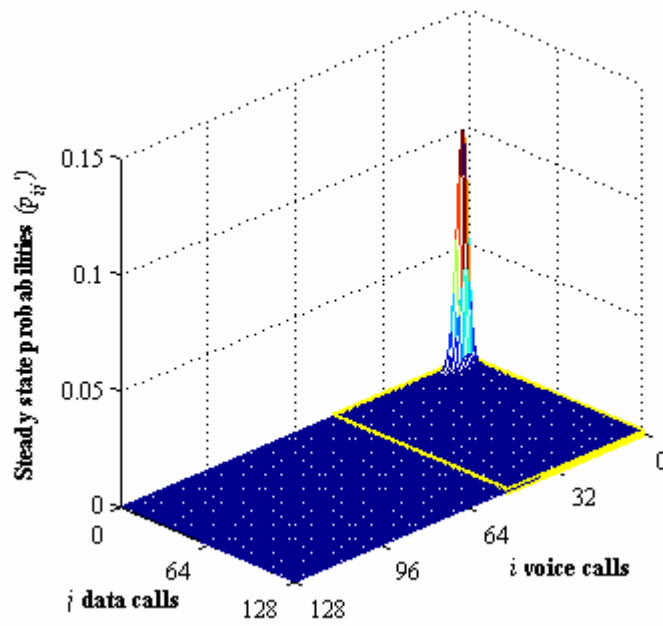
(b) p_{ij}' for an equitable distribution of resources.

Figure C.11 – Steady-states $[(2\tau, 2\tau_d), (\lambda, \lambda_d)]$ or $[(\tau, \tau_d), (2\lambda, 2\lambda_d)]$, equitable distribution of resources and 150 m cell radius.

C. Scenario A, Program results

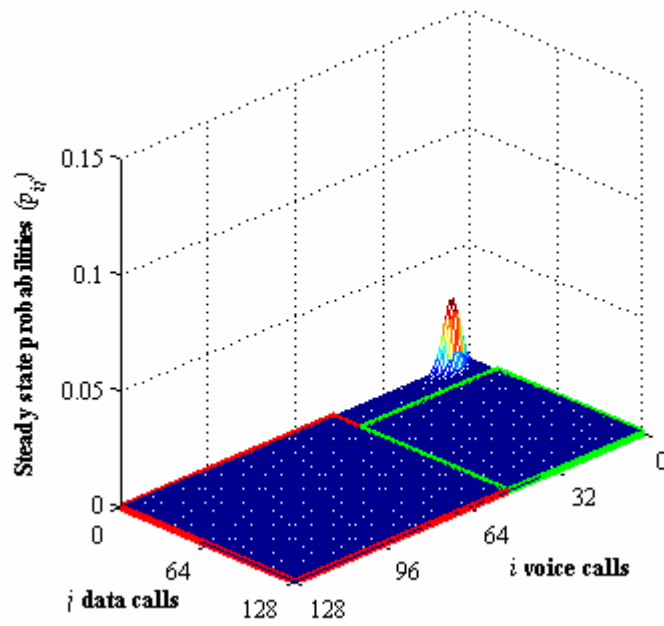


(a) p_{ij} for a proportional distribution of resources.

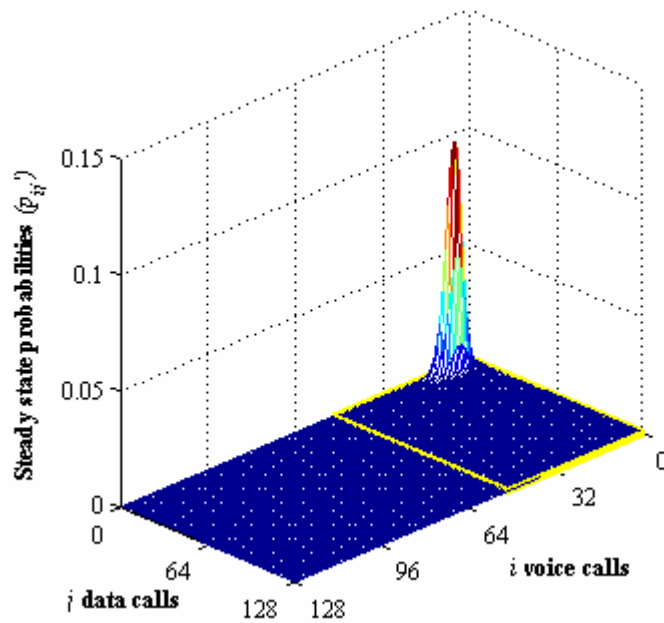


(b) p_{ij}' for a proportional distribution of resources.

Figure C.12 – Steady-states $[(\tau_s, \tau_d), (\lambda_s, \lambda_d)]$, proportional distribution of resources and 150 m cell radius.



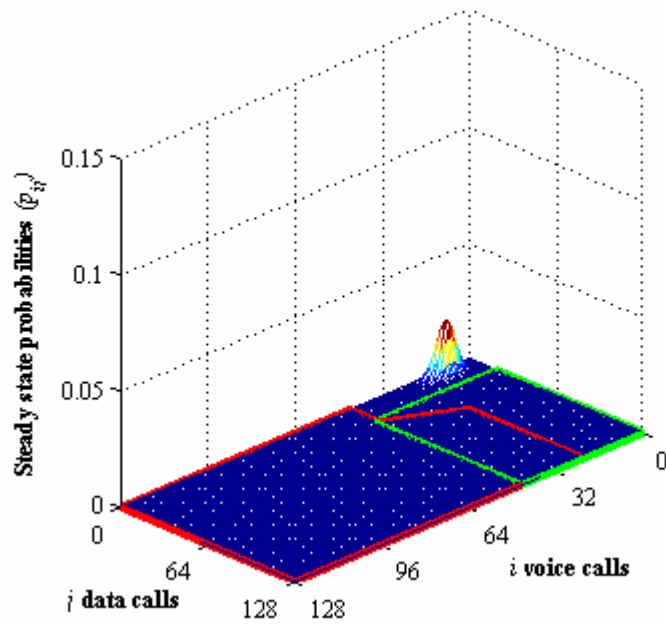
(a) p_{ij} for a proportional distribution of resources.



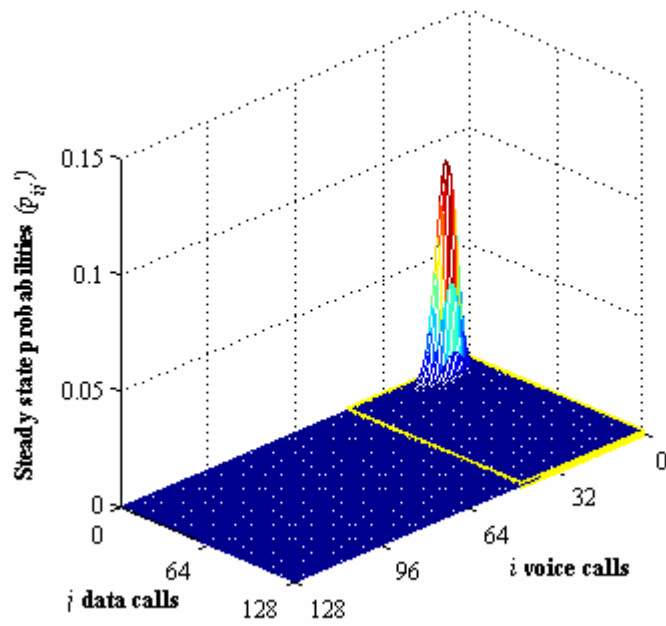
(b) p_{ij}' for a proportional distribution of resources.

Figure C.13 – Steady-states $[(2\tau, 2\tau_d), (\lambda_v, \lambda_d)]$ or $[(\tau, \tau_d), (2\lambda_v, 2\lambda_d)]$, proportional distribution of resources and 150 m cell radius.

C. Scenario A, Program results

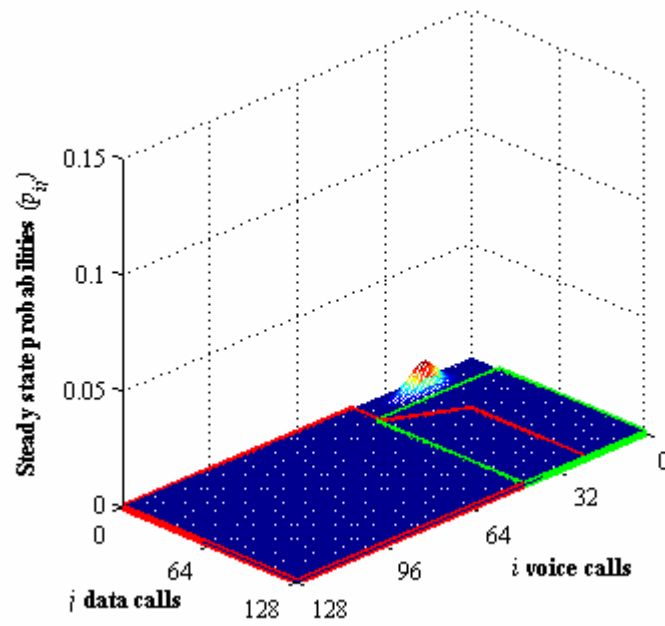


(a) p_{ij} for an equitable distribution of resources.

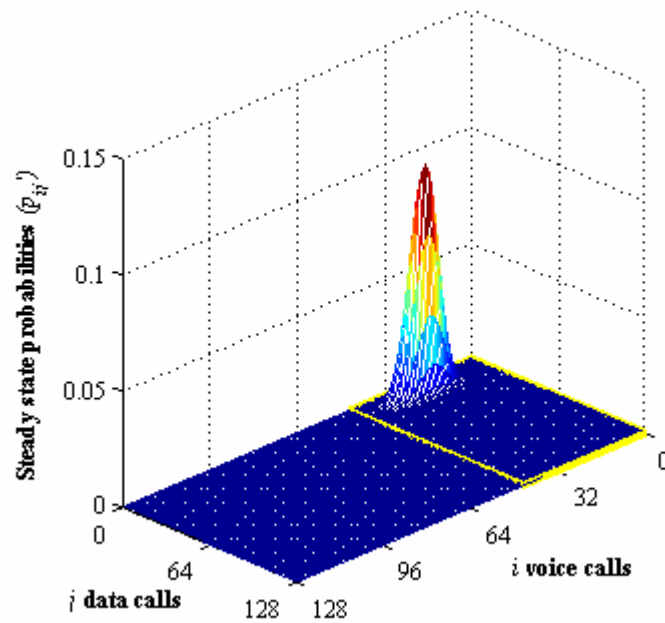


(b) p'_{ij} for an equitable distribution of resources.

Figure C.14 – Steady-states $[(\tau_v, \tau_d), (\lambda_v, \lambda_d)]$, equitable distribution of resources and 250 m cell radius.



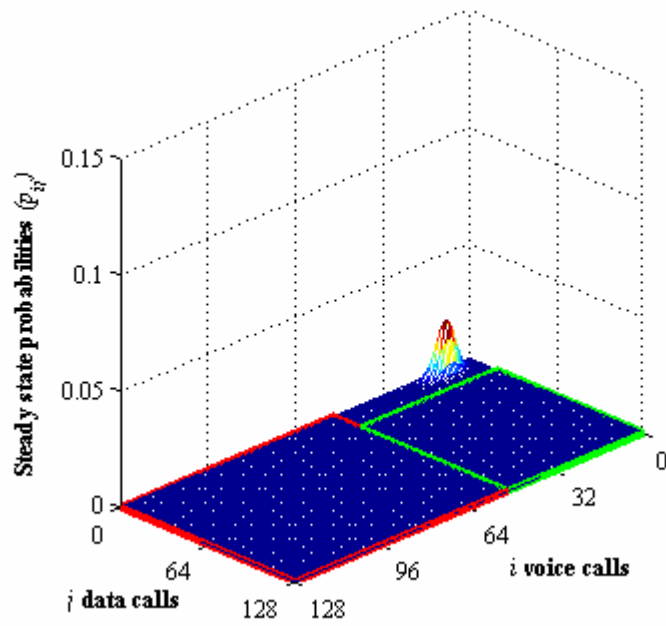
(a) p_{ij} for an equitable distribution of resources.



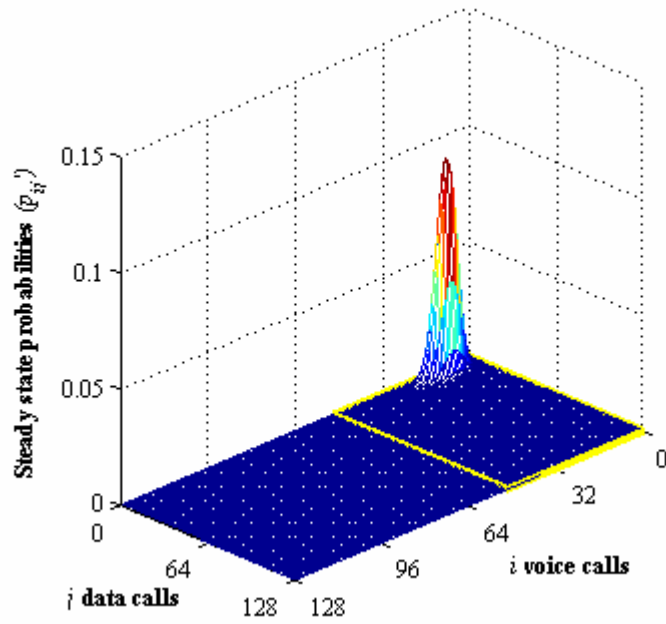
(b) p_{ij}' for an equitable distribution of resources.

Figure C.15 – Steady-states $[(2\tau, 2\tau_d), (\lambda, \lambda_d)]$ or $[(\tau, \tau_d), (2\lambda, 2\lambda_d)]$, equitable distribution of resources and 250 m cell radius.

C. Scenario A, Program results

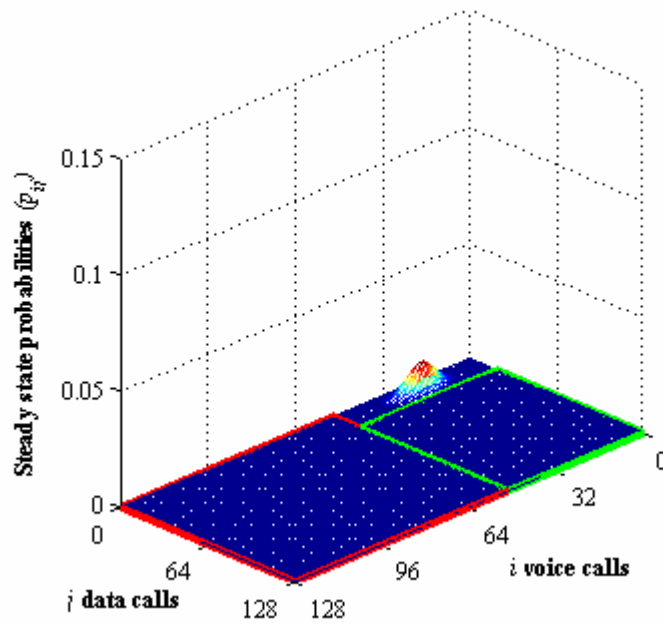


(a) p_{ij} for a proportional distribution of resources.

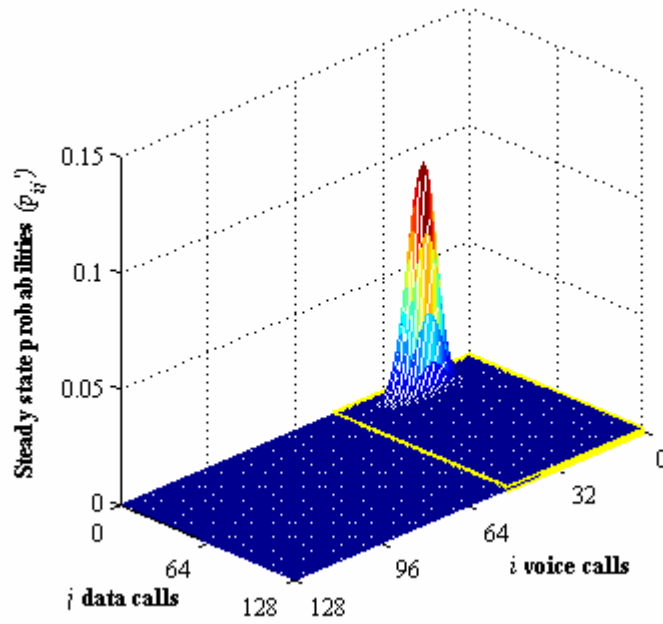


(b) p_{ij}' for a proportional distribution of resources.

Figure C.16 – Steady-states $[(\tau_s, \tau_d), (\lambda_s, \lambda_d)]$, proportional distribution of resources and 250 m cell radius.



(a) p_{ij} for a proportional distribution of resources.



(b) p_{ij}' for a proportional distribution of resources.

Figure C.17 – Steady-states $[(2\tau, 2\tau_d), (\lambda_v, \lambda_d)]$ or $[(\tau, \tau_d), (2\lambda_v, 2\lambda_d)]$, proportional distribution of resources and 250 m cell radius.

Annex D

Scenario B, Program results

Scenario B takes into account the number of users referred in Table 5.1, i.e., voice users will load considerably less the system than data users. The program is first run for a cell with 150 m radius; average speeds of 15 km/h and 60 km/h and buffer sizes of 20 and 10 MB are applied in particular situations. The program is run a second time for a cell with 250 m radius.

The numbers of channels obtained are presented in Figure D.1:

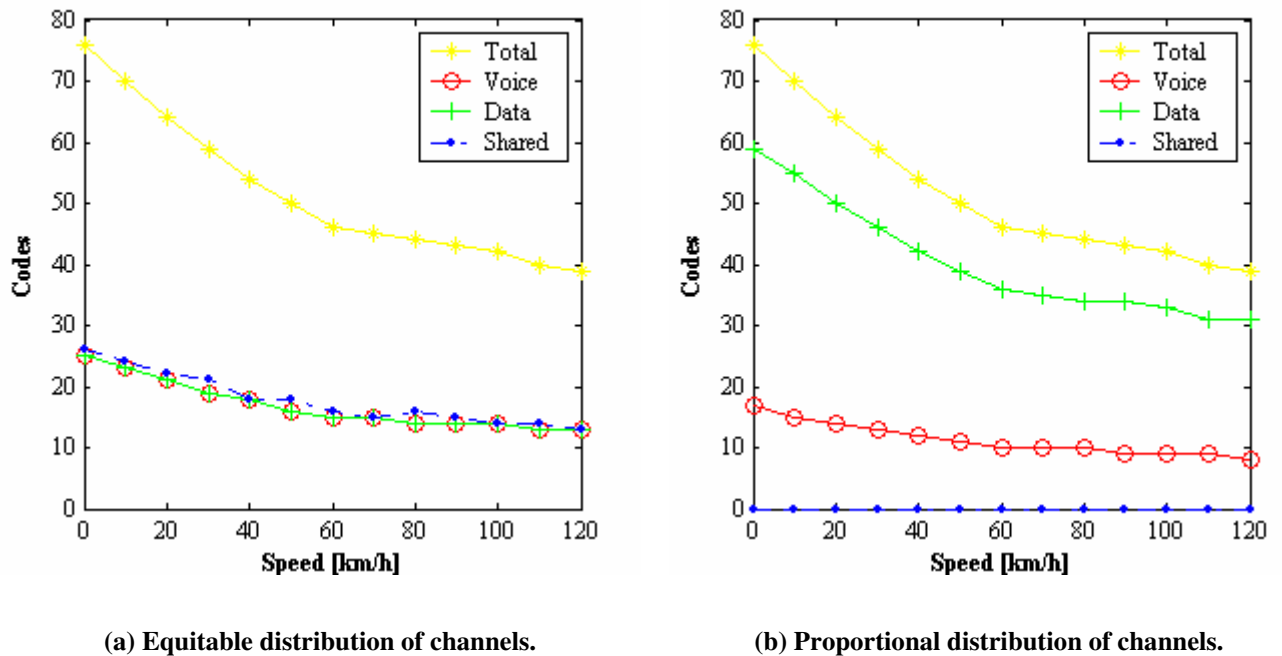
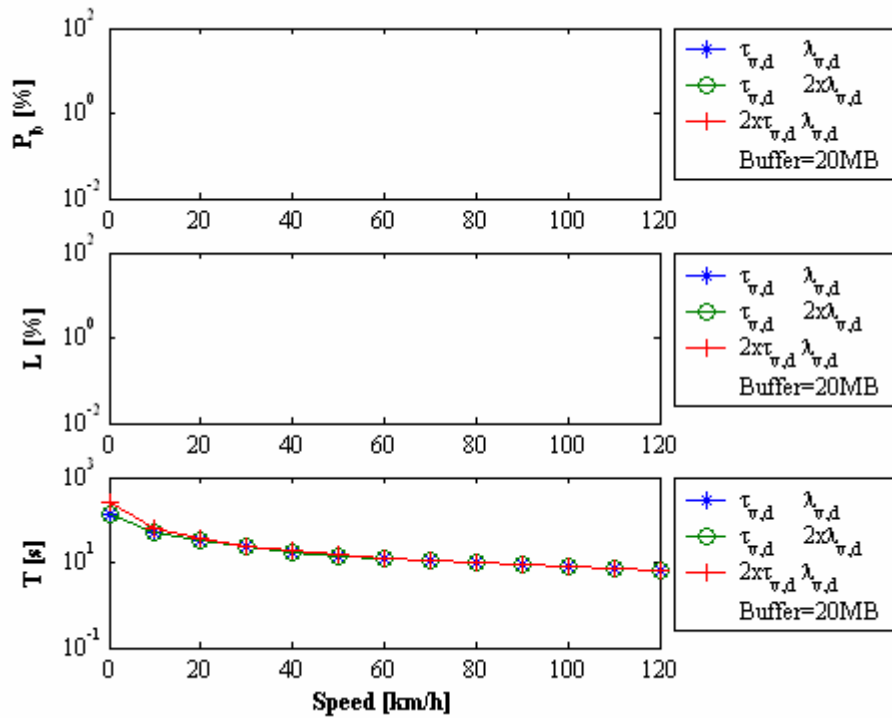


Figure D.1 – Number of channels for Scenario B.

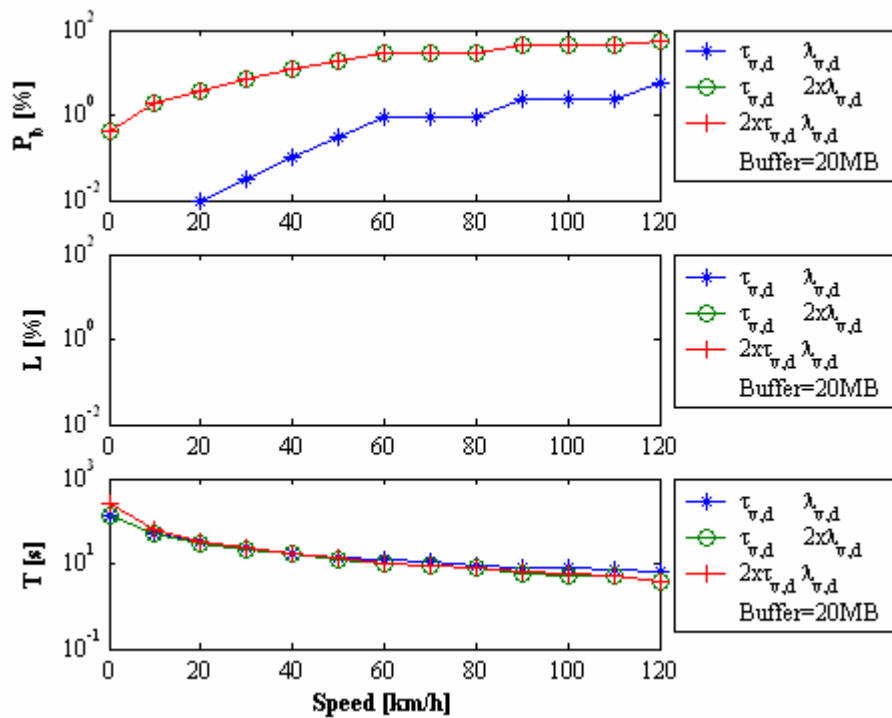
The performance results, as a function of users' speed, are presented in Figure D.2 to Figure D.5, and as a function of the buffer size, correspond to Figure D.6 to Figure D.9.

Figure D.10 to Figure D.13 show the p_{ij} and p_{ij}' matrices for a cell with 150 m radius, whereas the results for a 250 m cell are presented in Figure D.14 to Figure D.17.

D. Scenario B, Program results

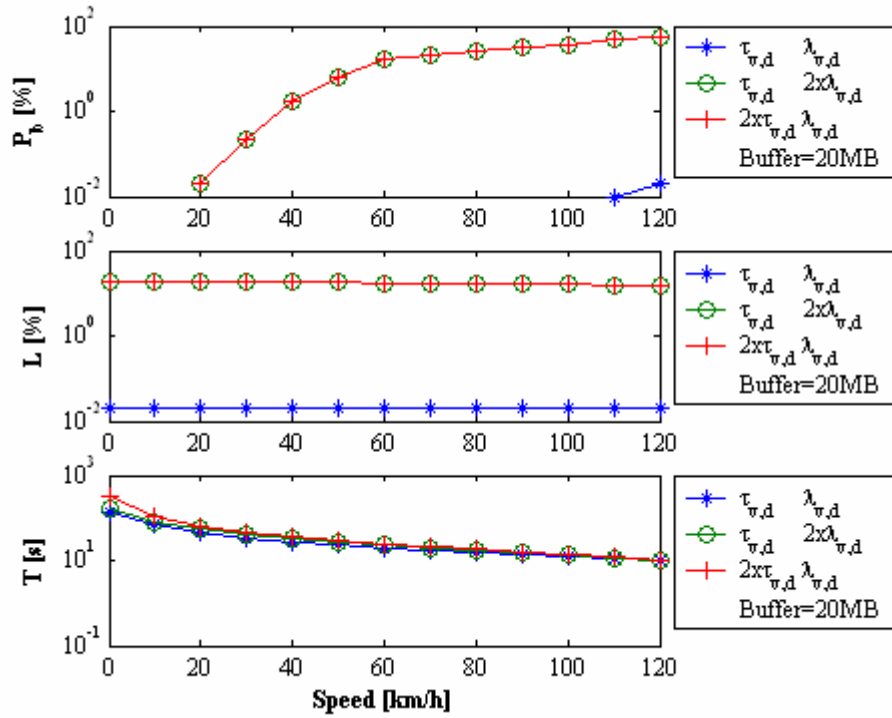


(a) Equitable distribution of channels.

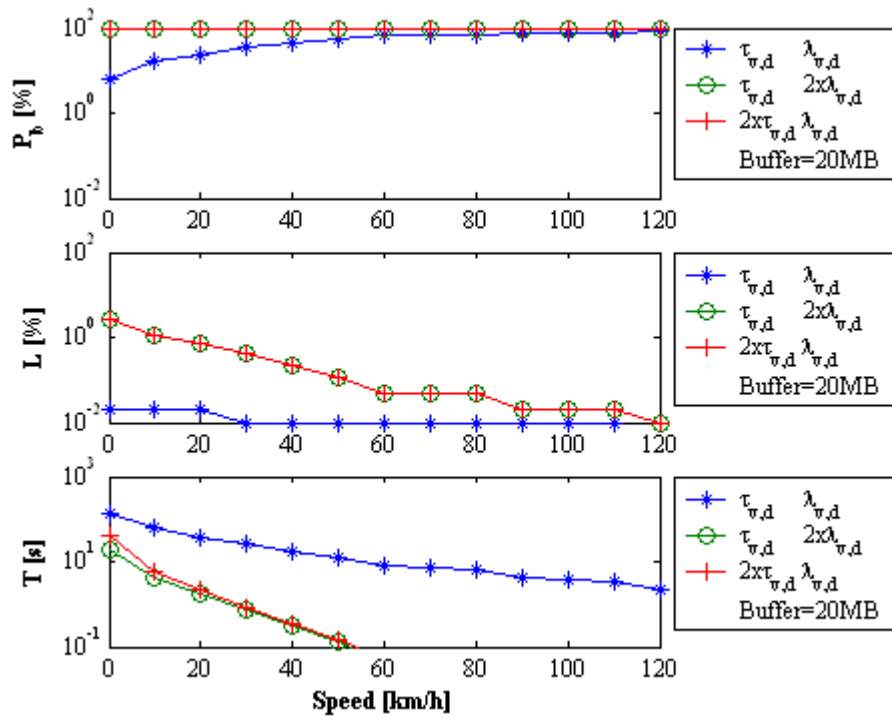


(b) Proportional distribution of channels.

Figure D.2 – System performance versus users' speed (150 m cell radius; 20 MB buffer size).



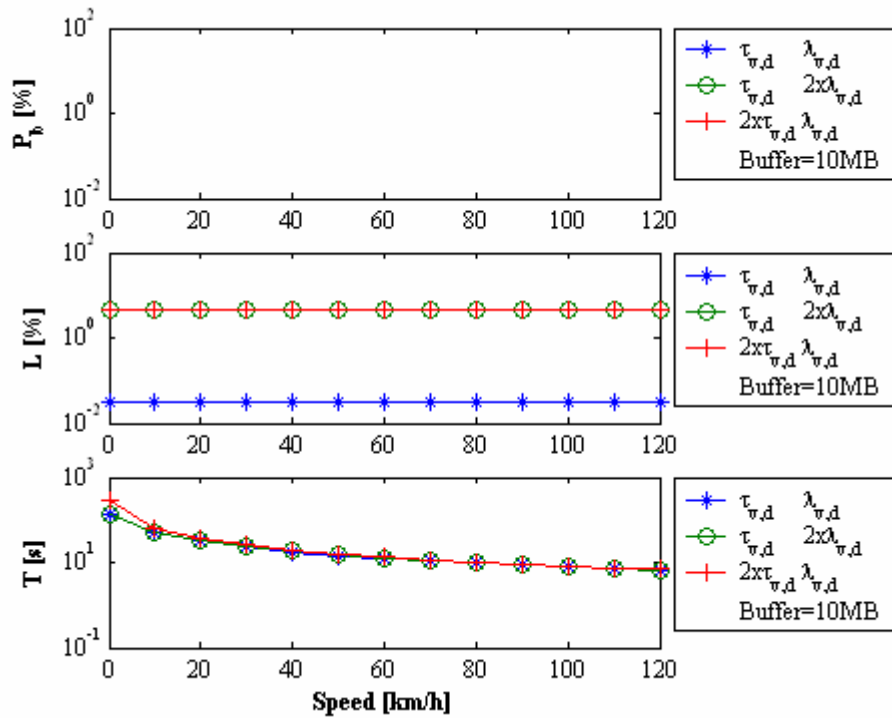
(a) Equitable distribution of channels.



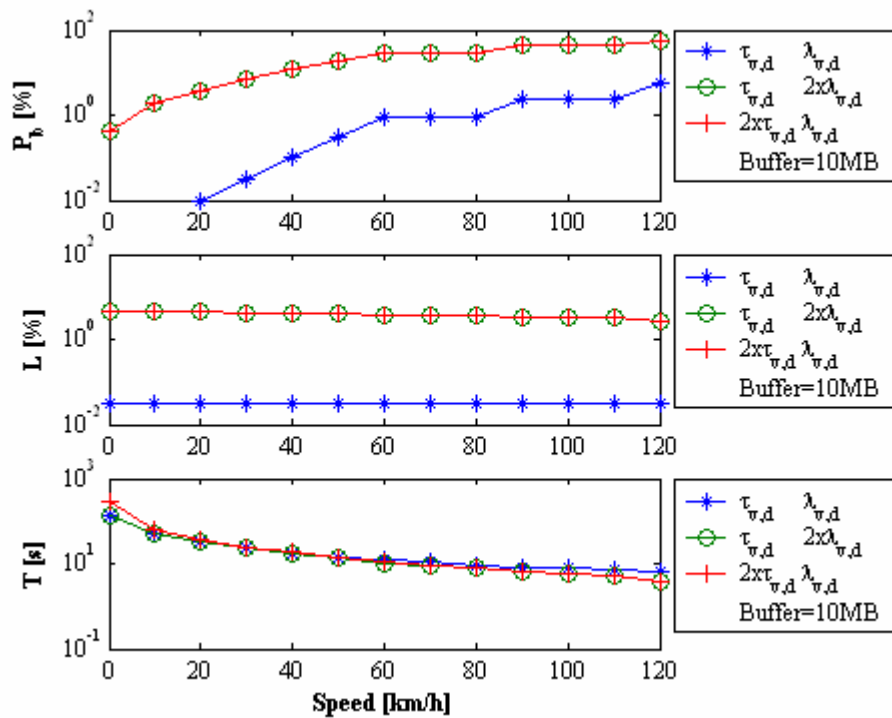
(b) Proportional distribution of channels.

Figure D.3 – System performance versus users' speed (250 m cell radius; 20 MB buffer size).

D. Scenario B, Program results

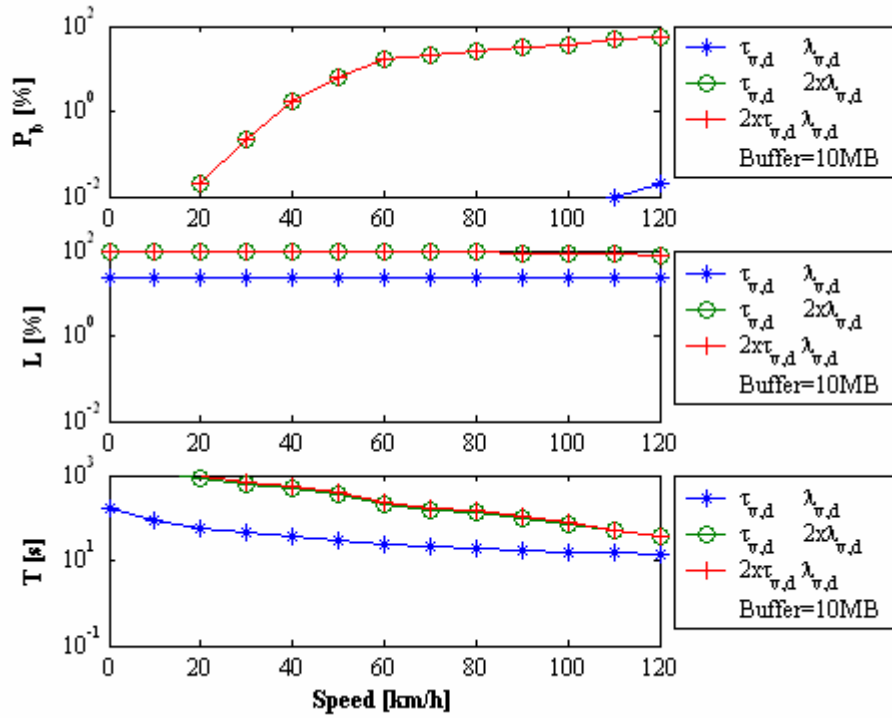


(a) Equitable distribution of channels.

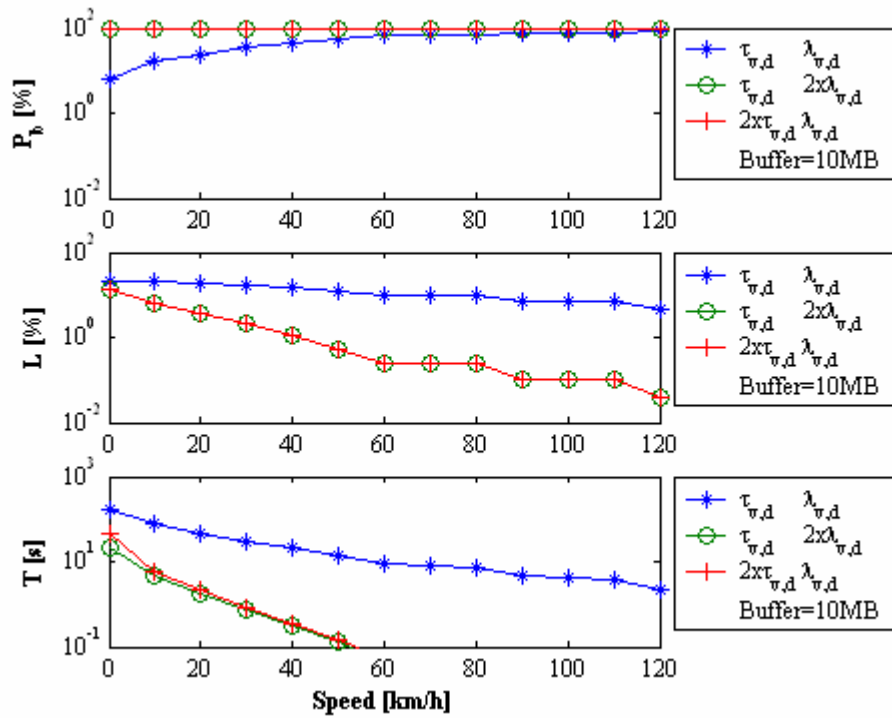


(b) Proportional distribution of channels.

Figure D.4 – System performance versus users' speed (150 m cell radius; 10 MB buffer size).



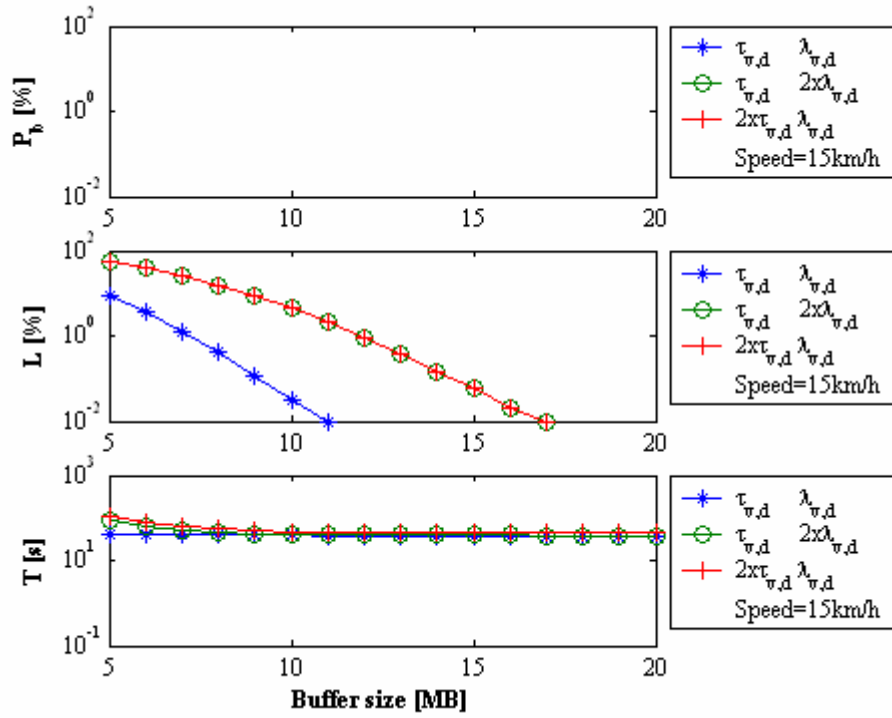
(a) Equitable distribution of channels.



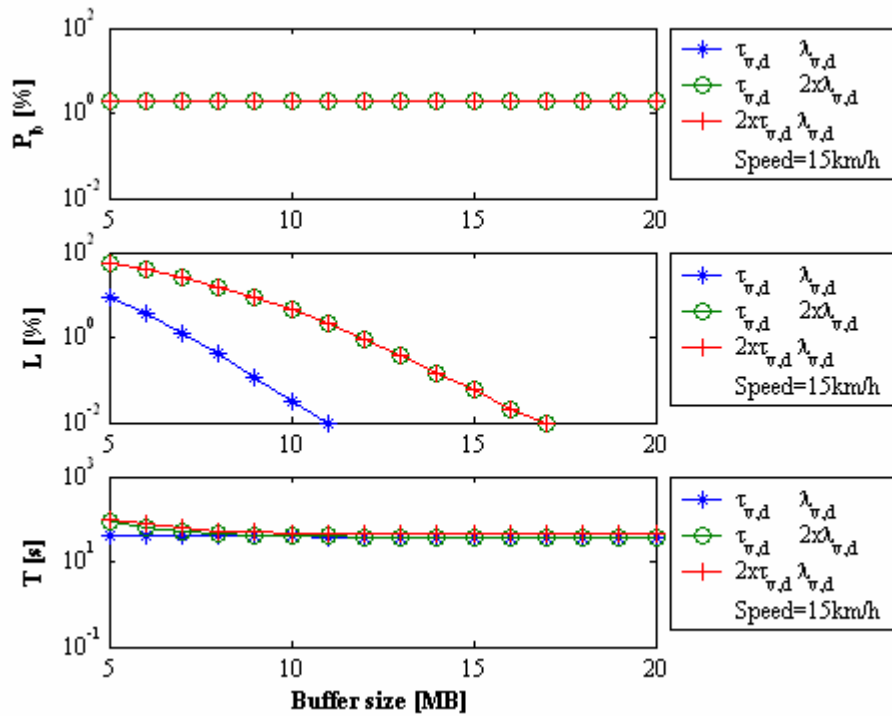
(b) Proportional distribution of channels.

Figure D.5 – System performance versus users' speed (250 m cell radius; 10 MB buffer size).

D. Scenario B, Program results

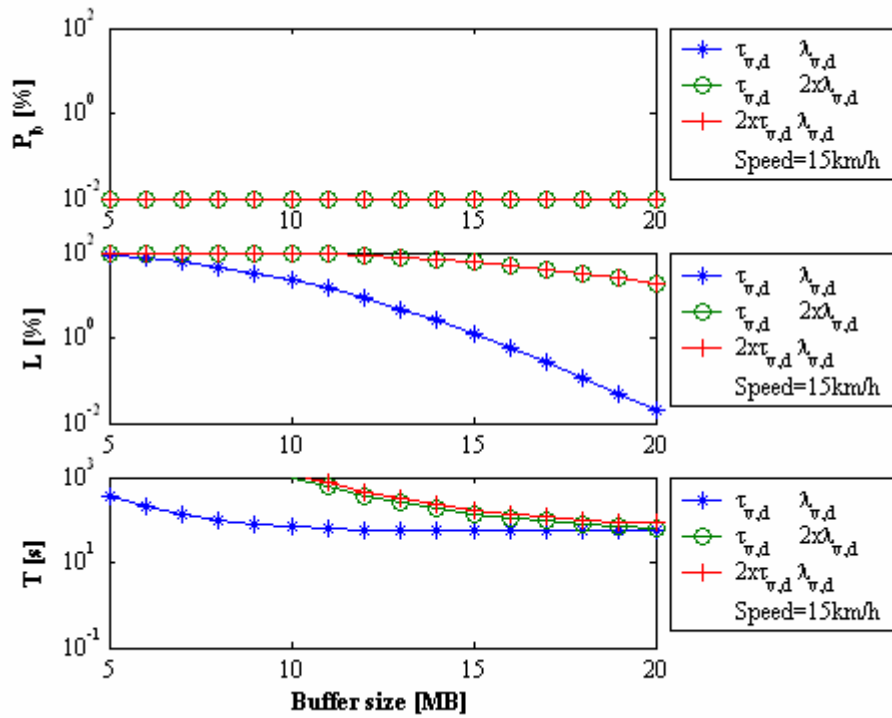


(a) Equitable distribution of channels.

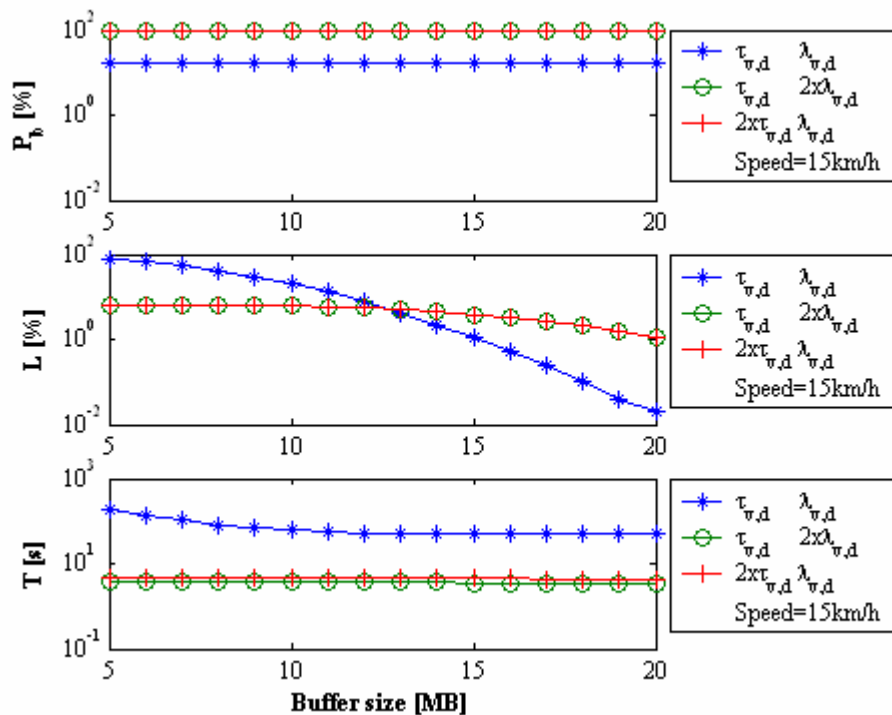


(b) Proportional distribution of channels.

Figure D.6 – System performance versus buffer size (150 m cell radius; 15 km/h average speed).



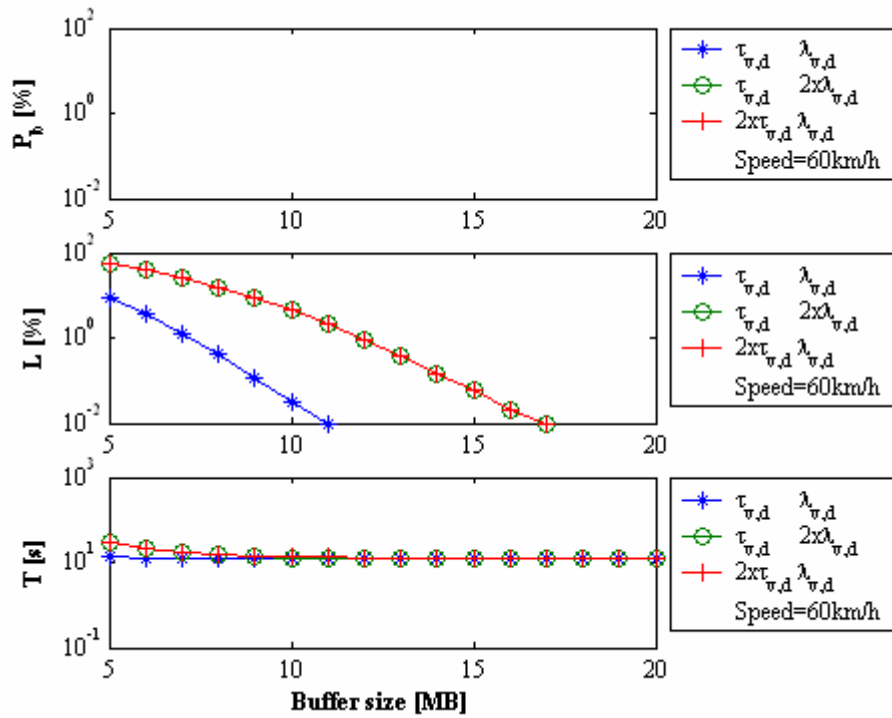
(a) Equitable distribution of channels.



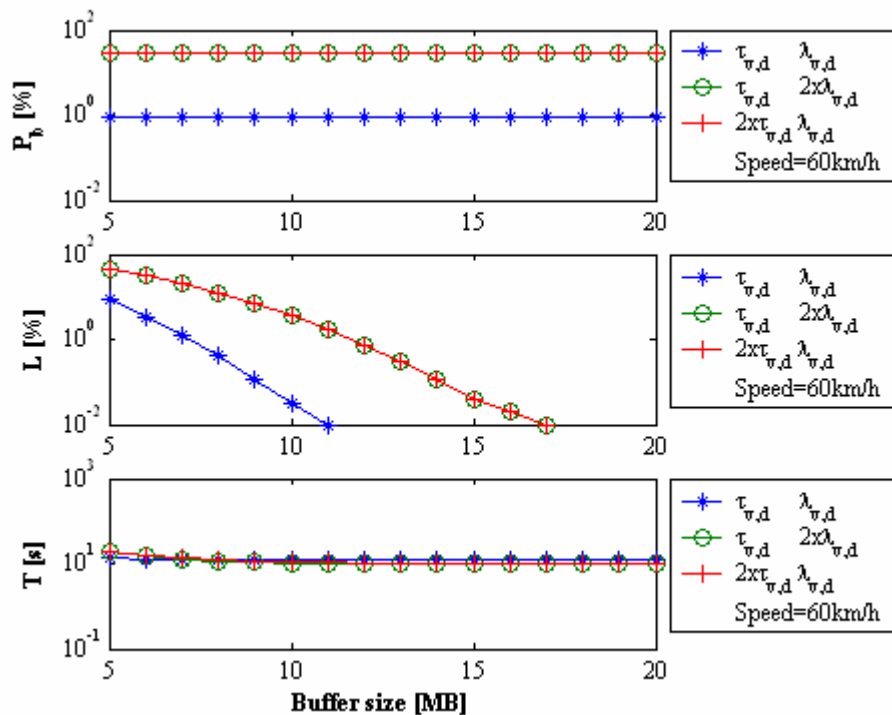
(b) Proportional distribution of channels.

Figure D.7 – System performance versus buffer size (250 m cell radius; 15 km/h average speed).

D. Scenario B, Program results

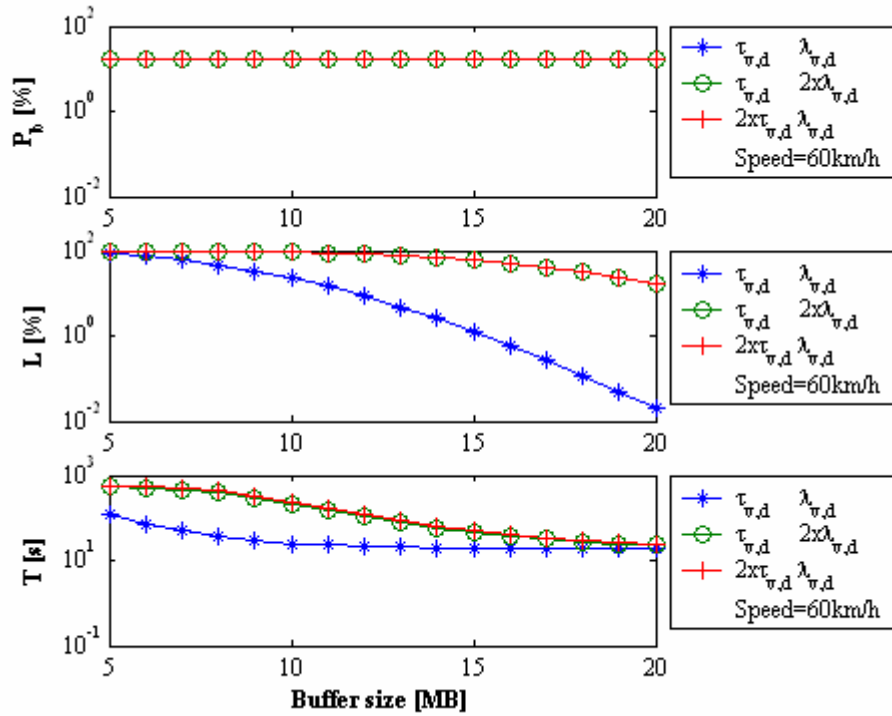


(a) Equitable distribution of channels.

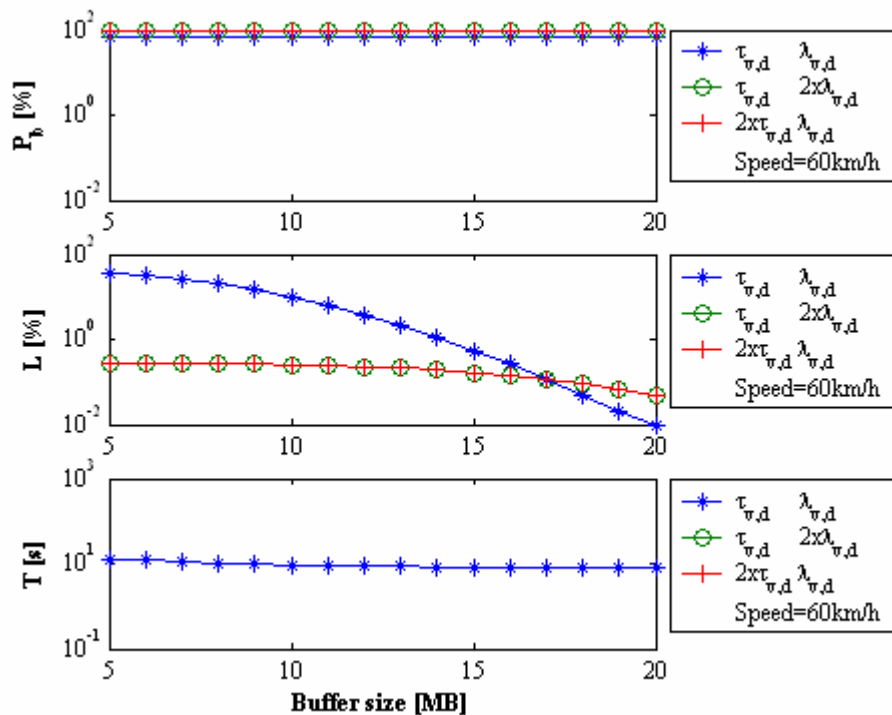


(b) Proportional distribution of channels.

Figure D.8 – System performance versus buffer size (150 m cell radius; 60 km/h average speed).



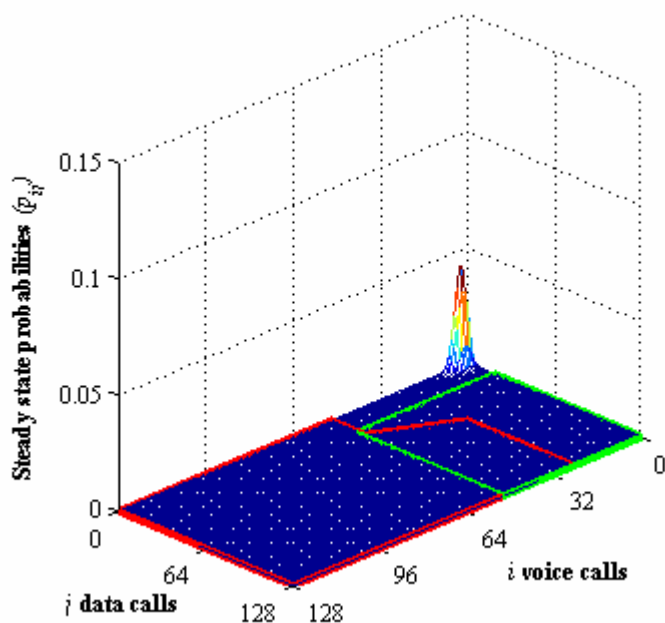
(a) Equitable distribution of channels.



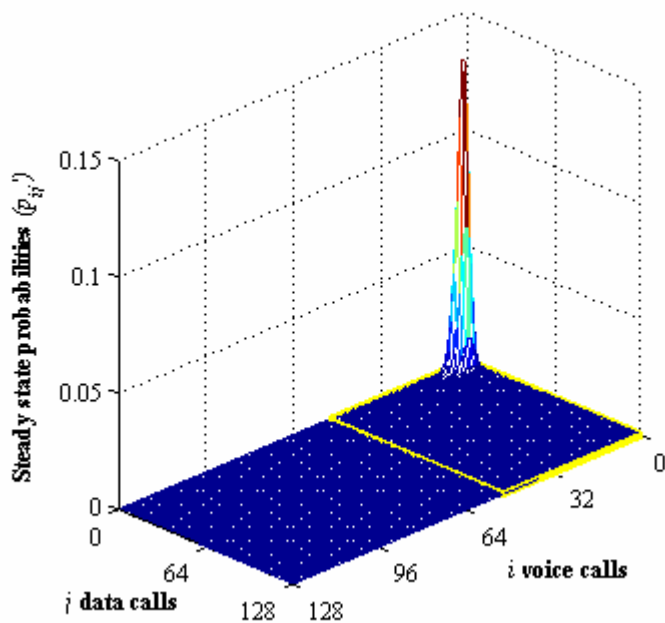
(b) Proportional distribution of channels.

Figure D.9 – System performance versus buffer size (250 m cell radius; 60 km/h average speed).

D. Scenario B, Program results

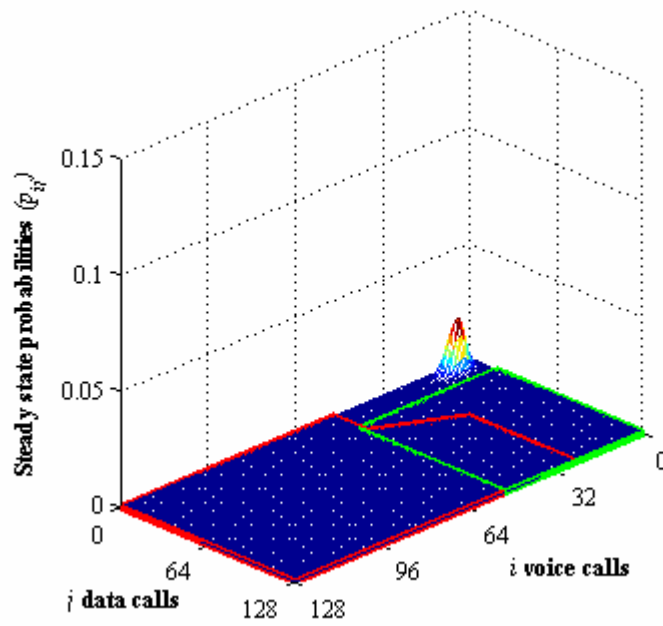


(a) p_{ij} for an equitable distribution of resources.

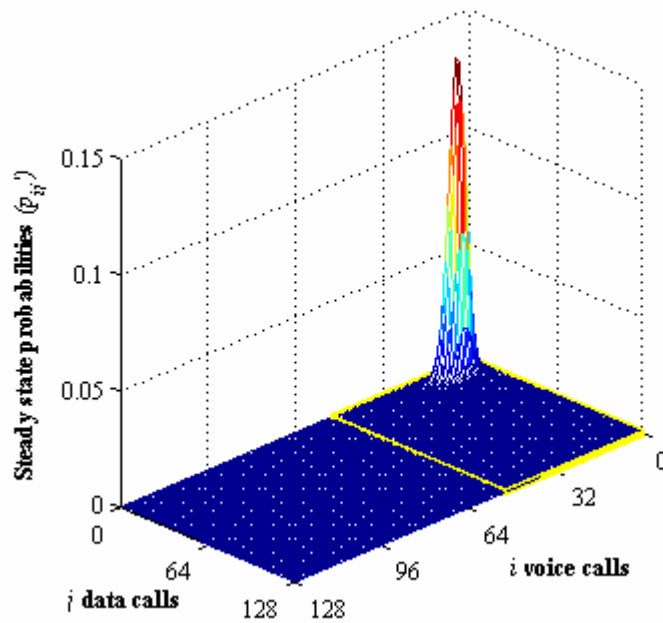


(b) p_{ij}' for an equitable distribution of resources.

Figure D.10 – Steady-states $[(\tau_v, \tau_d), (\lambda_v, \lambda_d)]$, equitable distribution of resources and 150 m cell radius.



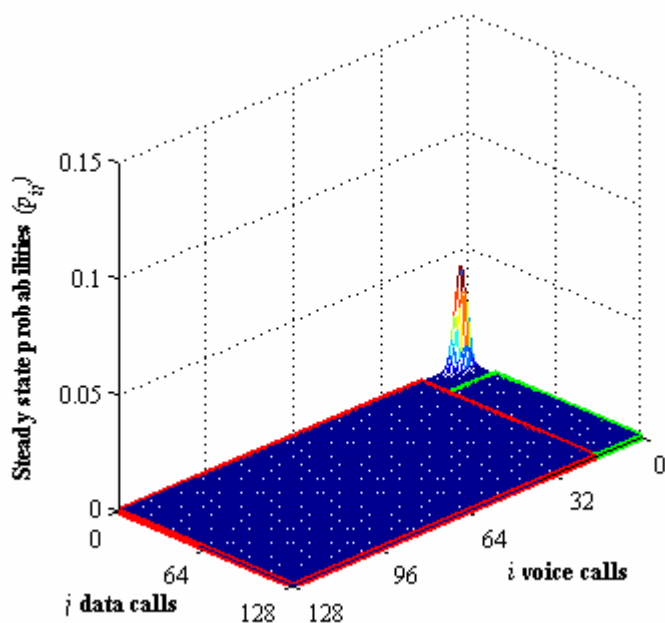
(a) p_{ij} for an equitable distribution of resources.



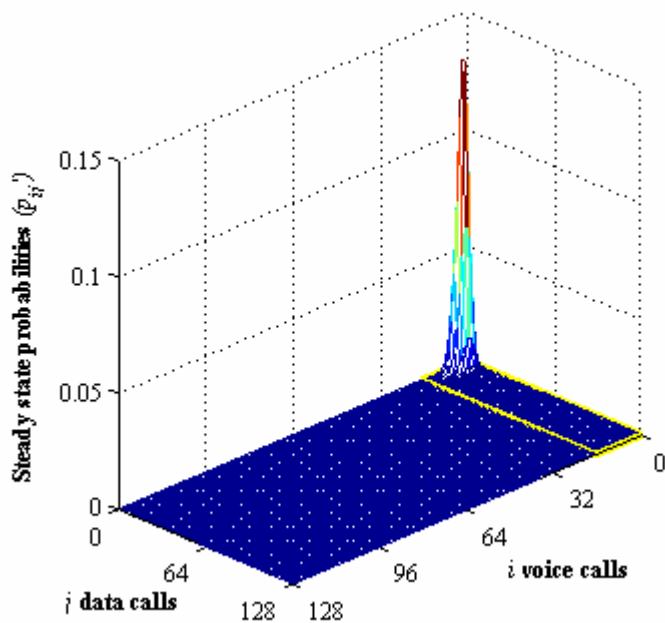
(b) p_{ij}' for an equitable distribution of resources.

Figure D.11 – Steady-states $[(2\tau, 2\tau_d), (\lambda, \lambda_d)]$ or $[(\tau, \tau_d), (2\lambda, 2\lambda_d)]$, equitable distribution of resources and 150 m cell radius.

D. Scenario B, Program results

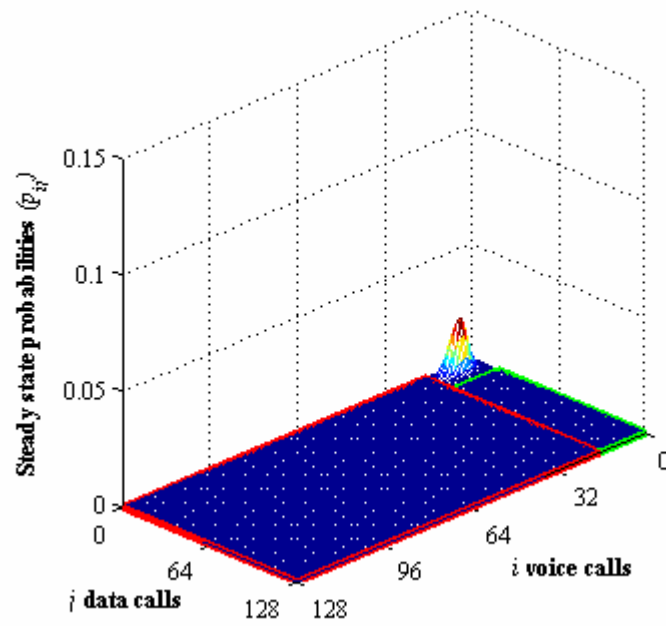


(a) p_{ij} for a proportional distribution of resources.

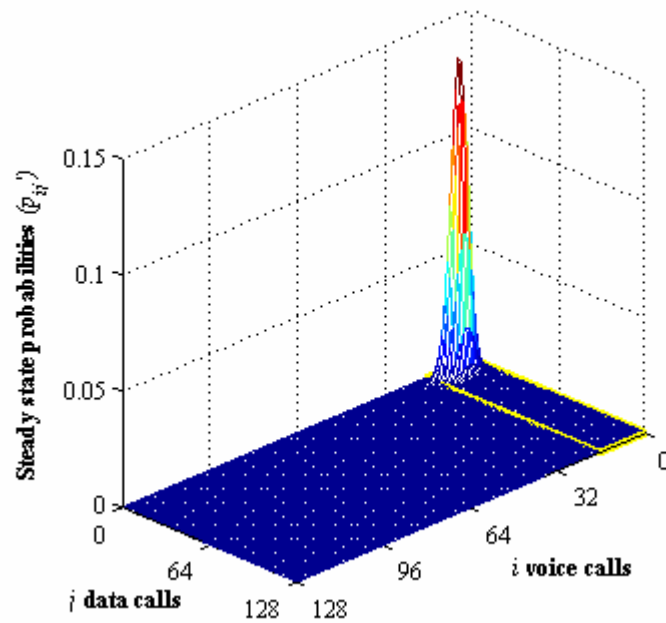


(b) p_{ij}' for a proportional distribution of resources.

Figure D.12 – Steady-states $[(\tau_s, \tau_d), (\lambda_s, \lambda_d)]$, proportional distribution of resources and 150 m cell radius.



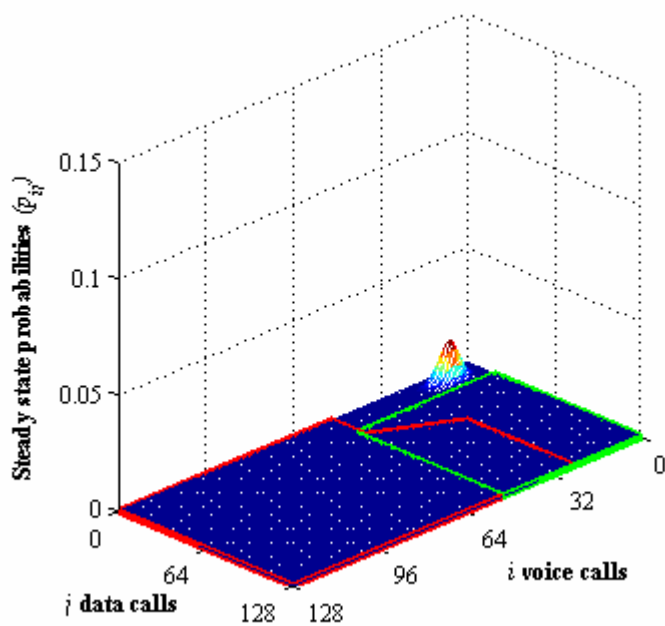
(a) p_{ij} for a proportional distribution of resources.



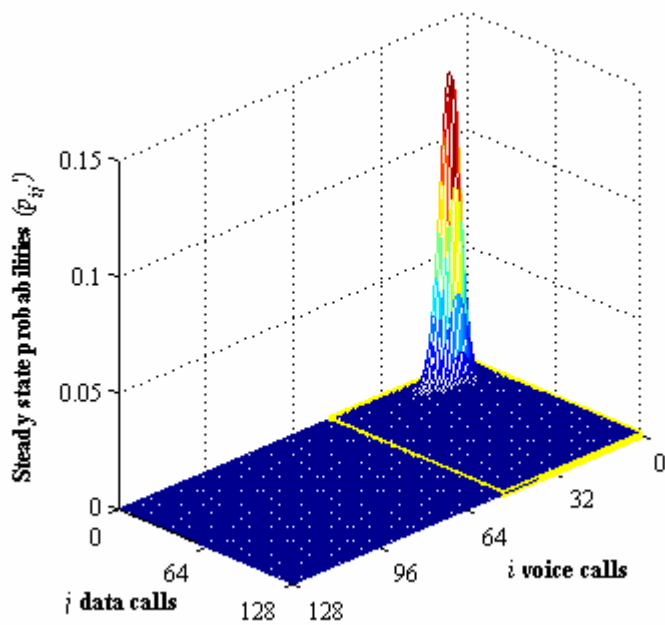
(b) p_{ij}' for a proportional distribution of resources.

Figure D.13 – Steady-states $[(2\tau, 2\tau_d), (\lambda_v, \lambda_d)]$ or $[(\tau, \tau_d), (2\lambda_v, 2\lambda_d)]$, proportional distribution of resources and 150 m cell radius.

D. Scenario B, Program results

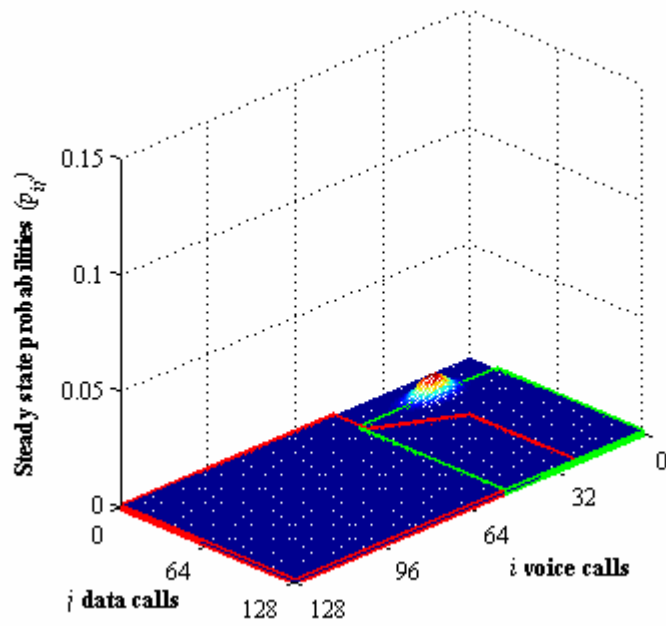


(a) p_{ij} for an equitable distribution of resources.

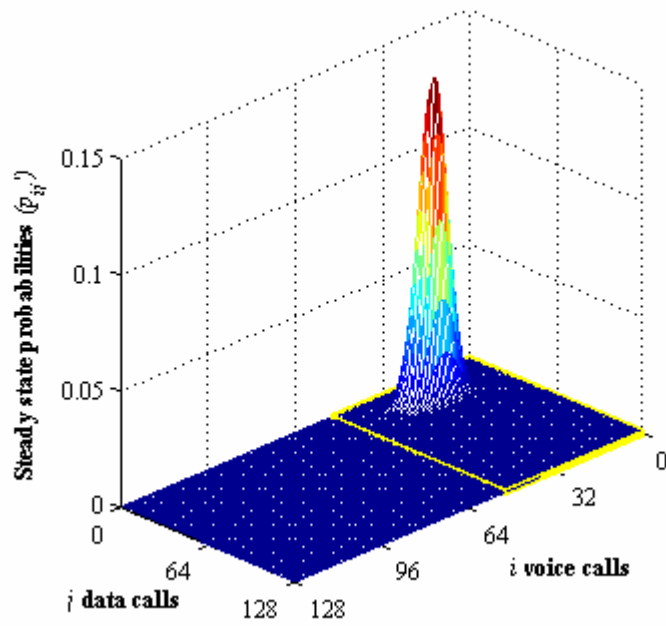


(b) p_{ij}' for an equitable distribution of resources.

Figure D.14 – Steady-states $[(\tau_v, \tau_d), (\lambda_v, \lambda_d)]$, equitable distribution of resources and 250 m cell radius.



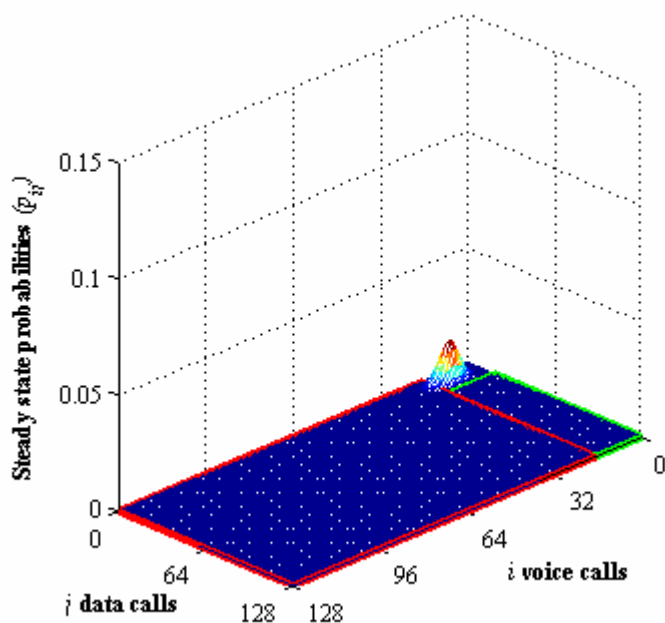
(a) p_{ij} for an equitable distribution of resources.



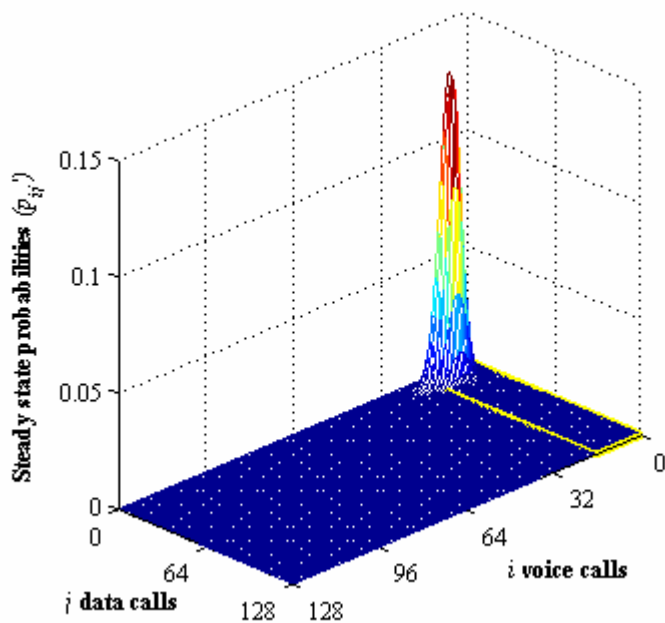
(b) p_{ij}' for an equitable distribution of resources.

Figure D.15 – Steady-states $[(2\tau, 2\tau_d), (\lambda, \lambda_d)]$ or $[(\tau, \tau_d), (2\lambda, 2\lambda_d)]$, equitable distribution of resources and 250 m cell radius.

D. Scenario B, Program results

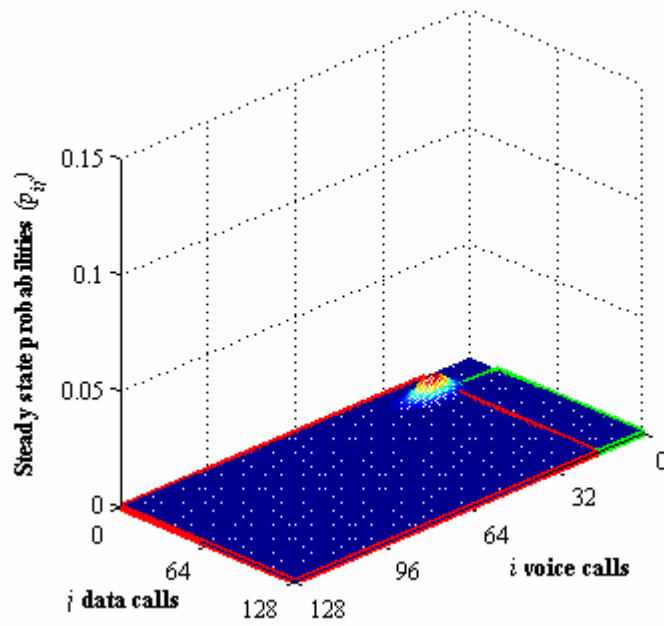


(a) p_{ij} for a proportional distribution of resources.

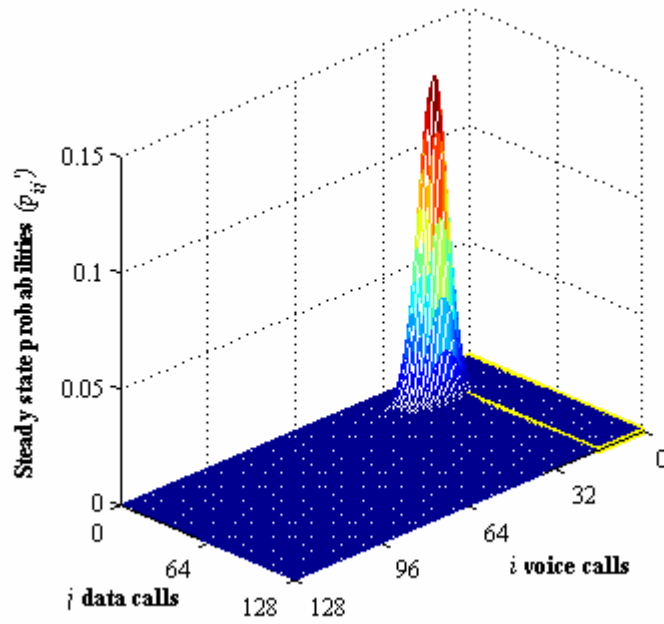


(b) p_{ij}' for a proportional distribution of resources.

Figure D.16 – Steady-states $[(\tau, \tau_d), (\lambda, \lambda_d)]$, proportional distribution of resources and 250 m cell radius.



(a) p_{ij} for a proportional distribution of resources.



(b) p_{ij}' for a proportional distribution of resources.

Figure D.17 – Steady-states $[(2\tau, 2\tau_d), (\lambda_v, \lambda_d)]$ or $[(\tau, \tau_d), (2\lambda_v, 2\lambda_d)]$, proportional distribution of resources and 250 m cell radius.

References

- [3GPP00a] 3GPP, *Spreading and Modulation (TDD)*, Technical Specification Group – Radio Access Network, Report No. 25.223 Ver. 3.2.0, Mar. 2000 (<http://www.3gppg.org>).
- [3GPP01a] 3GPP, *UTRAN Overall Description*, Technical Specification Group – Radio Access Network, Report No. 25.401 Ver. 4.0.0, Mar. 2001 (<http://www.3gppg.org>).
- [3GPP01b] 3GPP, *Spreading and Modulation (FDD)*, Technical Specification Group – Radio Access Network, Report No. 25.213 Ver. 3.5.0, Mar. 2001 (<http://www.3gppg.org>).
- [3GPP01c] 3GPP, *UE Radio Transmission and Reception (FDD)*, Technical Specification Group – Radio Access Network, Report No. 25.101 Ver. 5.0.0, Sep. 2001 (<http://www.3gppg.org>).
- [3GPP02a] 3GPP, *Quality of Service (QoS) concept and architecture*, Technical Specification Group – Services and System Aspects, Report No. 23.107 Ver. 5.6.0, Sep. 2002 (<http://www.3gppg.org>).
- [3GPP02b] 3GPP, *Physical channels and mapping of transport channels onto physical channels (FDD)*, Technical Specification Group – Radio Access Network, Report No. 25.211 Ver. 3.12.0, Sep. 2002 (<http://www.3gppg.org>).
- [3GPP02c] 3GPP, *Physical channels and mapping of transport channels onto physical channels (TDD)*, Technical Specification Group – Radio Access Network, Report No. 25.221 Ver. 3.11.0, Sep. 2002 (<http://www.3gppg.org>).

References

- [3GPP03] 3GPP, *Vocabulary for 3GPP Specifications*, Technical Specification Group – Services and System Aspects, Report No. 21.905 Ver. 5.8.0, Sep. 2003 (<http://www.3gppg.org>).
- [3GPP99a] 3GPP, *Physical Layer – General Description*, Technical Specification Group – Radio Access Network, Report No. 25.201 Ver. 3.0.1, Dec. 1999 (<http://www.3gppg.org>).
- [CaVa02] Carvalho,P. and Vasconcelos,A., *Traffic Models for Base Stations in UMTS* (in Portuguese), Graduation Report, Instituto Superior Técnico, Lisbon, Portugal, Sep. 2002.
- [CEPT00] CEPT, *Detailed Spectrum Investigation Phase III*, European Radiocommunications Committee, Final Report on DSI Phase III, Apr. 2000 (<http://www.ero.dk>).
- [CEPT02] CEPT, *European Common Allocation Table*, European Radiocommunications Committee, ERC Report 25, Jan. 2002 (<http://www.ero.dk>).
- [Corr03] Correia,L.M., *Mobile and Personal Communication Systems* (in Portuguese), Course Notes, Instituto Superior Técnico, Lisbon, Portugal, May 2003 (<http://fenix3.ist.utl.pt/publico>)
- [Corr99] Correia L.M., *Mobile Communications – Parts I and II* (in Portuguese), Course Notes, Instituto Superior Técnico, Lisbon, Portugal, Mar. 1999.
- [DaCo99] Damosso,E. and Correia,L.M., *Digital Mobile Radio Towards Future Generation Systems – COST 231 Final Report*, COST Office, Brussels, Belgium, 1999.
- [Dias03] Dias,C., *Traffic Analysis at the Radio Interface in UMTS FDD*, Master Thesis, Instituto Superior Técnico, Lisbon, Portugal, Dec. 2003.

- [ETSI01] ETSI, *General Packet Radio Service (GPRS); Mobile Station – Serving GPRS Support Node (MS-SGSN) Logical Link Control (LLC) Layer Specification*, Report No. 101 351 Ver. 8.7.0, Sophia-Antipolis, France, Dec. 2001 (<http://www.etsi.org>).
- [ETSI98] ETSI, *Selection procedures for the choice of radio transmission technologies of the UMTS (UMTS 30.03 version 3.2.0)*, Report TR 101 112 Ver. 3.2.0, Sophia-Antipolis, France, Apr. 1998 (<http://www.etsi.org>).
- [FCSC02] Ferreira,L., Correia,L.M., Serrador,A., Carvalho,G., Fledderus,E. and Perera,R., *UMTS Deployment and Mobility Scenarios*, IST-MOMENTUM Project, Deliverable D1.3, IST-TUL, Lisbon, Portugal, Oct. 2002 (<http://momentum.zib.de>).
- [FCXV03] Ferreira,L., Correia,L.M., Xavier,D., Vasconcelos,A. and Fledderus,E., *Final Report on Traffic Estimation and Services Characterisation*, IST-MOMENTUM Project, Deliverable D1.4, IST-TUL, Lisbon, Portugal, May 2003, (<http://momentum.zib.de>).
- [FMSC01] Ferreira,L., Marques,G., Serrador,A. and Correia,L.M., *Classification of Mobile Multimedia Services*, IST-MOMENTUM Project, Deliverable D1.1, IST-TUL, Lisbon, Portugal, Dec. 2001 (<http://momentum.zib.de>).
- [HaLH00] Haung,Y.-R., Lin,Y.-B. and Ho,J.-M., *Performance Analysis for Voice/Data Integration on a Finite-Buffer Mobile System*, IEEE Transactions on Vehicular Technology, Vol. 49, No. 2, Mar. 2000, pp. 367-378.
- [HaLi97] Hanselman,D. and Littlefield,B., *The Student Edition of Matlab*, Prentice Hall, Upper Saddle River, NJ, USA, 1997 (<http://www.mathworks.com/>).
- [HoTo01] Holma,H. and Toskala,A., *WCDMA for UMTS*, John Wiley & Sons, Chichester, UK, 2001.

References

- [Jabb96] Jabbari,B., “Teletraffic Aspects of Evolving and Next-Generation Wireless Communication Networks”, *IEEE Personal Communications*, Vol. 3, No. 6, Dec. 1996, pp. 4-9.
- [Keis89] Keiser,G.E., *Local Area Networks*, McGraw-Hill, Singapore, 1989.
- [KeRi88] Kernighan,B.W. and Ritchie,D.M., *The C Programming Language*, Prentice Hall, Englewood Cliffs, NJ, USA, 1988.
- [Leon94] Leon-Garcia,A., *Probability and Random Processes for Electrical Engineering*, Addison-Wesley, Massachusetts, USA, 1994.
- [Meye84] Meyer,P.L., *Introductory Probability and Statistical Applications* (in Portuguese), Livros Técnicos e Científicos Editora, Rio de Janeiro, Brazil, 1984.
- [MOME01] MOMENTUM, *Models and Simulations for Network Planning and Control of UMTS*, IST-MOMENTUM Project (<http://www.zib.de/projects/telecommunication/MOMENTUM/>).
- [MSDN03] Microsoft Developer Network Online (<http://msdn.microsoft.com>).
- [Rapp96] Rappaport,T.S., *Wireless Communications*, Prentice Hall, NJ, USA, 1996.
- [RFHL03] Rakoczi,B., Fledderus,E., Heideck,B., Lourenço,P. and Kürner,T., *Reference Scenarios*, IST-MOMENTUM Project, Deliverable D5.2, KPN, The Hague, The Netherlands, Nov. 2003.
- [SeCo03] Serrador,A. and Correia,L.M., *Protocol Buffering Effects on Traffic*, IST-FLOWS Project, Internal Report No. WP6_IST-TUL_TN_INT_065_01, IST-TUL, IST, Lisbon, Portugal, July 2003.
- [Serr02] Serrador,A., *Optimisation of Cell Radius in UMTS-FDD Networks*, Master Thesis, Instituto Superior Técnico, Lisbon, Portugal, Dec. 2002.

- [TWPL02] Türke,U., Winter,T., Perera,R., Lamers,E., Meijerink,E., Fledderus,E. and Serrador,A., *Comparison of different simulation approaches for cell performance evaluation*, IST-MOMENTUM Project, Deliverable D2.2, Siemens, Berlin, Germany, Oct. 2002 (<http://momentum.zib.de>).
- [UMTS01] UMTS Forum, *The UMTS Third Generation Market – Phase II: Structuring the Service Revenue Opportunities*, Report No. 13, London, UK, Apr. 2001 (<http://www.umts-forum.org/>).
- [UMTS98] UMTS Forum, *UMTS/IMT-2000*, Report No. 6, London, UK, Dec.1998 (<http://www.umts-forum.org/>).
- [Voda02] Vodafone-Telecel, IST-MOMENTUM Project, WP5 Reference Scenarios CD, Lisbon, Portugal, Oct. 2002.
- [Yaco93] Yacoub,M.D., *Foundations of Mobile Radio Engineering*, CRC Press, Boca Raton, FL, USA, 1993.

